National Library of Canada
Canadian Theses Service
Ottawa, Canada
K1A 0N4

Bibliothèque nationale du Canada
Service des thèses canadiennes

NOTICE

The quality of this microform is heavily dependent upon the quality of the original thesis submitted for microfilming. Every effort has been made to ensure the highest quality of reproduction possible.

If pages are missing, contact the university which granted the degree.

Some pages may have indistinct print especially if the original pages were typed with a poor typewriter ribbon or if the university sent us an inferior photocopy.

Reproduction in full or in part of this microform is governed by the Canadian Copyright Act, R.S.C. 1970, c. C-30, and subsequent amendments.

AVIS

La qualité de cette microforme dépend grandement de la qualité de la thèse soumise au microfilmage. Nous avons tout fait pour assurer une qualité supérieure de reproduction.

S'il manque des pages, veuillez communiquer avec l'université qui a conféré le grade.

La qualité d'impression de certaines pages peut laisser à désirer, surtout si les pages originales ont été dactylographiées à l'aide d'un ruban usé ou si l'université nous a fait parvenir une photocopie de qualité inférieure.

La reproduction, même partielle, de cette microforme est soumise à la Loi canadienne sur le droit d'auteur, SRC 1970, c. C-30, et ses amendements subséquents.

NL-339 (r. 88/04) c

Canada

UNIVERSITY OF ALBERTA

DESIGN GUIDELINES FOR BEDDED FOOTWALL SLOPES

BY

RICHARD DAWSON

A THESIS

SUBMITTED TO THE FACULTY OF GRADUATE STUDIES AND RESEARCH IN PARTIAL FULFILLMENT OF THE REQUIREMENTS FOR THE DEGREE OF MASTER OF SCIENCE

IN

MINING ENGINEERING

DEPARTMENT OF MINING, METALLURGICAL
AND PETROLEUM ENGINEERING

EDMONTON, ALBERTA

FALL, 1990

National Library of Canada
Bibliothèque nationale du Canada

Canadian Theses Service
Service des thèses canadiennes

Ottawa, Canada
K1A 0N4

The author has granted an irrevocable non-exclusive licence allowing the National Library of Canada to reproduce, loan, distribute or sell copies of his/her thesis by any means and in any form or format, making this thesis available to interested persons.

L'auteur a accordé une licence irrévocable et non exclusive permettant à la Bibliothèque nationale du Canada de reproduire, prêter, distribuer ou vendre des copies de sa thèse de quelque manière et sous quelque forme que ce soit pour mettre des exemplaires de cette thèse à la disposition des personnes intéressées.

The author retains ownership of the copyright in his/her thesis. Neither the thesis nor substantial extracts from it may be printed or otherwise reproduced without his/her permission.

L'auteur conserve la propriété du droit d'auteur qui protège sa thèse. Ni la thèse ni des extraits substantiels de celle-ci ne doivent être imprimés ou autrement reproduits sans son autorisation.

ISBN 0-315-65092-3

UNIVERSITY OF ALBERTA

RELEASE FORM

NAME OF AUTHOR:	RICHARD DAWSON
TITLE OF THESIS:	**DESIGN GUIDELINES FOR BEDDED FOOTWALL SLOPES**
DEGREE:	MASTER OF SCIENCE
YEAR THIS DEGREE GRANTED:	1990

PERMISSION IS HEREBY GRANTED TO THE UNIVERSITY OF ALBERTA LIBRARY TO REPRODUCE SINGLE COPIES OF THIS THESIS AND TO LEND OR SELL SUCH COPIES FOR PRIVATE, SCHOLARLY OR SCIENTIFIC RESEARCH PURPOSES ONLY.

THE AUTHOR RESERVES OTHER PUBLICATION RIGHTS, AND NEITHER THE THESIS NOR EXTENSIVE EXTRACTS FROM IT MAY BE PRINTED OR OTHERWISE REPRODUCED WITHOUT THE AUTHOR'S WRITTEN PERMISSION.

(SIGNED) R Dawson

PERMANENT ADDRESS:

9758 86 Ave
Edmonton, Alta
T6E 2L4

Date: Oct 12, 1990

THE UNIVERSITY OF ALBERTA

FACULTY OF GRADUATE STUDIES AND RESEARCH

THE UNDERSIGNED CERTIFY THAT THEY HAVE READ, AND RECOMMEND TO THE FACULTY OF GRADUATE STUDIES AND RESEARCH FOR ACCEPTANCE, A THESIS ENTITLED **DESIGN GUIDELINES FOR BEDDED FOOTWALL SLOPES** SUBMITTED BY RICHARD F. DAWSON IN PARTIAL FULFILLMENT OF THE REQUIREMENTS FOR THE DEGREE OF MASTER OF SCIENCE IN MINING ENGINEERING.

K. Barron
Dr. Ken Barron
(Supervisor)

J.M. Whiting
Dr. J.M. Whiting

Dr. N. Stuart

Dr. N.R. Morgenstern

Date: Sept. 26, 1990

ABSTRACT

The design of bedded footwalls is discussed as a class of rock slope problems where the slope face is excavated parallel to persistent bedding planes. During this study a thorough literature review, sensitivity analysis, minesite investigations, and recent mining experience have been drawn upon to develop a consistent set of guidelines for bedded footwall slopes with particular reference to mountain coal mines. Findings from the study of significance to the design process are as follows:

i. Groundwater pressures in bedded footwall strata are often artesian due to the preferred hydraulic conductivity parallel to bedding.

ii. The peak shear strength of persistent bedding joints is equal to or slightly greater than the ultimate friction angle. There does not appear to be any precedent for using a design peak strength with a dilation angle greater than 3° to 5°.

iii. Rock mass shear strength is best assessed by empirical criterion such as the Hoek-Brown formulation.

iv. Limit equilibrium based analytical techniques normally involve consideration for the failure mechanics of planar, bilinear, ploughing, or buckling slabs. Flexural buckling does not appear to be a realistic failure mechanism except perhaps for very thin slabs. Bilinear slab mechanics with failure through the rock mass toe is the critical failure mechanism where unfavorably oriented discontinuities are not present. Analyses incorporating this mechanism are very sensitive to an assessment of rock mass quality

v. Anchoring of bedded footwall slopes in surface mining environments is best accomplished with post tensioned resin grouted bars.

Rational design of bedded footwalls, incorporating anchor support, for Western Canadian mountain coal mines has proven to be economically beneficial by reducing waste requirements and/or increasing coal release. In many cases, however, the footwall is developed on a hard, thickly bedded basal sandstone unit which can stand unsupported up to the required depth to pit bottom, even where steeper dips are in evidence. Thus each individual rock slope must be assessed on its own merits.

ACKNOWLEDGEMENTS

The research project for which this report is submitted was funded in part by the Canada Centre for Mineral and Energy Technology (CANMET); Energy, Mines and Resources Canada. The financial assistance provided by CANMET is gratefully acknowledged.

The author is grateful to Professor Ken Barron under whose supervision the research for this thesis was conducted. His technical assistance and continued encouragement have been deeply appreciated.

Appreciation is extended to Howard Lutley and Bill Shaw of Esso Resources Canada Limited for supporting and overseeing the contract under which the research for this thesis was carried out. In addition, the author wishes to thank Bob Fong and Brian McEwan of Byron Creek Collieries for providing access to the minesite.

Special thank is also extended to Dave Fawcett of Smoky River Coal Limited for supporting the project's concept and providing access to the minesite. Also, the author wishes to mention that Dave's enthusiasm and continuous flow of fresh and innovative thinking have left a lasting impression.

The word processing skills of Louise Bohachyk are acknowledged with appreciation.

Finally, the author wishes to acknowledge, with many thanks, the continual encouragement, support and patience rendered by his wife, Sandra. Without her this thesis would not have been possible.

TABLE OF CONTENTS

CHAPTER PAGE

1.0 INTRODUCTION 1
2.0 SHEAR STRENGTH 3
  2.1 Rock Joint Shear Strength 4
  2.2 Rock Mass Shear Strength 13
  2.3 Shear Strength of Bedded Footwall Slopes 16
    2.3.1 Shear Strength of Bedding Joints 17
    2.3.2 Rock Mass Strength of Bedded Slopes 20
3.0 GROUNDWATER AND DRAINAGE 25
  3.1 Water Pressures in Footwall Slopes 25
  3.2 Drainage Measures for Footwall Slopes 28
  3.3 Conclusions 31
4.0 STABILITY ANALYSIS 32
  4.1 Planar Slab Failure 36
  4.2 Bilinear Slab Failure 43
  4.3 Ploughing Slab Failure 50
  4.4 Buckling Failure 59
    4.4.1 Flexural Buckling 59
    4.4.2 Hinge Buckling 64
  4.5 Deep Seated Failure 65
  4.6 Conclusions 66
5.0 ROCK ANCHOR DESIGN 69
  5.1 Shear Strength and Active/Passive Systems 71
  5.2 Design Capacity of Anchor Systems 74
    5.2.1 Steel Tendon Failure 74
    5.2.2 Bond Strength 75

5.2.3 Rock Mass Failure 79

5.3 Anchor Patterns 82

5.4 Conclusions 85

6.0 BEDDED FOOTWALL SLOPES IN WESTERN CANADIAN MOUNTAIN COAL MINES 87

6.1 General Geology 90

6.2 Engineering Geology 92

6.3 Design Studies 96

6.3.1 Smoky River Coal Limited 96

6.3.2 Byron Creek Collieries 108

6.4 Conclusions 113

7.0 DESIGN GUIDELINES 115

REFERENCES 117

APPENDIX A Sensitivity Analysis 122

APPENDIX B Planar Slab Failure Mechanics 131

APPENDIX C Bilinear Slab Failure Mechanics 136

APPENDIX D Ploughing Slab Failure Mechanics 148

APPENDIX E Digital Footwall Modelling 159

APPENDIX F Smoky River Coal Field Study 163

APPENDIX G Byron Creek Collieries Field Study 167

LIST OF TABLES

TABLE PAGE

TABLE 2.1 Approximate Ranges for Basic Friction Angle 5

TABLE 2.2 Unadjusted RMR Parameters 16

TABLE 2.3 Mobilized Dilation Angles (i) 18

TABLE 4.1 Parameters for Factor of Safety Comparison 40

TABLE 4.2 Factor of Safety Comparison Sensitivity Analysis 42

TABLE 4.3 Optimum Anchor Angle Relationships 43

TABLE 4.4 Parameters for Bilinear Slab Analysis 47

TABLE 4.5 Bilinear Slab Sensitivity Analysis 49

TABLE 4.6 Parameters for Ploughing Analysis 55

TABLE 5.1 Properties of High Strength Pre-Stressing Steel Bars (After ASTM.A.722) 70

TABLE 5.2 Properties of Seven Wire Pre-Stressing Steel Strand (after ASTM.A.779) 70

TABLE 5.3 Cement Based Grout versus Polyester Resin Bonding Systems 76

TABLE 5.4 Strength of Polyester Resin With Rock 77

TABLE 5.5 Recommended Anchor Design Safety Factor for Mining Applications 86

TABLE 6.1 Intact Rock Uniaxial Compressive Strength 92

TABLE 6.2 Bedding Joint Strength Parameters 96

TABLE 6.3 Upper East Limb Rock Analysis Slope Parameters 102

TABLE 6.4 Bilinear Slab Failure Sensitivity Analysis in the E-2 Pit (dry slope) 106

TABLE 6.5 Ploughing Failure Sensitivity Analysis in No. 51 Pit (dry slope) 111

LIST OF FIGURES

FIGURE PAGE

FIGURE 2.1 Idealized Rock Joint Load-Displacement Relationships 7

FIGURE 2.2 Rock Joint Strength Envelopes 8

FIGURE 2.3 Roughness Profiles and JRC Ranges 11

FIGURE 2.4 Mobilized Dilation Angles for Rock Slopes..................... 19

FIGURE 2.5 Ladanyi & Archambault's Brickwall Model 22

FIGURE 3.1 Equipotential Distribution in Slopes with Varying Anisotropies 27

FIGURE 3.2 Water Pressures on Bedded Footwall Slopes.................... 29

FIGURE 4.1 Footwall Failure Modes 35

FIGURE 4.2 Planar Slab Failure Forces and Nomenclature.................... 38

FIGURE 4.3 Comparison of Different Factors of Safety 41

FIGURE 4.4 Bilinear Slab Failure Forces and Nomenclature 45

FIGURE 4.5 Bilinear Slab Failure-Influence of Cross Joint.................. 48

FIGURE 4.6 Bilinear Slab Failure-Influence of β and RMR 51

FIGURE 4.7 Bilinear Slab Failure-Influence of Slab Thickness 52

FIGURE 4.8 Ploughing Slab Failure Forces and Nomenclature 54

FIGURE 4.9 Ploughing Failure-Influence of Plough Height.................. 56

FIGURE 4.10 Ploughing Failure-Influence of Ploughing Angle............... 57

FIGURE 4.11 Ploughing Failure-Influence of Slab Thickness 58

FIGURE 4.12 Buckling Failure Modes.. 60

FIGURE 4.13 Euler-Buckling-Influence of Slab Thickness 63

FIGURE 4.14 Deep Seated Failure Mechanics................................ 67

FIGURE 5.1 Dilation and Passive Bolt Reinforcement......................... 73

FIGURE PAGE

FIGURE 5.2 Fixed Anchor Length Design Chart (For FS = 1) 78

FIGURE 5.3 Uplift Capacity Design Chart (For FS = 1) 81

FIGURE 5.4 Anchor Load Distribution (2:1 Rule) 83

FIGURE 5.5 Anchor Spacing Design Charts (for 1 m Slab Thickness 84

FIGURE 6.1 Western Canadian Rocky Mountain Coal Mines Reserve Areas 88

FIGURE 6.2 Coal Measures Stratigraphy of the Western Canadian Rocky Mountains 91

FIGURE 6.3 Bedding Joint Direct Shear Test Results 95

FIGURE 6.4 Smoky River Coal's Upper East Limb Pit 98

FIGURE 6.5 Upper East Limb Pit Failure Back Analysis 101

FIGURE 6.6 Smoky River Coal's E-2 Pit 104

FIGURE 6.7 E-2 Pit Deep Seated Design Chart 107

FIGURE 6.8 Byron Creek Collieries 51 Pit 109

LIST OF SYMBOLS AND ABBREVIATIONS

Distances/Angles

h = slab/block length
$h_1 - h_9$ = miscellaneous lengths (as specified)
h_W = length of water table
h_B = buckling slab length
h_D = driving slab length
h_n = field scale block length
h_o = lab sample scale block length

H = slope height
H_W = water table height
H_P = height of plough discontinuity

T = slab thickness

m = moment arm
$m_1 - m_4$ = miscellaneous moment arms (as specified)

d = groundwater head
d_h = hydrostatic head
d_p = pressure head

α = slope angle/slope dip

β = dip of daylighting surface/dip of critical rock mass failure surface

θ = ploughing angle (with respect to bedding)

ψ = upper slope angle

ω = orientation of σ_1' with respect to failure surface

ε = $90° - \omega$

Strength/Material Properties

τ = shear strength
τ_P = peak
τ_U = ultimate

Strength/Material Properties (continued)

τ_I = intact rock

τ_{RM} = rock mass

C = cohesion C_a = apparent cohesion

C_{RM} = rock mass cohesion

ϕ = friction angle ϕ_P = peak

ϕ_U = ultimate

ϕ_R = residual

ϕ_B = basic

ϕ_J = cross joint

ϕ_{PL} = plough discontinuity

ϕ_i = instantaneous

ϕ_a = apparent

i = dilation angle

σ_c = uniaxial compressive strength σ_{cmass} = rock mass

E = Young's modulus E_{RM} = rock mass

RMR = rock mass rating

γ = total unit weight

γ_w = unit weight of water

a_s = proportion of sheared joint surface

$\dot{v}$ = dilation rate at peak strength

JRC = joint roughness coefficient: subscript o = lab/sample scale

JRC = joint roughness coefficient: subscript n = field scale

Δ = joint shear displacement Δ_P = peak displacement

e = joint normal displacement (dilation)

Strength/Material Properties (continued)

m and s: Hoek-Brown failure criterion material constants: subscript I = intact rock

subscript RM = rock mass

Ω and y: intermediate variables for Hoek-Brown failure criterion

Forces

W = total weight of rock
W_T = weight of toe slab
W_D = weight of driving slab

V = water force
V_T = water force on toe slab
V_D = water force on driving slab

S = shear resistance
S_T = shear resistance of toe slab
S_D = shear resistance of driving slab
S_J = shear resistance of cross joint

N = normal force
N_T = normal force on toe slab
N_D = normal force on driving slab

P = axial force
P_{cr} = critical buckling resistance
P_D = axial force of driving slab

Anchors

Q = anchor load (tension)

δ = anchor installation angle with respect to the horizontal

L_A = anchor length/spacing
L_{AT} = tensioned length
L_{AF} = fixed length
L_{AU} = pull-out length
L_{AH} = horizontal spacing
L_{AV} = vertical spacing

Anchors (continued)

D_D = anchor drillhole diameter

D_A = anchor diameter

A_A = anchor area

τ_{AB} = anchorage bond strength

Stress/Pressure

σ = total stress

σ' = effective stress

σ'_n = effective normal stress

σ'_1 = minor principal effective stress

σ'_3 = major principal effective stress

u = pore pressure

Statistics

X = random variable

x = value of a random variable

μ = mean

σ^2 = variance

SD = standard deviation

E = expectation function

Miscellaneous

FS = factor of safety

FS_A = active

FS_P = passive

FS_{ES} = excess shear

I = moment of inertia

K = Euler buckling constant

k = h_B/h for Euler buckling

1.0 INTRODUCTION

Bedded footwalls form a class of rock slopes where the slope face is excavated parallel to persistent bedding planes. The bedding normally exhibits a dominant control on slope stability. In surface mining, bedded footwalls are common in coal mines where it is desirable to excavate slopes parallel to bedding thus minimizing waste extraction and preventing the undercutting of potentially unstable strata.

1.1 Purpose and Scope

The objectives of the study were to develop a set of guidelines for rational engineering design of bedded footwall slopes. In particular, emphasis was placed on determination of appropriate shear strength parameters, proper consideration for groundwater pressures, and a refinement of available analytical techniques for footwall design. In addition, terms of reference for the project gave special consideration to design of anchor systems for surface mine bedded footwall slopes.

The design and construction of stable rock slopes involves a consideration of the following factors:

i. Engineering Geology
ii. Shear Strength
iii. Stability Analysis
iv. Artificial Support
v. Blasting and Excavation
vi. Monitoring

In this study design methods for bedded footwall slopes are developed with special consideration for points (ii) through (iv). The other factors are discussed with reference to case histories in the mountain coal mines of Western Canada. During the course of the study pertinent technical literature was examined and summarized, stability analysis techniques were reviewed and refined, and site studies at two Western Canadian mountain coal mines were carried out. The stability analysis techniques were applied to back analyze a failed footwall slope and to the design of two other slopes at the two minesite study areas.

Sections 2.0 and 3.0 contain a summary of the available literature on shear strength and groundwater respectively with special reference to the design of bedded footwalls. Section 4.0 describes and examines analytical techniques for limit equilibrium analysis of bedded footwall slopes. In section 5.0 design of anchoring systems for bedded footwalls are considered with an emphasis for those systems applicable to surface mining environments. Section 6.0 exhibits the manner in which rational engineering of bedded footwalls in Western Canadian mountain coal mines can be carried out . Finally, Section 7.0 offers design guidelines for bedded footwall slopes.

2.0 SHEAR STRENGTH

The determination of appropriate strength parameters for rock slopes design is a continuing challenge for the geotechnical engineer. Laboratory testing of rock specimens permits only a glimpse of actual mechanical characteristics mobilized in the field. In addition, in situ testing of rock materials is expensive and logistically very difficult. As a result, pragmatic design relationships to describe mechanical response of engineered rock structures are dominated by empirical criteria.

Engineering solutions to rock mechanics design issues are best dealt with by considering three classes of problems:

i. Persistent through-going discontinuities - Rock Joints
ii. Intact Rock dissected by impersistent discontinuities - Competent Rock Mass
iii. Weak Rock - Incompetent Rock Mass

For the purpose of this report the distinction between classes 2 and 3 above is arbitrarily made at a rock mass rating (RMR [19]) of 40. Engineering problems in weak rocks (eg. clay-shales) are normally dealt with by incorporating soil mechanics principles and this class of problems is not considered further here.

Shear strength parameters for rock slopes are calculated in terms of effective stress (σ') according to the well established relationship [1]:

$$\sigma' = \sigma - u \tag{2.1}$$

Where: σ = total stress

u = pore pressure

On a fundamental level and with special consideration for rock mechanics problems equation 2.1 involves the following assumptions:

i. The pore fluid must be inert.

ii. There must be a fully connected pore space such that the pore pressure is transmitted to the rock fabric.

iii. The rock matrix is incompressible.

In most cases these are reasonable assumptions for rock slope engineering problems and further use is made of equation 2.1 without reference to these assumptions.

2.1 Rock Joint Shear Strength

The shear strength (τ) of smooth, non-dilatant rock joints is a function of the friction angle of the rock material (ϕ) and the applied normal effective stress (σ_n'). For continuous joints, cohesion is normally assumed negligible and the shear strength is expressed as:

$$\tau = \sigma_n' \tan \phi \tag{2.2}$$

Equation 2.2 is the well known Mohr-Coulomb linear strength envelope. The smooth friction angle is an intrinsic property of the rock surface and can be measured in the laboratory from direct shear tests [3] or tilt table tests [4]. The terminology concerning the non-dilatant or smooth friction angle in the literature is somewhat confusing as the terms basic friction angle (ϕ_B) ultimate friction angle (ϕ_U), and residual friction angle (ϕ_R) are variously used without proper distinction. Strictly speaking, the basic friction angle is measured from a smooth saw cut laboratory specimen. Krahn [5] has shown that ϕ_B for the same rock varies according to the microscopic surface roughness. For this reason Krahn recommends using the term ultimate friction angle (ϕ_U) to describe non-dilatant frictional resistance on the actual surface under consideration. Several workers use the term residual friction angle (ϕ_R) to describe non-dilatant rock joint behaviour. In soil mechanics, ϕ_R is used to describe large strain post peak resistance which is independent of previous displacement history and dependent only upon grain size and mineralogy. In general, it is preferable to use the term ultimate friction angle to describe the non-dilatant friction angle properties of actual rock surfaces.

Table 2.1 shows typical values of basic friction angle (ϕ_B) derived from the literature for various rock types (after Hoek and Bray, [4]).

Table 2.1 Approximate Ranges for Basic Friction Angle

Lithology	ϕ_B (degrees)
Basalt	31 – 38
Conglomerate	35 – 40
Limestone	33 – 40
Sandstone	25 – 40
Shale	23 – 28
Granite	29 – 35

Krahn [5] back-analyzed 25 hard-rock slope failures and found that the mobilized friction angle corresponding to a factor of safety of unity was generally in the range of 25° - 35° (assuming zero cohesion). This corresponds to the general range of basic friction angles in Table 2.1 and thus the basic friction angle forms a useful first estimate of rock joint shearing resistance. Note however that this approach may not always yield conservative results if weathering or previous sliding has taken place. Hassani and Scoble [6] tested several hundred coal measures rocks under wet and dry conditions and found a percentage reduction of up to 10% (average of 5%) between the dry and saturated basic friction angles.

Following the pioneering work of Patton [7], Barton [8], Ladanyi [9], and others it is well recognized that the peak shearing behaviour along rock joints is markedly dilatant owing to the irregular surfaces of actual discontinuities. The peak friction angle (ϕ_P) of such real rock joints is expressed as:

$$\phi_P = \phi_U + i \tag{2.3}$$

The dilation angle (i) is comprised of an asperity failure component and a geometrical component. With reference to Figure 2.1, as a rough rock joint is sheared under conditions of constant normal stress dilation begins after the intrinsic friction (ϕ_U) has been fully mobilized. Maximum dilation occurs just at the point of peak shearing resistance as the opposing joint surfaces ride over the "critical" asperities. Peak strength (τ_P) is often accompanied by crushing of the asperities. Following peak strength, shearing resistance drops rapidly to a lower ultimate strength (τ_U) value representing the non-dilatant strength.

For perfectly rigid material the strength envelope of rough rock joints would be bilinear. Due to gradual crushing of asperities the envelope is actually curvilinear as shown in Figure 2.2. In practice, three different approaches to represent peak strength envelopes have been adopted.

The first approach is to approximate the strength envelope over the stress range of interest as:

$$\tau_P = C_a + \sigma_n' \tan \phi_a \tag{2.4}$$

Where C_a is the apparent cohesion and (ϕ_a) is the apparent friction angle. Equation 2.4 is valid only over the design stress range and is applicable where testing has been carried out at the appropriate scale or where back analyses are available.

The second approach is to approximate laboratory data with a best fit power curve [10] of the form:

$$\tau_P = A\,\sigma_n^B \tag{2.5}$$

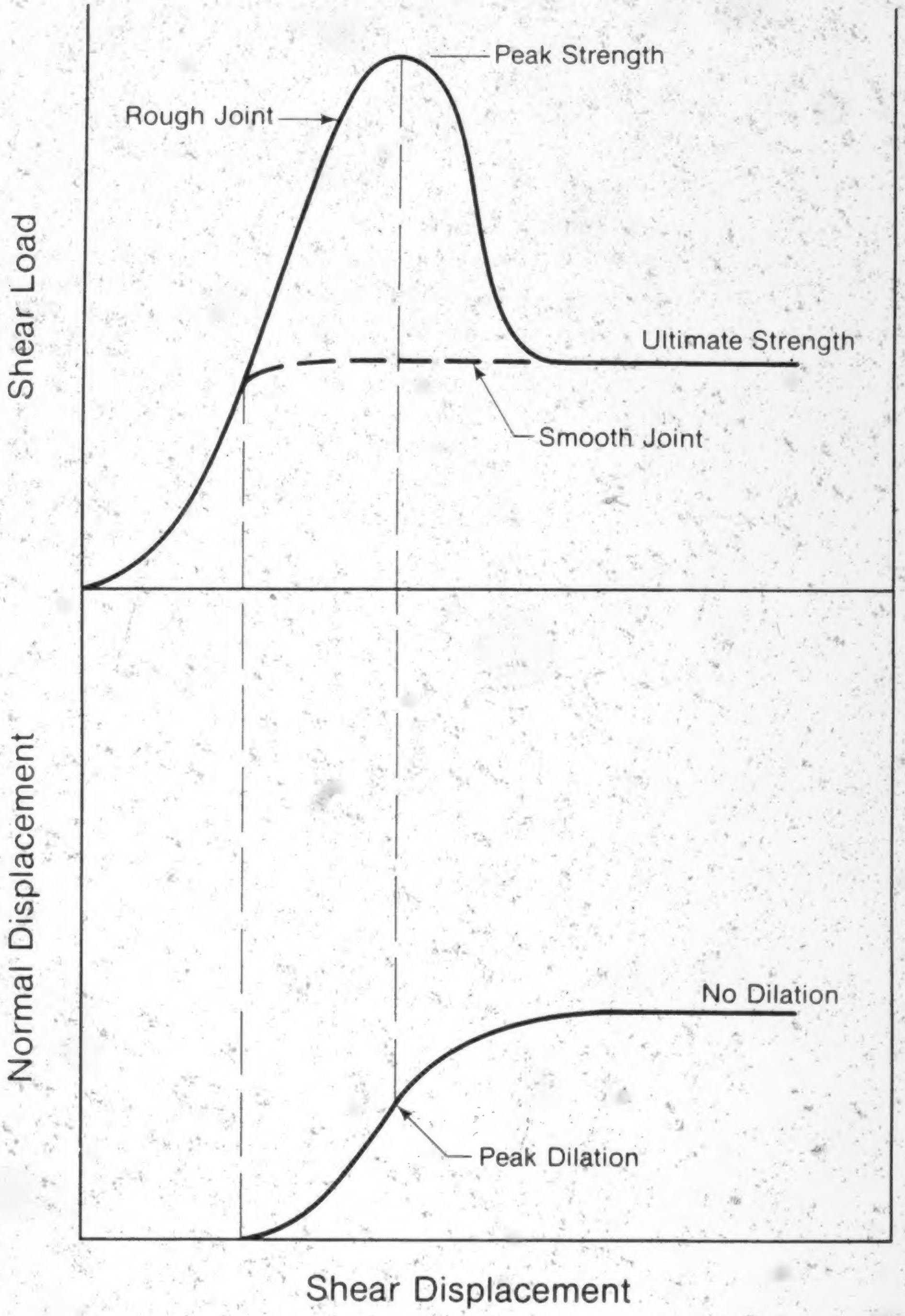

Figure 2.1 Idealized Rock Joint Load-Displacement Relationships

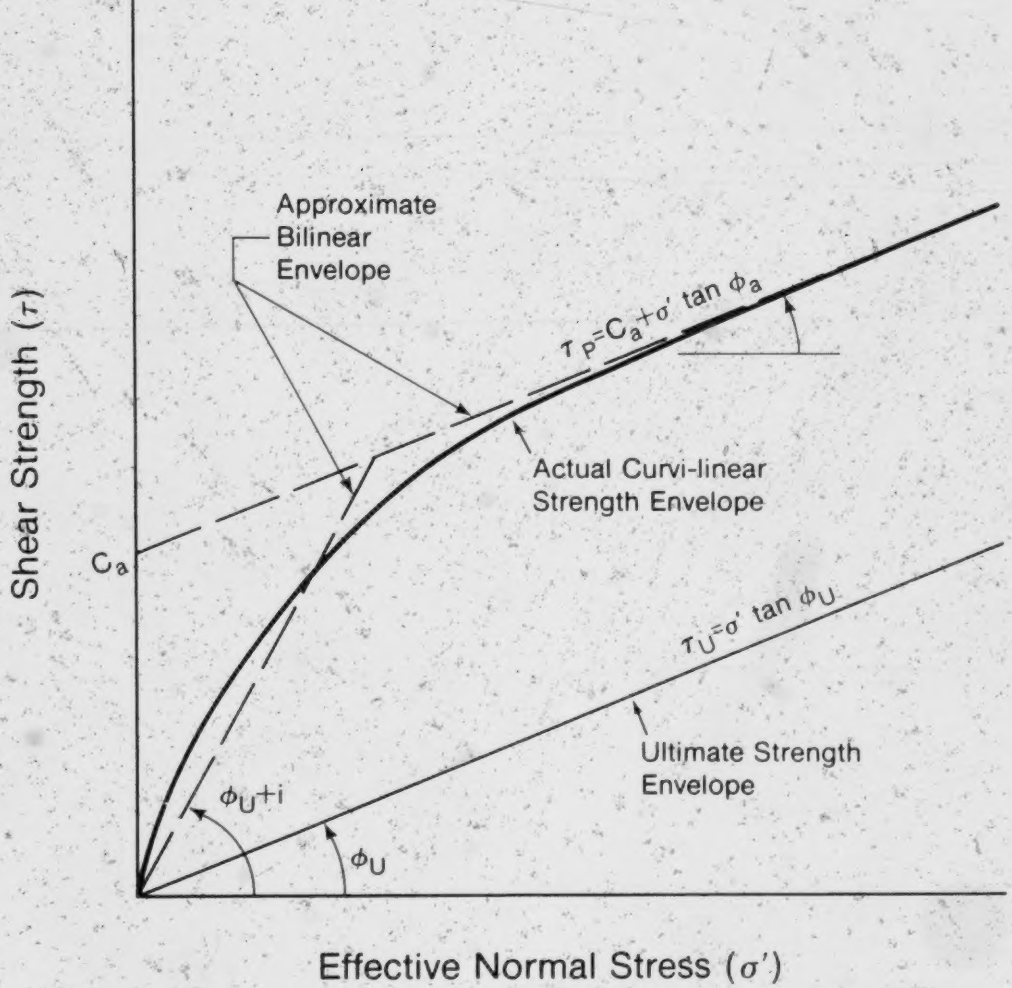
Shear Strength (τ)
Approximate
Bilinear
Envelope
$\tau_P = C_a + \sigma' \tan \phi_a$
Actual Curvi-linear
Strength Envelope
C_a
$\tau_U = \sigma' \tan \phi_U$
Ultimate Strength
Envelope
$\phi_U + i$
ϕ_U
Effective Normal Stress (σ')

Figure 2.2 Rock Joint Strength Envelopes

A and B are curve fitted constants. These constants have no physical meaning and the form of the envelope is very sensitive to small differences in B. Most importantly, scale effects are difficult to rationalize with this approach.

The last approach is to use empirical relationships to estimate peak rock joint shearing resistance (τ_P). The most popular empirical formulations are those of Ladanyi and Archambault [9] and Barton [8]. Ladanyi and Archambault developed their shear strength criteria relationships on theoretical grounds following the work of Rowe [59] on stress dilatancy and energy components of dense sand.

$$\tau_P = \frac{\sigma_n' (1 - a_s)\left(\dot{v} + \tan \phi_u\right) + a_s \cdot \tau_I}{1 - (1 - a_s)\,\dot{v} \tan \phi_u} \qquad (2.6)$$

Where: a_s = proportion of discontinuity surface sheared through projections of intact rock material

$\dot{v}$ = dilation rate at peak shear strength

τ_I = shear strength of intact rock material

The values a_s and $\dot{v}$ are very difficult to determine and therefore Ladanyi and Archambault developed empirical relationships for these values. Any suitable shear strength relationship may be substituted for the intact rock strength (τ_I). For very low normal stresses a_s approaches zero and τ_P approaches $\sigma'_n \tan(\phi_u + i)$. At very high normal stresses a_s approaches 1 and τ_P approaches τ_I.

Barton's empirical peak strength formula was developed from phenomenological behaviour:

$$\tau_P = \sigma_n' \tan\left[\phi_U + \text{JRC} \log\left(\frac{\text{JCS}}{\sigma_n'}\right)\right] \qquad (2.7)$$

Where: JRC = Joint Roughness Coefficient

JCS = Joint Compressive Strength

Barton's JRC values for natural rock joints vary between 0 and 20. Figure 2.3 shows typical roughness profiles which the engineer can use as a guide in determining design values. Tse and Cruden [12] have correlated the standard profiles with surface parameters used by mechanical engineers to describe the finish on milled metallic surfaces.

Barton advocates determining JRC values from tilt tests on actual rock blocks in the field. Equation 2.7 and simple statics are combined to solve for the JRC parameter as follows:

$$\mathrm{JRC} = \frac{\alpha - \phi_U}{\log\left(\frac{\mathrm{JCS}}{\sigma_n'}\right)} \tag{2.8}$$

Where: α = joint plane dip at onset of sliding

σ_n' = effective normal stress

In direct contrast to the Ladanyi and Archambault equation, Barton's formula predicts that τ_P approaches τ_U at very high normal stress. The reason for this apparent contradiction is that Barton's JCS is normally taken to be the joint wall uniaxial compressive strength, a reasonable assumption for most rock slope situations where little confining pressure resisting joint asperity crushing is apparent. In fact, Barton recommends that at high normal loads (as σ_n' approaches σ_c) the JCS term be replaced by the differential stress ($\sigma_1 - \sigma_3$) necessary to cause failure.

Following Barton's work, Bandis et al. [13] conducted an intensive investigation into the scale effects of rock joint shear behaviour. This very revealing study, based on several model prototype replicas and actual joint surfaces, resulted in several important findings and very clearly demonstrates the importance of scale effect on peak shear behaviour.

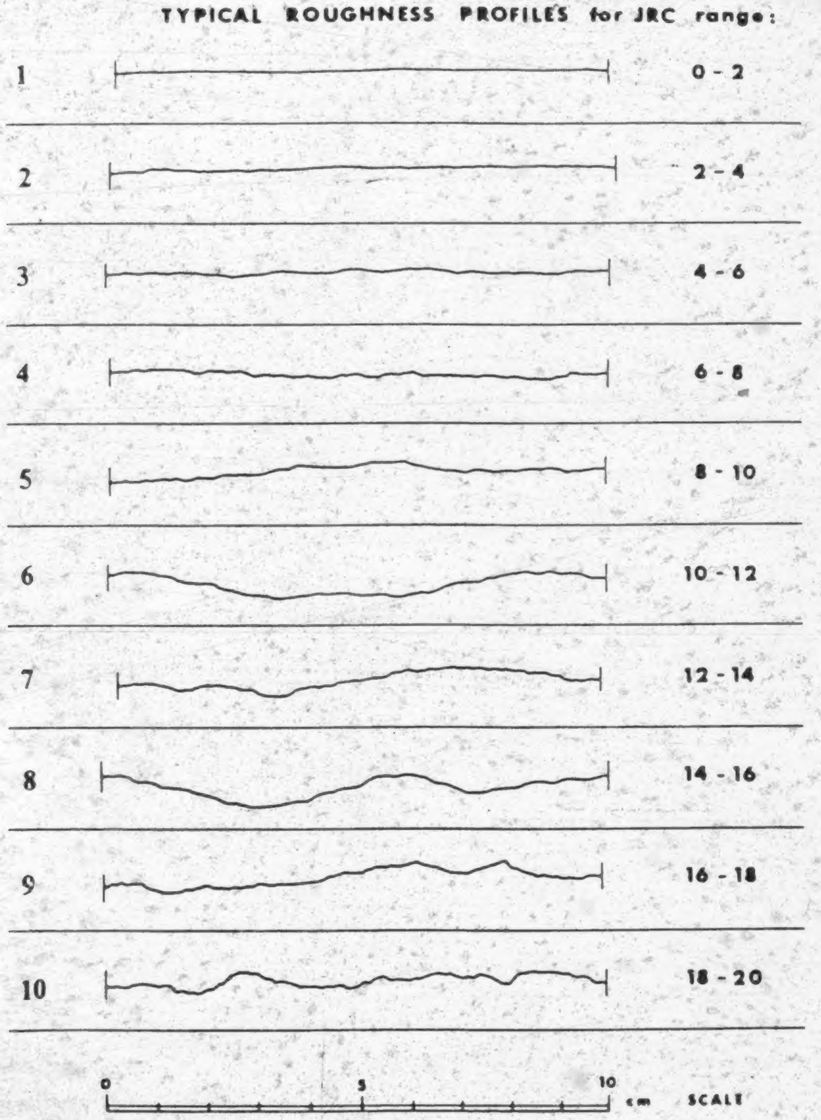
TYPICAL ROUGHNESS PROFILES for JRC range:
1
0 - 2
2
2 - 4
3
4 - 6
4
6 - 8
5
8 - 10
6
10 - 12
7
12 - 14
8
14 - 16
9
16 - 18
10
18 - 20
0
5
10
cm
SCALE

Figure 2.3 Roughness Profiles and JRC Ranges (after Barton [11])

> *"Peak shear displacement is effectively a measure of the distance a joint has to travel until effective contact is made between the asperities controlling its peak resistance. The displacement scale effect clearly implies that under the same level of normal stress the peak behaviour of different joint lengths is controlled by irregularities of different size or base length."*

The above quotation from the Bandis paper succinctly points out the influence of base length or block size on peak shearing resistance. Earlier work by Rengers [14] showed how the dilation angle decreased with increasing base length on a rough surface and Bandis' more recent work extended these concepts while also incorporating the asperity failure component of dilation. Important findings from Bandis' study and in subsequent publications by Barton [15, 16] are summarized below:

i. The roughness angle is controlled by the natural block size determined by cross jointing. These blocks have sufficient freedom to rotate and "feel" the smaller steeper asperities. Beyond the natural block size deviations from planarity or waviness may be treated as an increase or decrease in slope dip.

ii. Increased block size increases displacement at peak shear strength (Δ_P), reduces JRC, and reduces JCS.

iii. The peak shear displacement (Δ_P) can be estimated by the following empirical relationship:

$$\Delta_P = \frac{L}{500}\left(\frac{JRC}{h}\right)^{0.33} \tag{2.9}$$

Where h = block length (in meters)

As a rule of thumb Δ_P is approximately 1% of the block or sample size.

iv. Field JRC and JCS values can be estimated from laboratory values by the following empirical relationships

$$JRC_n = JRC_o\left(\frac{h_n}{h_o}\right)^{-0.02\ JRC_o} \tag{2.10}$$

$$JCS_n = JCS_o \left(\frac{h_n}{h_o}\right)^{-0.03\ JRC_o} \qquad (2.11)$$

Where: 'n' subscript = field scale

'o' subscript = lab scale

v. Average base length of critical asperities was estimated to be 4% of block size.

2.2 Rock Mass Shear Strength

Determining the shear strength of a regularly jointed rock mass is a more difficult task than the shear strength of a well defined through-going rock joint. In ideal terms, in order to fully describe rock joint shear strength the following information would be required:

i. Detailed knowledge of rock joint geometry

ii. Ability to integrate the geometry into a model describing the collective mechanics of individual rock blocks.

iii. The extent to which individual blocks are crushed and sheared at edges and corners.

If these parameters were fully understood and providing that the associated field information could be readily obtained, then failure criteria such as the stress dilatancy relationship proposed by Ladanyi and Archambault [9] discussed with respect to rock joints in the previous section, might be appropriate. However, this level of mechanical characterization and understanding is not available. Thus purely empirical criteria, particularly the Hoek-Brown failure criterion, dominate practical solutions for rock mass shear strength determination.

Hoek and Brown [11] have proposed the following relationship for defining rock mass strength:

$$\sigma_1' = \sigma_3' + \sqrt{m\,\sigma_c\,\sigma_3' + s\sigma_c^2} \tag{2.12}$$

Where: σ_1' = major principal effective stress at failure

σ_3' = minor principal effective stress at failure

σ_c = uniaxial compressive strength of intact rock

m and s are material constants

For intact rock s = 1 and the intact m (m_I) coefficient has typical values as shown below from Hoek and Brown [17]:

i. Carbonate rocks with well developed crystal cleavage (dolomite, limestone, and marble); $m_I = 7$.

ii. Lithified arenaceous rocks (mudstone, shale and slate; normal to cleavage); $m_I = 10$

iii. Arenaceous rocks with strong crystals and poorly developed crystal cleavage (sandstone and quartzite); $m_I = 15$

iv. Fine grained polymnerallic igneous crystalline rocks (andesite, dolerite, diabase and rhyolite); $m_I = 17$

v. Coarse grained polymnerallic igneous and metamorphic rocks (amphibilite, gabbro, gneiss, granite, norite and granodiorite); $m_I = 25$.

The uniaxial compressive strength of the rock mass (σ_{cmass}) is determined by substitution of $\sigma_3' = 0$ into equation 2.12:

$$\sigma_{c\ mass} = \sqrt{s}\,\sigma_c \tag{2.13}$$

For rock slope problems it is more convenient to express failure criterion in terms of the shear strength (τ). Following Hoek and Brown [18]:

$$\tau = \left(\cot\phi_i - \cos\phi_i\right)\frac{m\sigma_c}{8} \tag{2.14}$$

Where: $\phi_i = \arctan\left(\frac{1}{\sqrt{4y\cos^2\Omega - 1}}\right)$

$$\Omega = 1/3\left[90 + \arctan\left(\frac{1}{\sqrt{y^3 - 1}}\right)\right]$$

$$y = 1 + \frac{16\, m\sigma_n' + s\,\sigma_c}{3\, m^2\, \sigma_c}$$

Equations 2.12 and 2.14 represent the strength of intact rock, for s = 1 or the strength of a regularly jointed rock mass, for $0 \geq s < 1$. Strictly speaking, these equations are valid only when the rock mass can be considered to exhibit strength isotropy. For the case of an anisotropic rock mass the values of the material constants (m and s) vary with the principal stress directions relative to joint set orientations. Hoek and Brown show that it is valid to treat the rock mass as being isotropic when dissected by four or more discontinuity sets of approximately equal strength.

Field values of m and s are difficult to determine without extensive very large scale triaxial testing. Hoek and Brown [18] have proposed further empirical relationships relating peak strength m and s values to the value of Bieniawski's [19] rock mass rating (RMR) system. For disturbed rock masses the following expressions are suggested.

$$m = m_I \exp\left(\frac{RMR - 100}{14}\right) \qquad s = \exp\left(\frac{RMR - 100}{6}\right) \tag{2.15}$$

For peak strength of undisturbed or interlocked rock masses, slightly higher m and s values are recommended:

$$m = m_I \exp\left(\frac{RMR - 100}{28}\right) \qquad s = \exp\left(\frac{RMR - 100}{9}\right) \tag{2.16}$$

In general, equations 2.15 are recommended for rock slope design and equations 2.16 are recommended for tunnel design where disturbance is minimized.

The RMR values to be used in equations 2.15 and 2.16 are the so-called unadjusted RMR values. The unadjusted RMR incorporates five basic parameters which are easily obtained from field mapping data and simple tests. Table 2.13 summarizes these parameters and shows the allowable ranges that may be assigned to each.

Table 2.2 Unadjusted RMR Parameters

Parameter	RMR Range	Comment
1. Intact Rock Strength	0 - 15	• Estimate from point load or Schmidt hammer index tests
2. Rock Quality Designation	0 - 20	• From drillcore or scan-line surveys
3. Discontinuity Spacing	5 - 20	• Spacing of "controlling set" most appropriate
4. Joint Condition	0 - 30	• Incorporates continuity and infilling
5. Groundwater	0 - 15	• Use 10 - 15 for analyses incorporating effective stress

NOTE: See Charts A - E in Bieniawski, 1989 [19] for rating guidelines.

The adjusted RMR incorporates a sixth parameter, joint orientation. Romana [20] has proposed a modified joint adjustment rating for rock slope design. When the limit equilibrium method incorporates joint orientation the joint adjustment rating is not required and thus it is not used in this study.

2.3 Shear Strength of Bedded Footwall Slopes

Most bedded rock slopes can be described by orthogonal joint system models [21]. Such a model consists of 3 orthogonally oriented joint sets. For rational design purposes joint system models should recognize the natural variation inherent to the orientation, persistence, and joint spacing within each joint set. Within the context of an orthogonal joint system model, bedded footwall slopes exhibit persistent bedding joints dissected by two mutually orthogonal impersistent cross joints. For design purposes the bedding joints can normally be expected to be completely pervasive at the scale of most rock slopes, especially where bedding joints at lithological contacts are being considered. Cross joints terminate at bedding joints, often within one or two bedding joint spacings. On the basis of such a bedded footwall orthogonal model, selection of suitable shear strength criteria involves consideration of sliding along persistent bedding joints (Section 2.1) and shear surfaces developed through the rock mass (Section 2.2).

2.3.1 Shear Strength of Bedding Joints

The very nature of bedding joint genesis suggests a fairly uniform process whereby bedding joint surfaces are fairly smooth. Thus dilation angles to be incorporated into shear strength formulations, such as those in equations 2.3, 2.6 and 2.7 would be expected to be fairly low. Table 2.3 shows some mobilized rock joint dilation angles extracted from the literature based on back analysis of sliding and evaluation of ϕ_U.

Table 2.3 Mobilized Dilation Angles (i)

Joint Description	Calculated Value	Estimated σ_n'
1. Precambrian gneiss foliation shears, Sri Lanka [22]	3°	50 - 75 kPa
2. Limestone bedding joints, China [22]	2 - 3°	NA
3. Limestone fault plane, China [22]	5°	NA
4. Sandstone Bedding, Australia [23]	2°	410 kPa
5. Shale Bedding, Australia [23]	2°	240 kPa
6. Claystone Bedding, Australia [23]	4°	220 kPa
7. Mudstone Bedding, Australia [23]	4°	450 kPa
8. Siltstone, Canada [24]	5°	20 kPa
9. Shale, South Africa [25]	5°	NA
10. Sandstone, Canada [26]	2 - 4°	NA

NOTE: Case histories for i = 0 have not been included.

All the case histories in Table 2.3 show instabilities occurred at normal stress (σ_n') below 500 kPa, an observation confirmed by Denby et al. [10] while studying rock slope case histories in British coal mines. In addition, calculated dilation angles lie within the 2° to 5° range. Figure 2.4 shows results from Table 2.3 plotted alongside estimated i values calculated from Barton's shear strength equation:

$$i = JRC \log\left(\frac{JCS}{\sigma_n'}\right) \qquad (2.17)$$

Where: JRC = 1 and 2

JCS = 60 MPa (reasonable average for sedimentary rock)

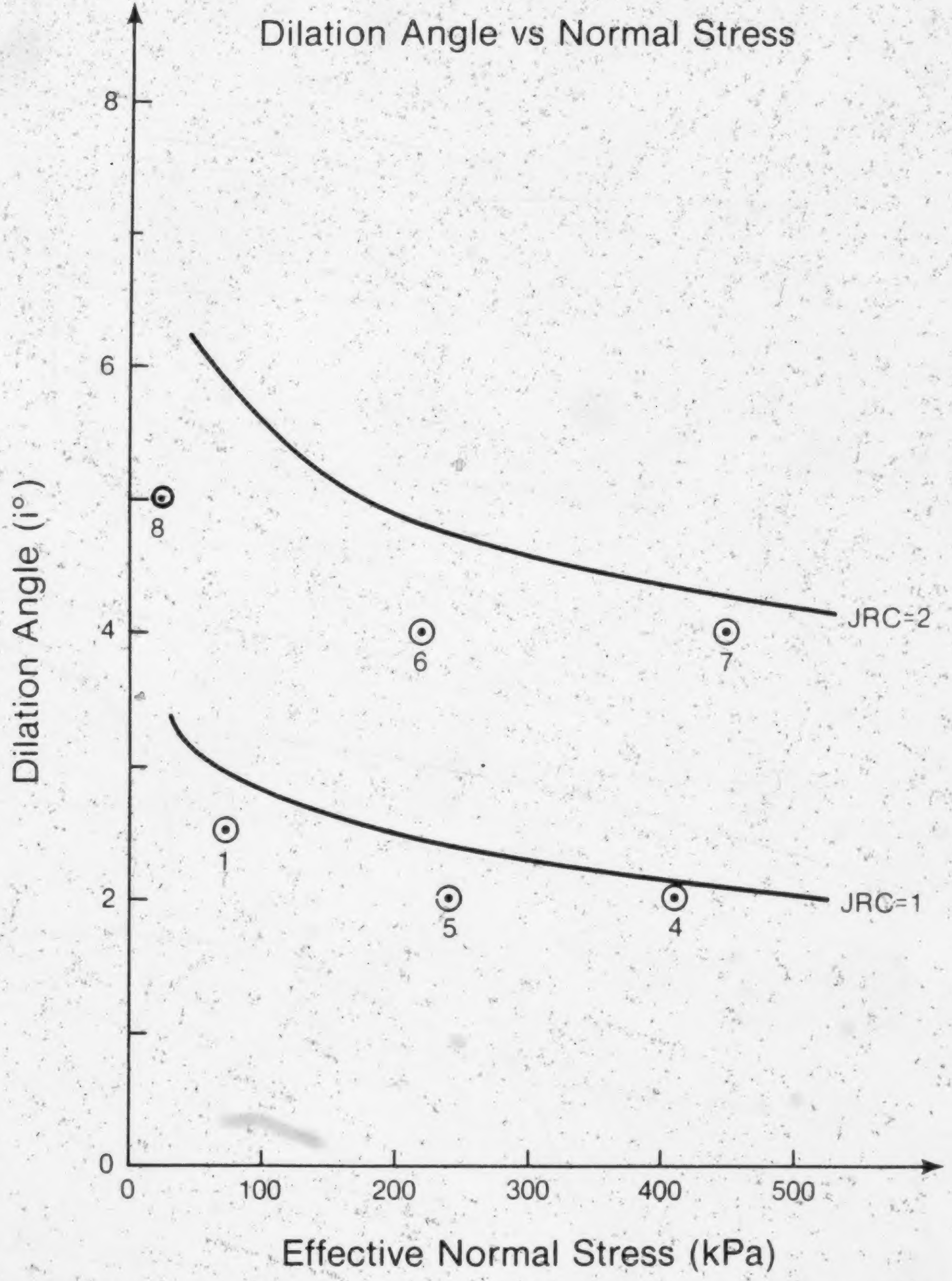

Figure 2.4 **Mobilized Dilation Angles for Rock Slopes (see Table 2.4)**

Although the data comprising Table 2.3 is rather limited, Figure 2.4 follows the previously stated intuitive reasoning that bedded joints exhibit low roughness values. In fact, it would seem that for bedding planes slope design purposes JRC values between 0 and 2 are suitable.

For this study, surface modelling of a steeply dipping siltstone bedding plane was conducted at Byron Creek Collieries, Sparwood, B.C. The modelling was carried out incorporating digital photogrammetric techniques provided by Douglas Curran of Prometric Technologies Inc. from Calgary, Alberta. The modelling was done at two different scales in order to examine small scale roughness and large scale waviness. Plan views normal to average bedding dip and representative profiles for the detailed 1 m and large scale 4.8 m grid are shown in Appendix E. Examination of the profiles shows that the small scale roughness is fairly smooth and that the large scale upslope and downslope waviness angles almost cancel each other out.

Following the above discussion the following design recommendations are made with respect to shear strength parameters of bedding joints on footwall slopes:

i. Bedding joints on footwall slopes normally dominate shear strength considerations and can usually be considered all pervasive at the scale of most design slopes.
ii. Mobilized dilation angles normally lie within the 0 - 5° range under conditions of normal stress normally of interest in rock slope design (100 to 500 kPa).
iii. Corresponding JRC values for use in curvilinear strength approximations appear to be within the 0 to 2 range for most situations.

2.3.2 Rock Mass Strength of Bedded Slopes

The most critical failure modes on bedded footwall slopes involves sliding along the persistent bedding joints or other through-going discontinuities such as fault planes.

However, if the bedding has not been undercut and if unfavorably oriented faults or joints do not exist, then the critical failure mode may involve shearing through the rock mass at the toe of the slope followed by sliding along bedding updip of the sheared area (see Bilinear Failure in Section 4.2). In this case it is necessary to evaluate the rock mass shear strength.

Hoek and Brown's rock mass shear strength criteria discussed in Section 2.2 is strictly only valid for isotropic rock masses; a rock mass can be considered isotropic when dissected by four or more discontinuity sets of approximately equal strength. Hoek, in his 1983 Rankine lecture [27], reviewed some brickwall test model results by Ladanyi and Archambault [28]. With reference to Figure 2.5, it is worthwhile to review Hoek's discussion in order to justify selection of rational design criteria for rock mass strength in bedded footwall slopes. Figure 2.5.A shows the configuration of the brickwall model tested by Ladanyi and Archambault. The model consists of primary through-going joints dissected by impersistent orthogonal cross joints and thus, without consideration for natural joint orientation scatter, fairly represents the orthogonal bedded footwall discussed with reference to this study. The model is quite obviously highly anisotropic with respect to variations in shear strength with principal stress direction. Hoek estimated the shear strength envelopes of the primary joints, cross joints, and the intact material as shown in Figure 2.5.B. The strength of the model is expected to vary between that of the primary joints and the intact material depending upon model orientation with respect to the principal stress direction. On theoretical grounds the axial strength $\left(\sigma_1'\right)$ of the brickwall model can be calculated from joint inclinations with respect to principal stress direction and the intact rock/discontinuity strength envelopes (Hoek and Brown [17]). Figure 2.5.C shows the predicted strength results; regions of failure through the intact rock, cross joints, and primary joints are clearly delineated. The actual model strength is shown in Figure 2.5.D as observed from Ladanyi's and Archambault's

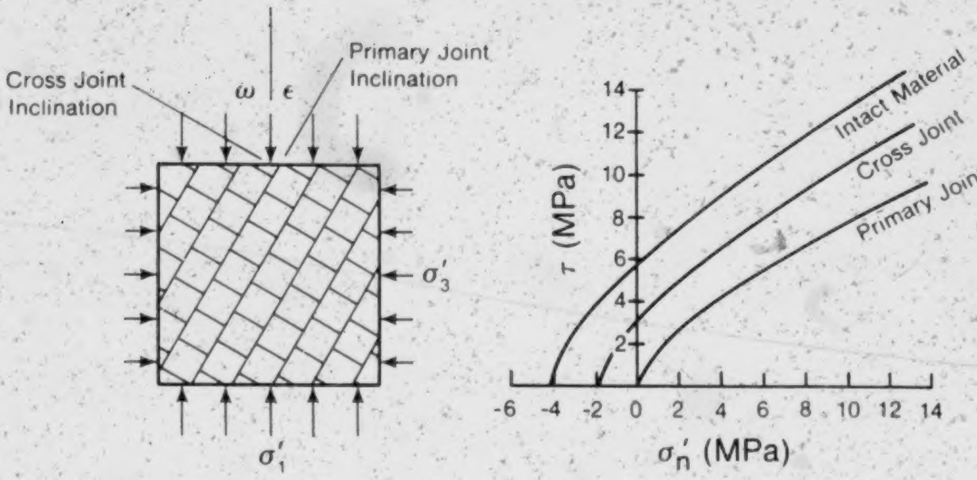
Primary Joint Inclination
Cross Joint Inclination
ω
ϵ
σ'3
σ'1
Intact Material
Cross Joint
Primary Joint
τ (MPa)
14
12
10
8
6
4
2
-6
-4
-2
0
2
4
6
8
10
12
14
σ'n (MPa)

A) Configuration of Brickwall

B) Brickwall Model Failure Envelopes

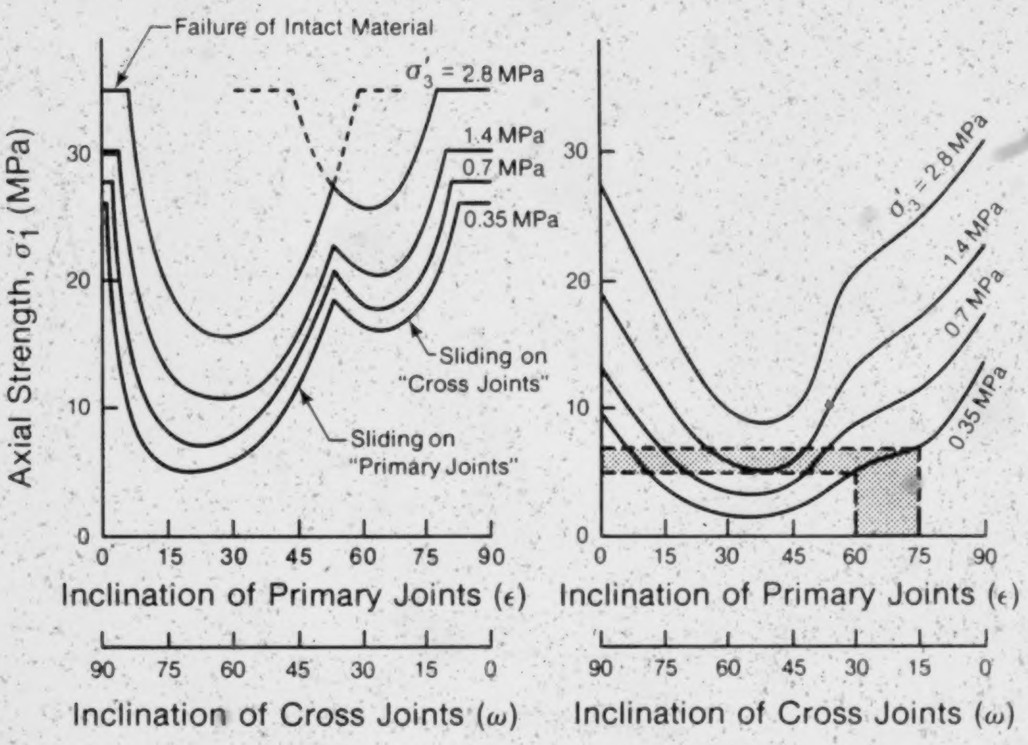

C) Predicted Model Strength

D) Observed Model Strength

Figure 2.5 **Ladanyi & Archambault's Brickwall Model (after Hoek [27])**

test results. A comparison of the predicted and observed test results leads to the following conclusions:

i. There is a general similarity between the form of the predicted and observed model strengths.

ii. Observed strengths are generally lower than predicted and this was attributed to rotation/crushing of individual blocks. The intact rock strength is not achieved even at the most favorable orientation.

On a footwall slope the maximum principal stress is approximately parallel to the slope face and hence parallel to bedding. The minor principal stress for shallow slab failures can be assumed to be zero. If unfavorably oriented discontinuities do not daylight out of the slope then failure can only occur through the rock mass. An approximation of the orientation angle of the slip surface (ω) with respect to the principal stress axis is derived from:

$$\omega = 45 - \frac{\phi_i}{2} \tag{2.18}$$

Where ϕ_i = instantaneous friction angle.

For most rock masses the friction angle varies from 30 - 50° and thus ω\` can be expected to be between 20 and 30°. Figure 2.6.D shows that at the lowest confined stress $\left(\sigma_3' = 0.35 \text{ MPa}\right)$ the axial strength is "reasonably" constant over the range ω = 20 - 30°. In addition, the 20 - 30° range of ω values represents the average strength of the model. Thus, as long as the critical failure surface is found, with due regard for slope kinematics, then an estimate of rock mass strength for failure through the slope toe can be made from the Hoek-Brown isotropic rock mass failure criterion.

In conclusion, the following design suggestions are offered with respect to rock mass strength in bedded footwall slopes:

i. Hoek-Brown failure criterion can be used to search for the critical failure surface with regard for overall slope kinematics.

ii. An estimate of the m and s values required for rock mass strength determination can be made from laboratory or otherwise representative values of intact σ_c and m_I and an assessment of Rock Mass Rating through equation 2.16.

3.0 GROUNDWATER AND DRAINAGE

Groundwater flow through rock is controlled by the discontinuities, as the permeability of fractures and fissures is generally several orders of magnitude greater than the intact rock. Seepage and drainage characteristics are complex and governed by the following factors:

i. Orientation, spacing, roughness, and continuity of the rock joints.

ii. Effective stress versus permeability relationships of the rock mass. Most hard rock slopes are considered free draining and thus excess pore pressures due to loading/ unloading effects are not normally considered. However, a change in loading conditions will result in dilation/contraction of the jointed mass and a consummate change in permeability. Rock slopes are particularly sensitive to large changes in permeability with unloading.

iii. Recharge/discharge boundary conditions. The groundwater boundary conditions of rock slopes are complex and affected by climatic conditions, runoff and infiltration characteristics.

Mechanics and measurement of hydraulic properties through rock masses are covered by Sharp et al. [29]. Hoek and Bray [4], and in the Pit Slope Manual [2]. More recently Barton et al. [16] have studied hydraulic conductivity of rock joints. Numerical techniques incorporating finite element code are very popular and provide a useful basis for preliminary design.

3.1 Water Pressures in Footwall Slopes

Groundwater has an adverse effect on the stability of rock slopes by reducing effective stress and to a lesser extent by softening of the rock materials. The latter effect is more pronounced in rocks containing clay minerals and can be taken into account by utilizing saturated ϕ_U and σ_c values in shear strength formulations. Time effects of softening processes are normally considered negligible for hard rock slopes.

The unstabilizing effect of groundwater is directly related to the pore pressure through equation 2.1:

$$\sigma' = \sigma - u \qquad 2.1$$

For isotropic and homogeneous material the steady state pore pressure is independent of permeability and controlled only by boundary conditions. In anisotropic and non-homogeneous materials, such as bedded rocks, the spatial and directional permeability variations will have a significant influence on pore pressures. Figure 3.1, after Hoek and Bray [4], demonstrates the effect of different permeability configurations on the phreatic surface and on the distribution of equipotentials. For both Figure 3.1.A (isotropic permeability) and Figure 3.1.B (maximum permeability in the horizontal direction) an assumption of a hydrostatic pressure profile results in conservative pore pressure predictions. However, where the permeability is markedly higher parallel to the slope face (Figure 3.1.C) an assumption of hydrostatic pressure is grossly unconservative.

Figure 3.1.C shows an increase in head of about 270% between the hydrostatic head (d_h) and the pressure head (d_p) at Point A. Robert et al [30] examined theoretical pressure distributions in different topographic and geologic situations using finite element methods. They computed a pressure head difference of 30 m on a hypothetical failure plane located on a mountain dip slope (305 m high) between an assumption of horizontal to slope-parallel anisotropy [10 (maximum) : 1 (minimum) hydraulic aniotropy]. Serious errors in stability analysis can result by not properly accounting for seepage anisotropy on bedded footwall slopes.

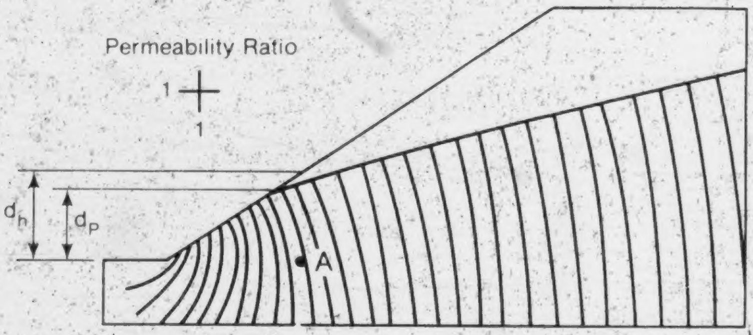
Permeability Ratio
1
1
d_h
d_p
A

A) Isotropic Rock Slope

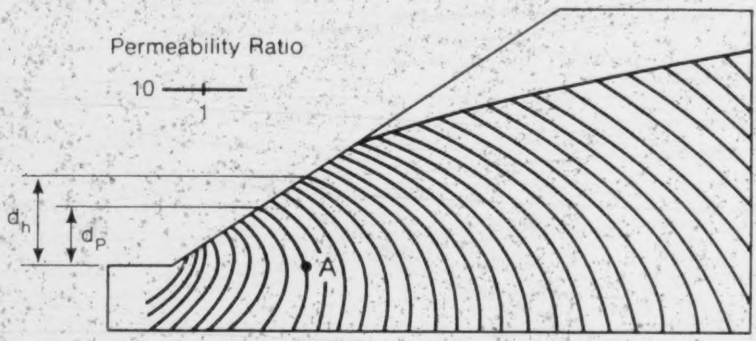
Permeability Ratio
10
1
d_h
d_p
A

B) Anisotropic Rock Mass — Horizontally Bedded Strata

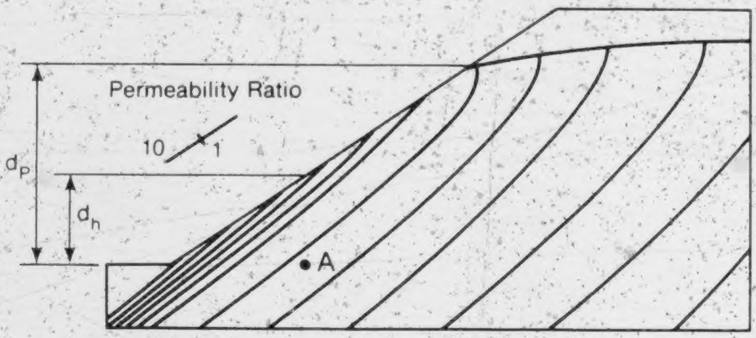
Permeability Ratio
10
1
d_p
d_h
A

C) Anistropic Rock Mass — Strata Dipping Parallel to Slope

d_h = Hydrostatic Head

d_p = Pressure Head

Figure 3.1 **Equipotential Distribution in Slopes with Varying Anisotropies (after Hoek and Bray [4])**

Figure 3.2 shows a typical footwall situation in an open pit. This figure shows a potential failure plane, ABC, and a water table (phreatic surface) developing a seepage face on the footwall slope. For such a situation the pore pressure at A and C is clearly zero and a knowledge of the pore pressure at B (u_B) would allow for a reasonable estimate of the water pressure distribution and hence the estimation of water forces (V), along AB and BC. Therefore, assuming linear pressure distributions:

$$V_{AB} = \frac{\overline{AB}\, u_B}{2} \qquad V_{BC} = \frac{\overline{BC}\, u_B}{2} \tag{3.1}$$

Where $\overline{AB}$ and $\overline{BC}$ are distances along AB and BC

The pore pressure at B is seldom known very precisely but is best calculated from a down-dip sealed piezometer located within the same stratum. In this case the pore pressure at B would be estimated as:

$$u_B = \gamma_w D_{P2} \tag{3.2}$$

Note that an estimate of u_B using the hydrostatic head, d_h, is not reasonable as a large head loss does not occur along AB due to higher permeability parallel to bedding.

Patton [31] demonstrates how small variations in geology can lead to very significant and unexpected water pressure profiles. Multiple piezometers are necessary to monitor permeability contrasts between stratigraphic units. In addition, piezometers are necessary to record seasonal variations and sudden changes due to storm events.

3.2 Drainage Measures for Footwall Slopes

Drainage measures for rock slopes include horizontal drains, vertical wells, drainage galleries, and drainage trenches constructed down or along the slope. For

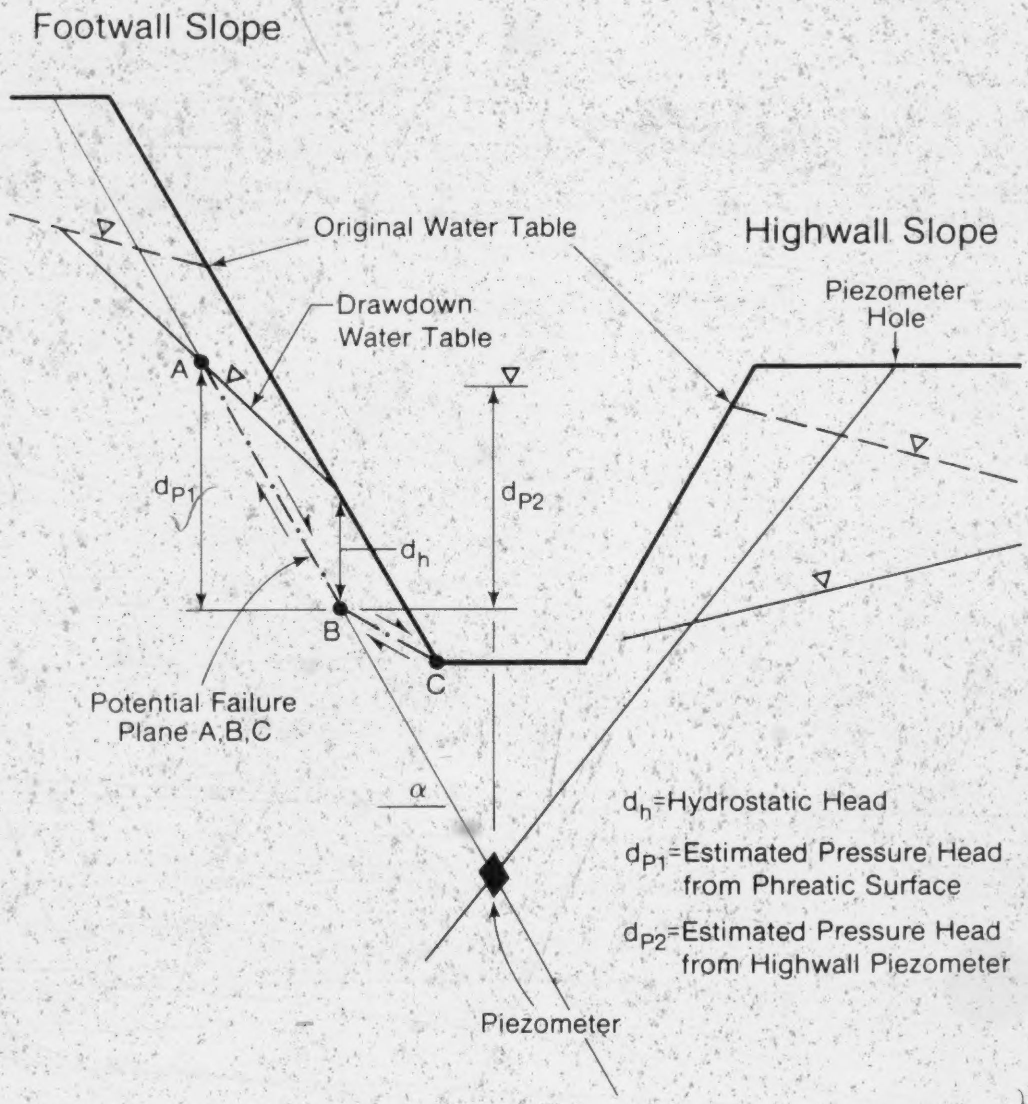
Footwall Slope
Original Water Table
Highwall Slope
Piezometer Hole
Drawdown Water Table
A
d_{P1}
d_{P2}
d_h
B
C
Potential Failure Plane A,B,C
α
d_h=Hydrostatic Head
d_{P1}=Estimated Pressure Head from Phreatic Surface
d_{P2}=Estimated Pressure Head from Highwall Piezometer
Piezometer

Figure 3.2 Water Pressures on Bedded Footwall Slopes

bedded footwall slopes effective and inexpensive drainage can normally be obtained with free draining sub-horizontal drainholes installed at a slight upward angle (2 - 5°). Due to the complexity of seepage and drainage characteristics on rock slopes design of horizontal drainhole system is best based on previous experience in similar strata and general rules-of-thumb.

Sharp et al. [29] offer the following design guidelines for horizontal drainholes in isotropic rock slopes:

i. For slopes with groundwater tables at 30 - 60 m above the toe, drainholes should be installed to a depth equivalent to the slope height (maximum of 90 m). A single line of 8 cm diameter holes spaced at 6 to 15 m intervals should provide adequate drainage.

ii. Where groundwater tables are at elevations greater than 60 m above the toe, rows of drains should be installed every 30 m.

In practice the depth of drain holes should be based on the influence of groundwater on stability for the slope under consideration. Drainhole spacing is best determined through observational design incorporating actual drainhole performance cross-checked against piezometer readings. Seegmiller [32] provides useful information on horizontal drain design, emplacement, performance, and costs for rock slopes. He recommends hole diameters of 7 to 10 cm, drain lengths varying from one-half to the total slope height, and horizontal spacing ranging from 3 to 30 m. Furthermore, Seegmiller recommends that actual drainhole spacing be determined based on measurable interference between drainholes as determined from individual drainhole flowrate recordings. Monitoring of flowrate with time and the effect of drainhole installation on piezometer readings constitutes a necessary design and monitoring practice of rational rock slope engineering.

3.3 Conclusions

i. Rational estimates of pore pressure along bedding are best determined from piezometers located down-dip of prospective failure surfaces. Alternatively, pore pressure estimates can be made from a linear profile measured from the phreatic surface in a down-dip direction.

ii. In most cases sub-horizontal drains drilled at a slight uphill gradient provide the most economically effective drainage option. Design of horizontal drain systems should be based on experience and through correlation with drainhole flow rates and piezometer response. In most cases drainholes of 5 to 10 cm diameter spaced at 3 to 30 m will provide adequate drainage. Depth of influence varies from one-half to the total slope height.

4.0 STABILITY ANALYSIS

Despite the popularity of numerical computer based stress-strain analysis, pragmatic rock slope engineering is carried out with limit equilibrium methods. The general principles of limit equilibrium methods for solving rock slope stability problems are as follows [60]:

i. Postulate a sliding mechanism with reference to the structural geology and associated slope kinematics.

ii. From rigid body statics estimate the shear strength required to keep the slip mechanism in limit equilibrium.

iii. Compare the shear strength with the shear resistance (i.e. calculate the safety factor).

iv. Find the mechanism with the lowest safety factor (i.e. the critical failure surface).

All limit equilibrium analyses result in the calculation of the safety factor defined as the ratio of available strength to mobilized forces along a given slip surface. The appropriate safety factor for a given design problem will be based on familiarity with the failure mechanics, consequences of failure, and sensitivity of the design parameters to uncertainties and natural variations. Although design safety factors for many rock slopes fall between 1.2 and 1.5, engineering judgement should be employed to assess each design problem and determine an appropriate safety factor. In mining applications, economics often dictates that lower safety factors be utilized (1.1 to 1.2) which is justifiable for short term appropriately monitored slopes.

Sensitivity analysis is an important component of the design methodology and helps the designer to get a feel for the important design parameters. In this study the sensitivity analysis is carried out with the VARSIM computer code developed within the Department of Mining, Metallurgical and Petroleum Engineering at the University of

Alberta. A summary of the concepts embodied in the program is provided in Appendix A.

The VARSIM program calculates the individual variance and bias terms for each variable. The sum of each of these terms is the estimated variance and bias for the function. The percentage contribution of the individual variance and bias terms to the totals for each parameter is written alongside the estimated mean and standard deviation values. This provides the user with an indication of the sensitivity of each parameter to the calculated result.

The designer should appreciate that the rigid body statics of limit equilibrium based techniques does not result in determination of deformations, it assumes average stress distributions, and does not allow for progressive failure. Note that the latter mechanism is common to the stress-strain behaviour of brittle rock materials. Despite these shortcomings limit equilibrium design of rock slopes has several advantages:

i. Detailed knowledge of rock material constitutive behaviour is not required.
ii. Different failure modes may easily be compared with one another.
iii. The safety factor is calculated relatively easily.
iv. Back analyses of previously failed slopes is easily carried out.

Economic surface mining recovery of stratiform ore deposits, such as coal and bedded iron deposits, is often contingent upon footwall design. In these and other bedded rocks it is desirable to excavate slopes parallel to bedding thus minimizing waste extraction and preventing the undercutting of potentially unstable strata. The extent to which a slope may be continuously excavated along a bedding unit relies upon the slope kinematics, shear strength and water forces, and the failure mechanics. The kinematics of rock slopes engineering are discussed by Hoek and Bray [4] and in Chapter 2 of the Pit Slope Manual [2]. Section 2.0 and 3.0 in this study deal with pertinent shear strength and hydrogeological issues respectively. In this section, limit equilibrium based methods to analyze the stability of footwall slopes will be reviewed and refined.

Hawley et al. [33] report on possible modes of failure on bedded footwall slopes. Their list of failure mechanisms is comprised of planar slab failure, bilinear slab failure, ploughing slab failure, buckling failure, toppling failure, wedge failure, deep seated failures and ravelling (rockfalls). The latter process, ravelling, is really a function of weathering and blasting practice and therefore is not conducive to static equilibrium analysis. Due to the kinematics normally present on footwall slopes stepped, toppling, and wedge failures are not common. Hoek and Bray [4] provide useful reviews of these processes. Further discussion and analysis is directed towards the four main modes of slab or bedding plane failures on footwall slopes, namely:

i. Planar
ii. Bilinear
iii. Ploughing
iv. Buckling

Figure 4.1 illustrates these mechanisms. In addition, a discussion of deep seated footwall failure will be presented.

The analyses that follow are based on simple static equilibrium models which incorporate the following assumptions and limitations:

i. The models are two dimensional. Thus lateral restraint is assumed to be negligible, resulting in a conservative analysis. Note, however, that shear strength parameters derived from two dimensional back analyses may result in an overestimate of stability when applied to future design .

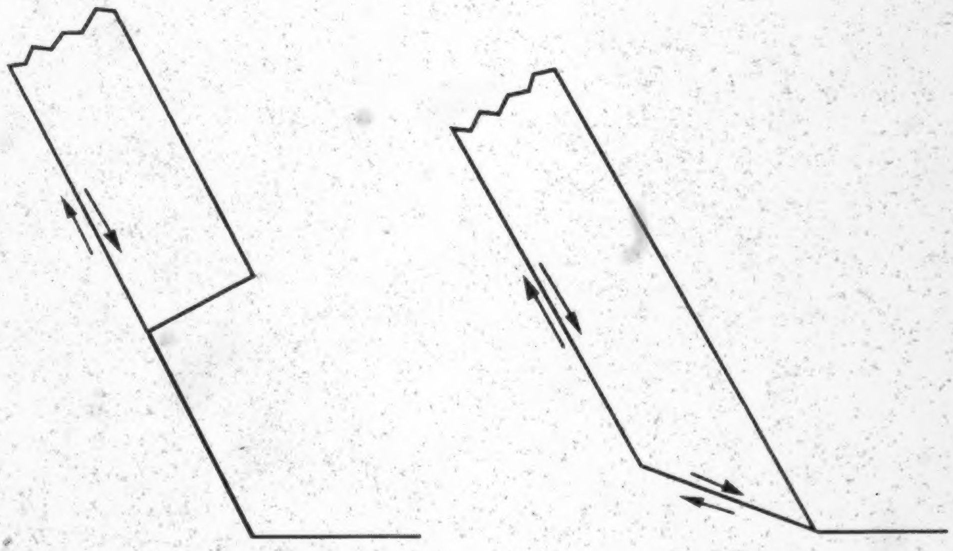

A. Planar

B. Bilinear

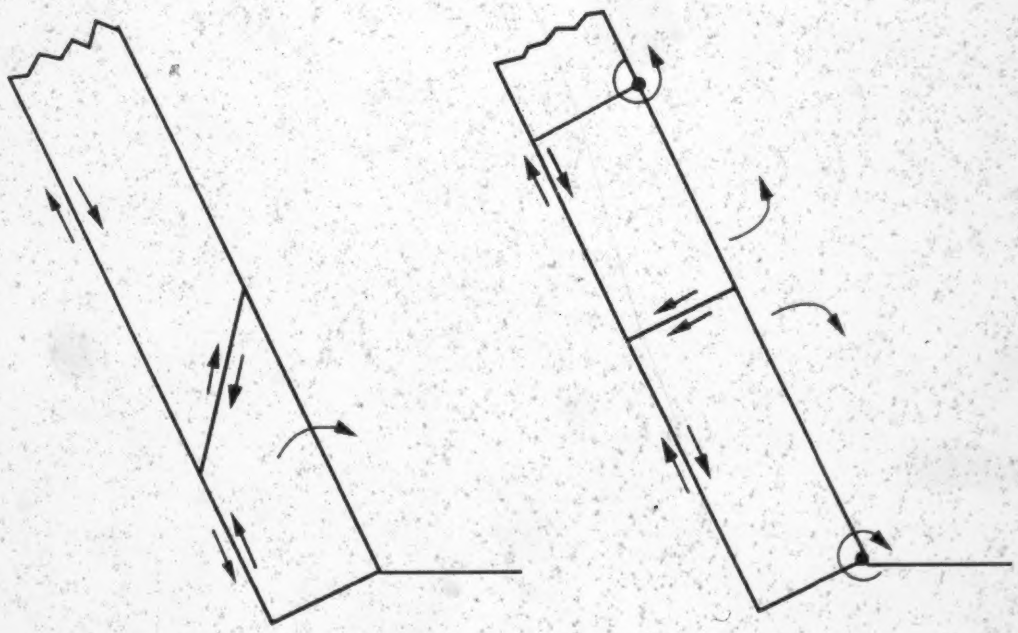

C. Ploughing

D. Buckling

Figure 4.1 Footwall Failure Modes

ii. Water pressures increase linearly with depth and static pressures behind bedded slabs are assumed to exist. A further discussion of groundwater conditions in bedded footwall slopes was presented in Section 3.0.

iii. Cohesion along bedding joints is always assumed to be zero.

4.1 Planar Slab Failure

Whenever slabs of bedding daylight on footwall slopes dipping greater than the angle of shearing resistance (friction angle) of the bedding joints the stability of the slope is at risk. In most circumstances it is not prudent design practice to assume that cohesion between bedding planes or lateral restraint along bedding strike will serve to prevent failures from occurring.

Daylighted bedding, where present, is always the most critical failure mode as the only contribution to stability is the shearing resistance of the bedding planes themselves. Occurrence of daylighted slabs of bedding on footwall slopes is primarily due to stratigraphic or structural geology processes, or as a result of undercutting bedding during excavation. Hardy Associates [41] discusses stratigraphic features of daylighted beds in sedimentary strata; pinchouts and various forms of cross beds are mentioned in this regard. Recent experience on the footwall slope of the Line Creek coal mine in southeastern British Columbia [41] has documented a large stratigraphic pinchout occurring very abruptly within a 2 m thick sandstone bed lying directly beneath the mined out coal seam. This feature extends diagonally down the 200 m high footwall and has necessitated anchor reinforcement of the 40° - 50° slope. Dawson and Sheehan [37] document daylighted beds up to 2 m thick resulting from shear displacement along cross joints normal to bedding in steeply dipping foothills coal measures rocks at Smoky River Coal, near Grande Cache, Alberta.

The limit equilibrium analysis of planar failure has been discussed by several workers [2, 4, 34]. For conditions where a linear Mohr-Coulomb strength envelope is appropriate and assuming zero water pressures, stability is independent of slab weight and the factor of safety (FS) is expressed as:

$$FS = \frac{\tan \phi}{\tan \alpha} \tag{4.1}$$

Where ϕ = friction angle along bedding

α = slope dip

Appendix B presents the details of planar slab analysis incorporating Barton's shear strength criteria [8], water pressures, and reinforcing anchor restraint. The analysis has been incorporated into the SLAB program which was linked and compiled with the VARSIM code for sensitivity analysis in this study.

When anchor loads are considered, the determination of the factor of safety may be calculated three different ways [4, 35]:

i. Active Factor of Safety (FS_A)

ii. Passive Factor of Safety (FS_P)

iii. Excess Shear Factor of Safety (FS_{ES})

When anchors are tensioned prior to completing the installation an active force is applied across bedding effectively creating a beam of rock. The anchor load may be considered to act directly against the disturbing forces. Therefore assuming a Mohr-Coulomb strength envelope, and with reference to Figure 4.2, the active factor of safety relationship (FS_A) is expressed as:

$$FS_A = \frac{\text{Resisting Forces}}{\text{Disturbing Forces} - Q\cos(\alpha - \delta)} \tag{4.2}$$

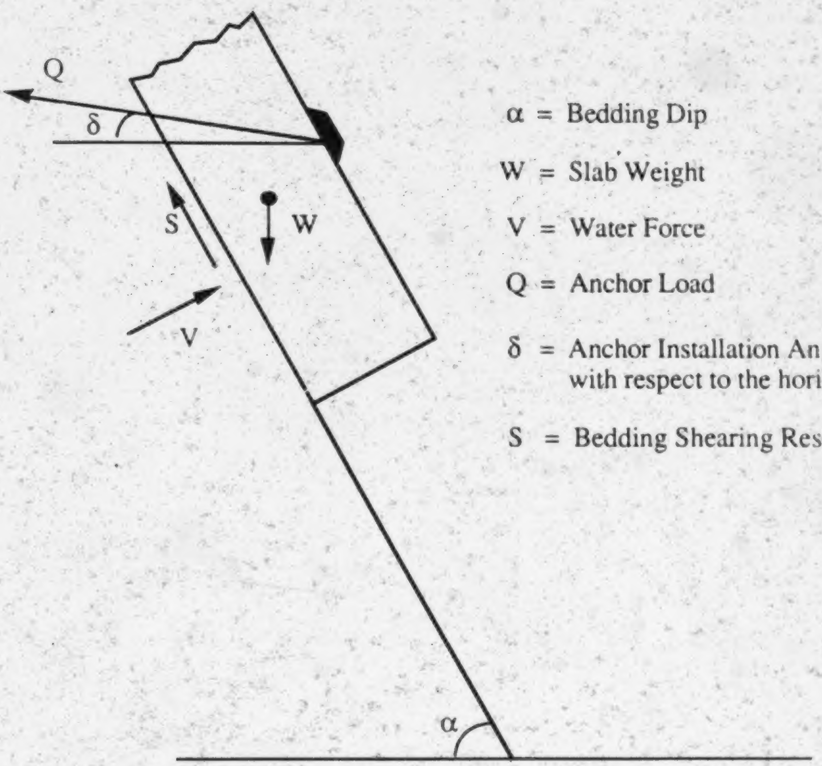

α = Bedding Dip

W = Slab Weight

V = Water Force

Q = Anchor Load

δ = Anchor Installation Angle with respect to the horizontal

S = Bedding Shearing Resistance

Figure 4.2 Planar Slab Failure Forces and Nomenclature

When anchors are installed without tensioning, movement in the slope must occur to initiate resistance from the anchors. In this case the anchor can be considered to resist movement in a passive manner similar to cohesion between rock joint surfaces. The passive safety factor (FS_P) is commonly expressed as:

$$FS_P = \frac{\text{Resisting Forces} + Q\cos(\alpha - \delta)}{\text{Disturbing Forces}} \tag{4.3}$$

An alternative approach considers the excess shear force (S_E) and the total anchor load contribution to shear strength (S_A) where:

$$S_E = \text{Disturbing Forces} - \text{Resisting Forces} \tag{4.4}$$

$$S_A = Q\left[\cos(\alpha - \delta) + \sin(\alpha - \delta)\tan\phi\right] \tag{4.5}$$

In this approach the excess shear factor of safety (FS_{ES}) is expressed as:

$$FS_{ES} = \frac{S_A}{S_E} \tag{4.6}$$

The excess shear factor of safety is zero without anchor support and negative when resisting forces are greater than disturbing forces. Thus, this approach cannot be used to compare unsupported versus supported slopes and it is not commonly used in practice.

Seegmiller [35] compares these three approaches and it is worthwhile to re-examine his findings with respect to nominal slope parameters pertinent to this study. Consider the following variable values for a dry slope:

Table 4.1 Parameters for Factor of Safety Comparison

	Mean	Standard Deviation*
Bedding Dip (α)	60°	6.0
Slope Height (H)	10 m	1.0
Daylighted Bedding thickness (T)	2 m	0.2
Unit Weight (γ)	25 kN/m^3	2.5
Friction Angle (ϕ) (JRC = 0)	30°	3.0

* Parameter coefficient of variation = 10%

Figures 4.3.A and B show anchor load ($\delta = 0$) versus safety factor versus the safety factor standard deviation respectively derived from the SLAB program. From these two figures the following conclusions are drawn:

i. All three methods yield identical anchor loads at FS = 1

ii. The active method is least conservative while the passive method is most conservative. The excess shear approach lies between the two extremes.

iii. The FS_A is increasingly sensitive to uncertainties as anchor load increases (Figure 4.3.B) as indicated by the increase in standard deviation with increasing load. This means that at higher loads and hence higher safety factors, the FS_A yields an apparent false sense of security if the design parameters are not well defined.

A useful appreciation for the sensitivity of various parameters on the safety factor is afforded by comparing the percentage contribution to the total variance made by each variable. This is done below from results of the SLAB program at a nominal FS = 1.2 and assuming the parameters previously listed.

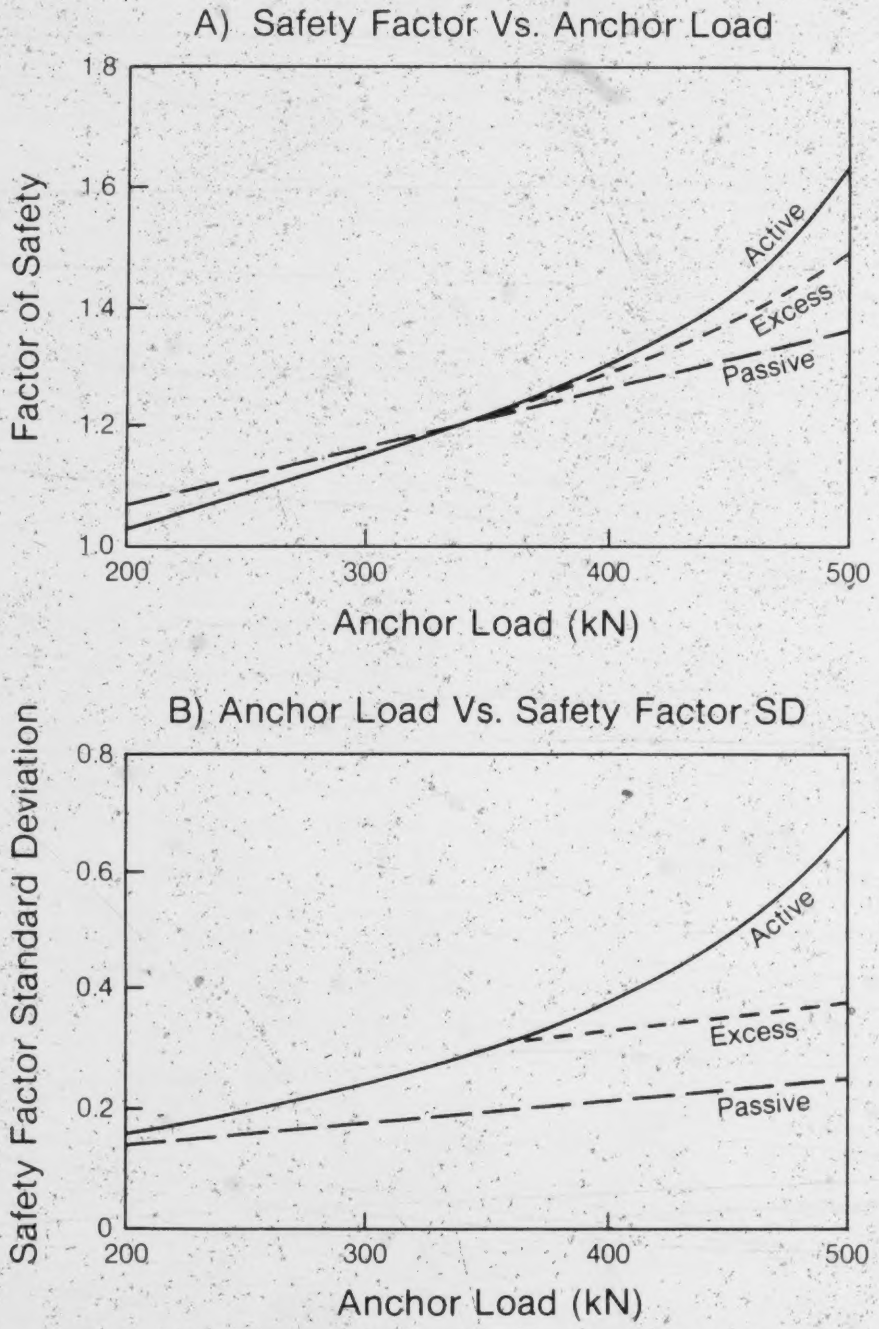

Figure 4.3 Comparison of Different Factors of Safety (see Table 4.1)

Table 4.2 Factor of Safety Comparison Sensitivity Analysis

	% of Total Variance		
	Active	Passive	Excess Shear
Bedding Dip (α)	40.1	36.2	42.4
Slope Height (H)	14.9	15.4	12.9
Bedding Thickness (τ)	14.9	15.4	12.9
Unit Weight (γ)	14.9	15.4	12.9
Friction angle (ϕ)	15.2	17.6	18.9
TOTAL Standard Deviation	0.37	0.22	0.33

All three safety factor approaches show that, in the light of uncertainty, the bedding dip is the most important variable in this particular case. This is not surprising as the estimated standard deviation of bedding, at a 10% coefficient of variation is twice the friction angle (6° versus 3°). A normal variation of 6° on a 60° dip slope, however, would not be unreasonable.

From the statics point of view the other important anchor design consideration is angle of installation. There will be an optimum inclination for maximum shear strength across bedding where the updip component of anchor tension and the normal component of anchor tension combine to maximize shear strength. The optimum tension can be derived by solving the safety factor equation for Q and differentiating with respect to the angle of installation. Setting this equation to zero for Mohr-Coulomb strength criteria, the three safety factor equations discussed above yield the following optimum angle relationships:

Table 4.3 Optimum Anchor Angle Relationships

Safety Factor Approach	Optimum Angle (δ) Relationship
SF_A	$\alpha - \arctan\left(\frac{\tan \phi}{FS}\right)$
SF_P / SF_{ES}	$\alpha - \phi$

Therefore the optimum active and passive installation angles for the preceding example at FS = 1.2 will be 34° and 30° respectively. The active angle increases relative to the passive optimum angles as the safety factor get higher. At FS = 1 both methods yield the same optimum angle. Note that the optimum angle from a statics point of view may not distribute the load appropriately across the slip surface, can result in excessively long anchors and may restrict installation procedures. Further discussion on design of anchoring systems in bedded footwalls is presented in Section 5.0.

4.2 Bilinear Slab Failure

Bilinear slab failure involves sliding parallel to bedding in combination with sliding along a secondary surface dipping out of the slope. The secondary surface may be a persistent discontinuity surface or, if unfavorably oriented discontinuities are not present, a shear zone developed through the rock mass. In the latter case, the critical failure surface attitude must be found.

Brawner [26] reports the occurrence of persistent shallow shears and fractures dipping at 20° out of a footwall in coal measures strata in southeastern British Columbia. Hawley et al. [33] document a bilinear mode of slope failure developed through the rock mass at the toe of a slope where bedding has thinned. Krahn [5], while re-examining the geology of the Frank Slide, documents a bilinear slab mode of failure developed along cross joints, bedding joints, and a fault zone daylighting from the slope.

Stability analysis for bilinear slab failure is carried out by dividing the bedding slab into a driving and a toe slab. Stimpson [36] and Hawley [33] describe analytical techniques that have been employed in the literature. Figure 4.4 shows the general geometry and forces employed in this study to examine bilinear slab failure. Details of the analysis are contained in Appendix C. The analysis has been incorporated into the BILIN program which was linked and compiled with the VARSIM code for sensitivity analysis in this study.

The BILIN program incorporates the following features and assumptions:

i. The boundary between the driving and toe slabs is assumed to consist of orthogonal cross joints. The analysis incorporates a shearing resistance (S_J) between these two slabs. The effect of S_J on slab stability is discussed below.

ii. Allowance is made for an upper slope angle (ψ). In this fashion, slopes in steep terrain or a series of berms can be accounted for by assuming an average angle above the crest of the continuous footwall slope.

iii. Analysis may be carried out incorporating a persistent secondary discontinuity or with failure through the rock mass. The latter option utilizes empirical relationships discussed in Section 2.0. In this case, the critical angle (β) is calculated by iteration.

iv. Water forces acting on the cross joint between the two slabs are assumed to be negligible.

v. The anchor load is assumed to act on the upper slab only. In this fashion the reinforcement acts to reduce the excess load transferred from the driving slab to the toe slab. An alternative would be to consider the anchor load as acting across

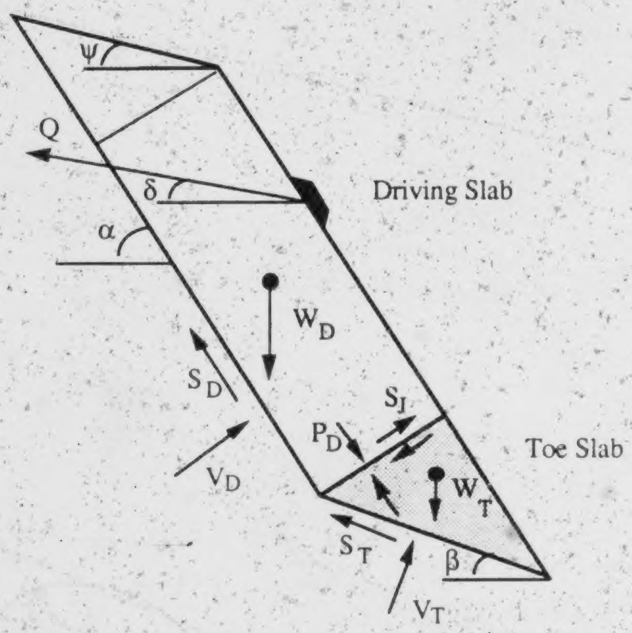
ψ
Q
δ
Driving Slab
α
W_D
S_D
S_J
P_D
Toe Slab
V_D
W_T
S_T
β
V_T

α = Bedding Dip
β = Secondary Surface Dip
ψ = Upper Slope Angle
δ = Anchor Installation Angle with respect to the horizontal

W = Slab Weights
V = Water Forces
S = Shear Resistances
Q = Anchor Loads
P_D = Driving Slab Axial Force

Figure 4.4 Bilinear Slab Failure Forces and Nomenclature

the secondary slip surface. In practice the accurate location of this surface may not be known or an alternate surface could daylight above the anchors resulting in ineffective reinforcement. Calculation of active and passive safety factors follows the same logic as that of planar slab reinforcement (Section 4.1).

Whether failure will occur through the rock mass or along a secondary discontinuity will depend on the relative strength of the discontinuity versus that of the rock mass and the orientation of the discontinuity relative to the maximum principal stress (σ_1) direction. If it is assumed that σ_1 acts downwards parallel to bedding and that σ_3 is zero, then the critical angle for failure along a secondary discontinuity is :

$$\beta = \frac{\phi}{2} + \alpha - 45 \qquad (4.7)$$

where β is the dip of the secondary discontinuity, α is the bedding dip, and ϕ is the discontinuity friction angle.

In order to compare bilinear slab stability considerations for failure along a persistent discontinuity dipping out of a slope (Case A) with failure through the rock mass toe (Case B) consider the following slope parameters:

Table 4.4 Parameters for Bilinear Slab Analysis

Bedding Dip (α) = 60°

Daylighting Discontinuity Dip (β) = 20°

Slab Thickness (T) = 2 m

Bedding Joint Friction Angle (ϕ) = 30° (JRC = 0)

Unit Weight (γ) = 25 kN/m^3

Uniaxial Compressive Strength (σ_c) = 60 MPa

Intact m coefficient (m_I) = 10

Rock Mass Rating (RMR) = 50

Slope height versus factor of safety (FS) relationships for Case A and Case B are exhibited in Figures 4.5.A and 4.5.B respectively. Both figures show the influence of frictional resistance (ϕ_J) along the cross joint between the driving and the toe slabs. Case A (Figure 4.5.A) is far more sensitive to consideration of sliding resistance along the intervening cross joint. Figure 4.5.B (Case B) shows a difference of 28 m between ϕ_J = 0 and ϕ_J = 30° for a critical slope height (FS = 1). Due to the highly empirical nature of the rock mass failure criteria, lack of well defined kinematic control during rock mass failure, and the very high calculated slope heights in Case B it seems rational to set ϕ_J = 0° for rock mass failure. On the other hand the rigidly defined kinematics of a pervasive daylighting continuity (Case A), large sensitivity to ϕ_J, and lower stable slopes suggest that a nominal cross joint frictional resistance is warranted for design in this case.

Note the large difference in the slope height scales between Figure 4.5.A and 4.5.B. Not surprisingly Figure 4.5.B predicts slope heights much greater than 4.5.A emphasizing the role that unfavorable kinematics plays on a rock slope. The design

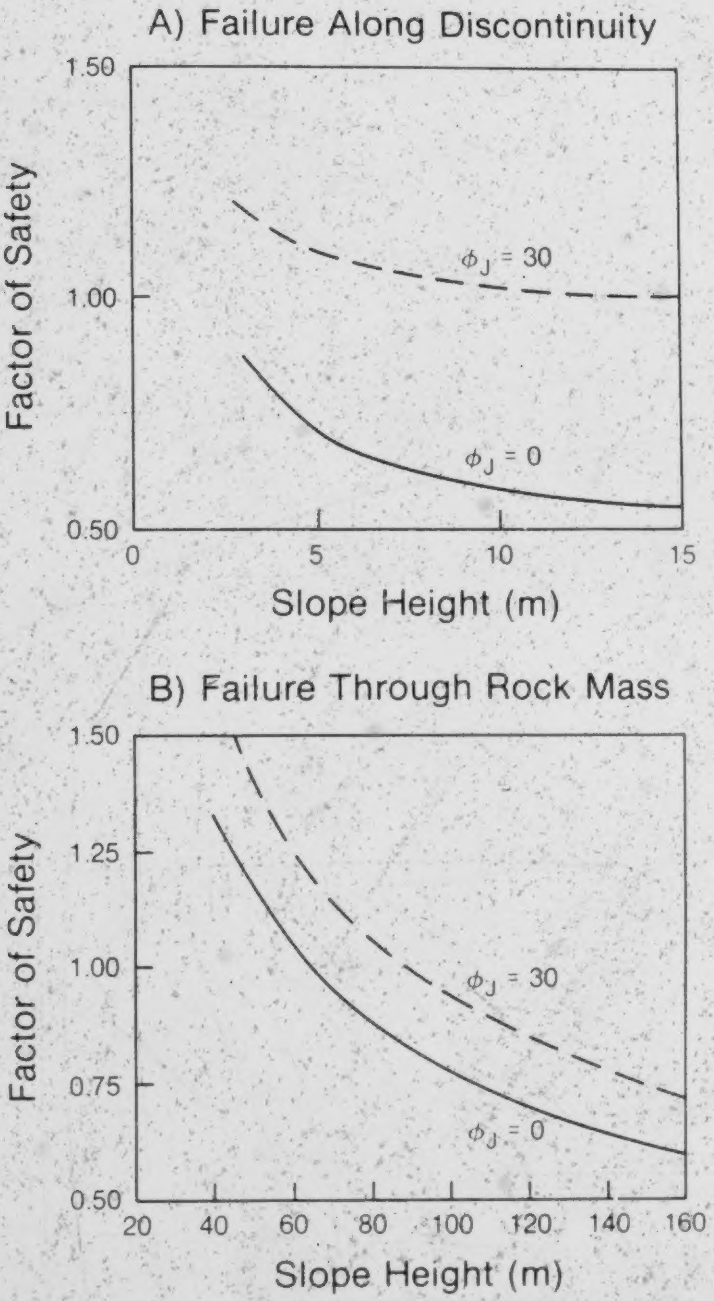
A) Failure Along Discontinuity

B) Failure Through Rock Mass

Figure 4.5 Bilinear Slab Failure – Influence of Cross Joint (see Table 4.4)

curve for Case A is far less sensitive to slope height than Case B. Therefore where unfavorably oriented discontinuities exist they may present a hazard at almost any slope height, similar to a daylighted bedding slab.

Table 4.5, derived from results of the BILIN program with the above mentioned mean parameters and a nominal coefficient of variation of 10%, shows a quantitative comparison of parameter sensitivities for the two cases at slope heights corresponding to FS = 1.2.

Table 4.5 Bilinear Slab Sensitivity Analysis

	CASE A			CASE B		
	Mean	S.D.	% Var.	Mean	S.D.	% Var.
dip of footwall (°)	60	6	10.5	60	6	12.8
dip of daylighting discontinuity (°)	20	**5	59.4	*35	–	–
height of slope (m)	3	.3	1.6	45	4.5	5.5
slab thickness (m)	2	.2	1.6	2	.2	.1
unit weight (kN/m^3)	25	2.5	0	25	2.5	4.3
bedding friction angle (°)	30	3	24.3	30	3	1.7
crossjoint friction angle (°)	30	3	2.6	0	–	–
Uniaxial Compressive Strength (MPa)	–		–	60	6	4.3
intact m (m_I)	–		–	10	1	.2
Rock Mass Rating (RMR)	–		–	50	5	71.1
Mean Factor of Safety	1.19			1.24		
Standard Deviation	0.23			0.28		

* Calculated by iteration

** Coefficient of Variation equal to 25% in order to represent more realistic field variations.

Results in Table 4.5 show the bilinear slab mechanism to be particularly sensitive to the daylighting discontinuity angle and the RMR (as indication of rock quality) for Case A and Case B respectively. Figure 4.6.A emphasizes the importance of first assessing a rock slope for unfavorable kinematics. At $\beta = 20°$ slope heights in excess of 15 m are unstable whereas for $\beta = 10°$ sliding along the daylighting discontinuity will not take place and failure can only occur through the rock mass toe (Case B). Figure 4.6.B shows that a difference in the critical slope height (FS = 1) of 100 m is obtained when the RMR is varied between 40 and 60 thus emphasizing the necessity for realistic assessment of rock mass quality.

Figure 4.7 shows the influence of slab thickness on the slope height versus critical slope dip (FS = 1) for Case B (bilinear slab failure through the rock mass toe). Note that beyond 60° slope dip the critical design curves exhibit a rapid increase in gradient indicating a higher sensitivity to this mode of failure for steeper slopes (> 60°). Beyond a slab thickness of 10 m very high slopes are necessary for failure to occur ("average" rock; RMR = 50). A 20 m slab on a 100 m high slope has a critical slope dip of 67°. Therefore in most cases it is the thinner slabs that dominate stability considerations on dry footwall slopes.

4.3 Ploughing Slab Failure

Ploughing slab failure involves sliding along a basal bedding plane and a secondary discontinuity dipping into the slope. The failure mechanics results in a rotational movement of the lower toe slab out of the slope.

Ploughing failures can occur where thrusts daylight at critical positions on footwall slopes. Few failures of this type have been documented. A small ploughing failure took

A) Failure Along Discontinuity

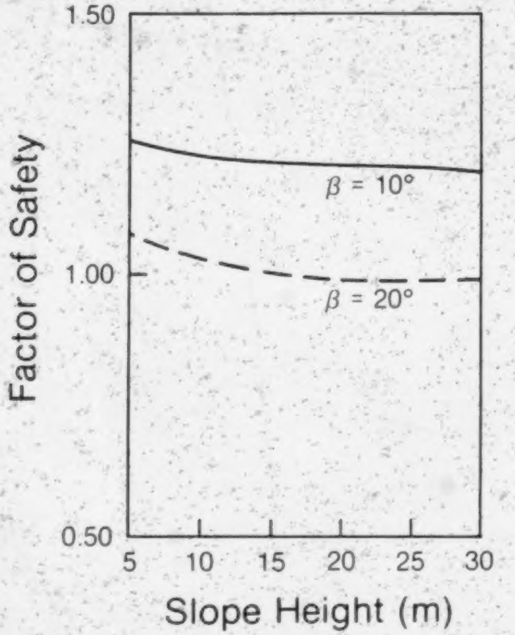

B) Failure Through Rock Mass Toe

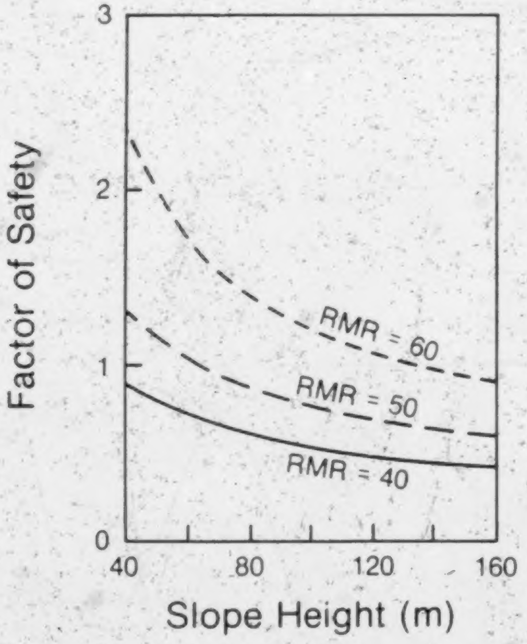

Figure 4.6 Bilinear Slab Failure – Influence of β and RMR (see Table 4.4)

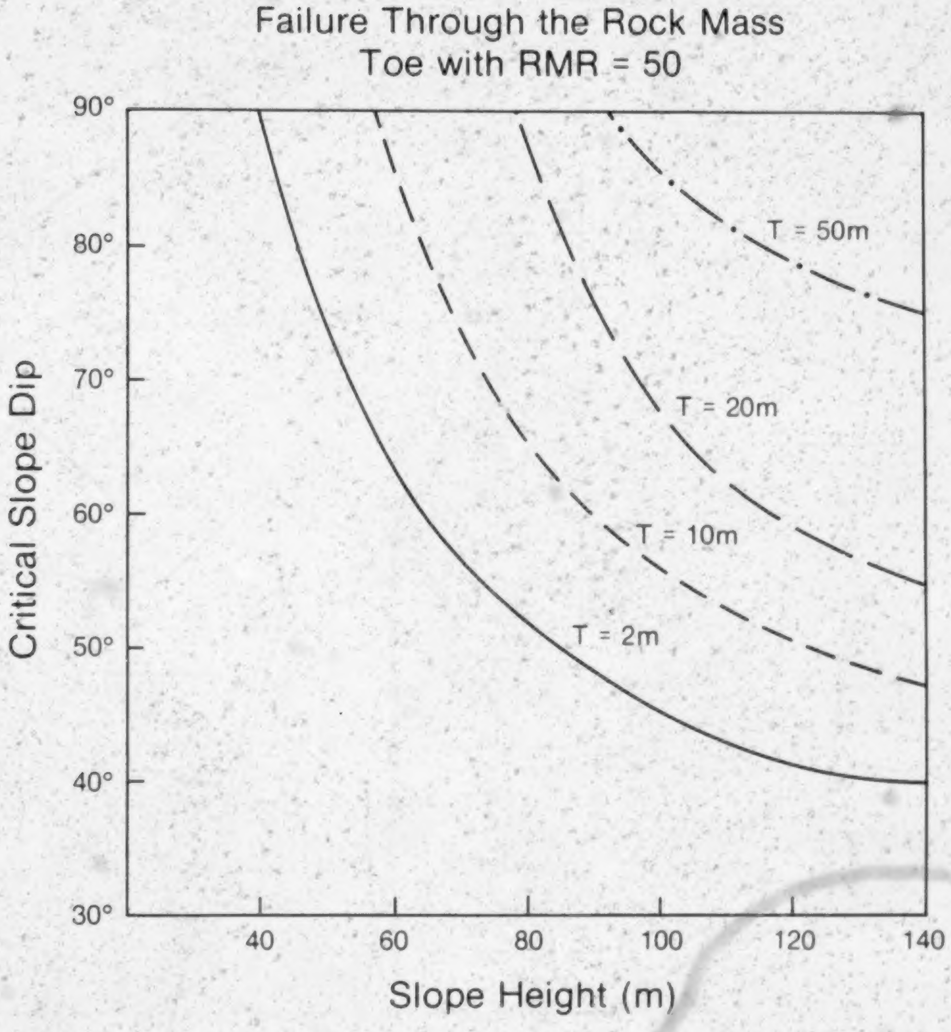

Figure 4.7 Bilinear Slab Failure - Influence of Slab Thickness (see Table 4.4)

place at Smoky River Coal in Grande Cache, Alberta [37]. This instability involved a 1 m slab which failed on a 65° slope over a 30 m bench height.

Stability analysis for ploughing slab failure is carried out by dividing the bedding slab into a driving and a toe slab. Figure 4.8 shows the general geometry and forces used in this study to examine ploughing failure. Details of the analysis are contained in Appendix D. The analysis has been incorporated into the PLOW program which was linked and compiled with the VARSIM code for sensitivity analysis in this study

The PLOW program first involves finding the minimum overturning moment about the slope toe necessary to initiate plowing of the lower toe slab. The force resulting from this equilibriating moment is then applied to the driving slab. A force equilibrium analysis is then carried out on the driving slab to investigate whether enough driving force (F_D) is available to initiate ploughing slab failure.

The analysis incorporates the following features and assumptions:

i. The boundary between the driving and toe slabs is defined by a ploughing discontinuity angle with respect to bedding. Ploughing discontinuities are commonly thrust faults oriented at shallow angles to bedding (20° - 40°).

ii. Allowance is made for an upper slope angle in the same fashion as the BILIN program.

iii. Water forces acting on the ploughing discontinuity between the two slabs are assumed negligible for stability purposes.

iv. The anchor load is assumed to act on the upper slab only, similar to the BILIN program.

In order to examine ploughing slab failure further consider the following dry slope parameters:

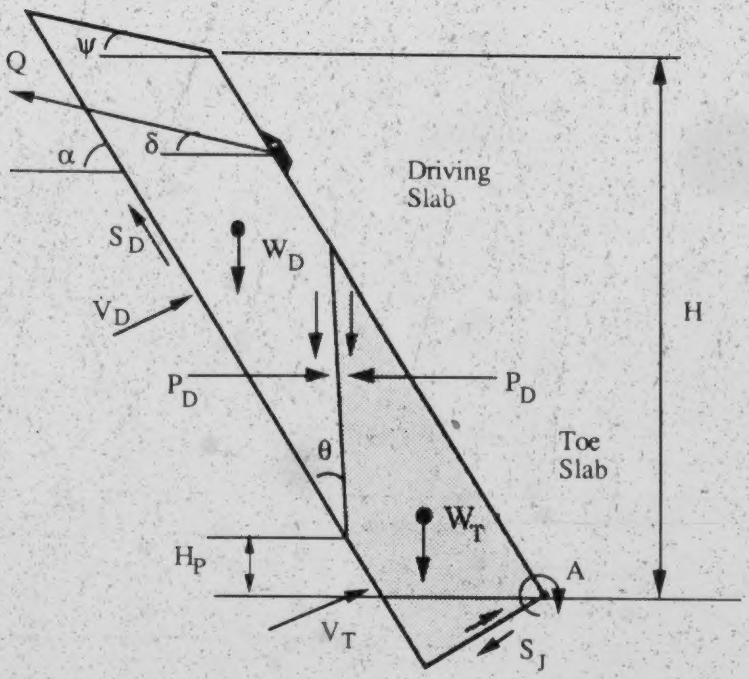
Q
ψ
α
δ
Driving Slab
S_D
W_D
V_D
P_D
P_D
θ
Toe Slab
W_T
H
H_P
A
V_T
S_J

α = Bedding Dip

θ = Ploughing Discontinuity angle with respect to bedding

ψ = Upper Slope Angle

δ = Anchor Installation Angle with respect to the horizontal

W = Slab Weights

V = Water Forces

S = Shear Resistances

TA = Anchor Load

H = Total Slope Height

H_P = plough discontinuity height

P_D = driving slab normal to plough discontinuity

Figure 4.8 Ploughing Slab Failure Forces and Nomenclature

Table 4.6 Parameters for Ploughing Analysis

Bedding Dip (α) = 60°

Ploughing Angle with respect to bedding (θ) = 20°; 40°

Slab Thickness (T) = 2 m

Friction Angle (ϕ) = 30° (JRC = 0)

Unit Weight (γ) = 25 kN/m^3

Slope Height (H) = 60 m

Figure 4.9 shows the relationship between the height of the ploughing discontinuity (H_P) and the factor of safety for a 60 m high slope with the above parameters. Note that the plough height reaches a minimum factor of safety at a nominal height above the slope toe. This is where the stabilizing moment generated by the toe slab is at a minimum. Beyond this minimum point the factor of safety increases with plough height (H_P). The critical plough height is defined as the uppermost plough height where the factor of safety is unity.

Figure 4.10 shows the relationship between the critical plough height (H_P) and the total slope height for ploughing discontinuity angles with respect to bedding of 20° and 40°. This figure shows that the critical plough height is 40% to 60% of the total slope height for the range of ploughing discontinuity angles (θ) normally encountered on bedded slopes ($\theta = 20° - 40°$). Thus, for $\theta = 30°$ the critical plough height is approximately one-half the total slope height (H).

Figure 4.11 shows the critical slope height versus slope dip relationships for different slab thicknesses where $\theta = 30°$ and $H_P = 1/2\ H$. The main point in this figure

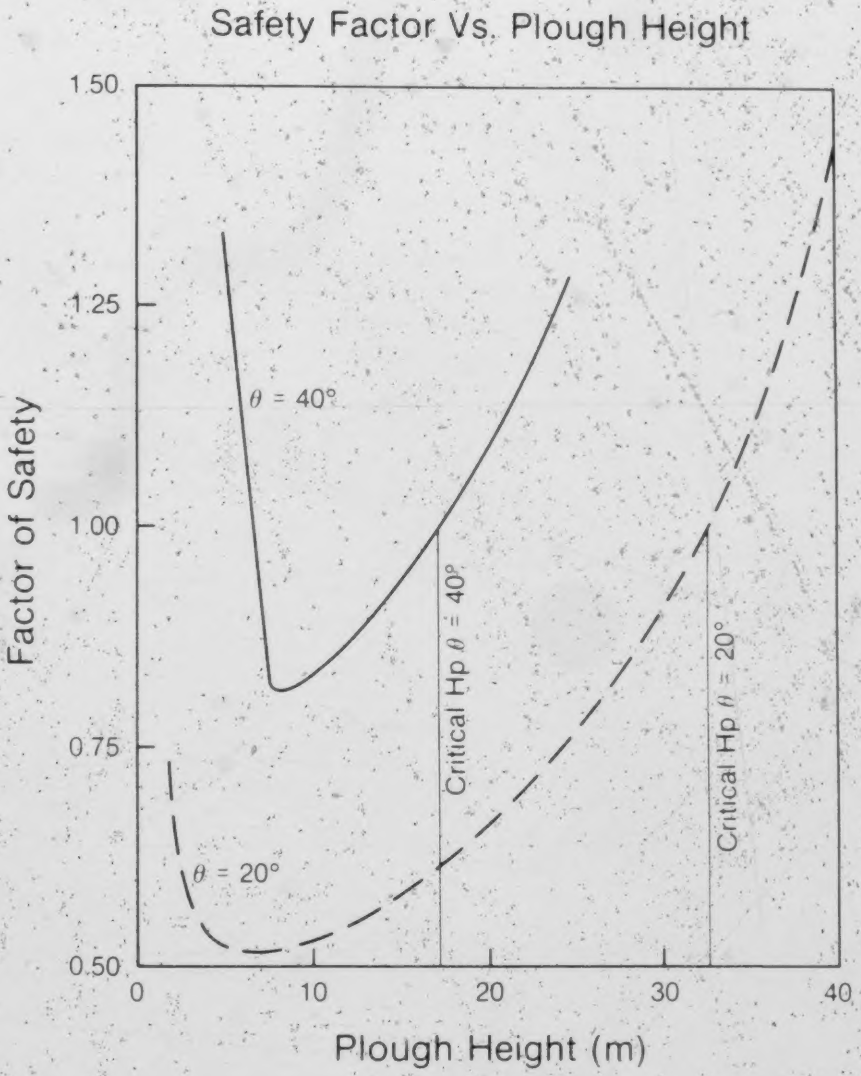

Figure 4.9 Ploughing Failure-Influence of Plough Height (see Table 4.6)

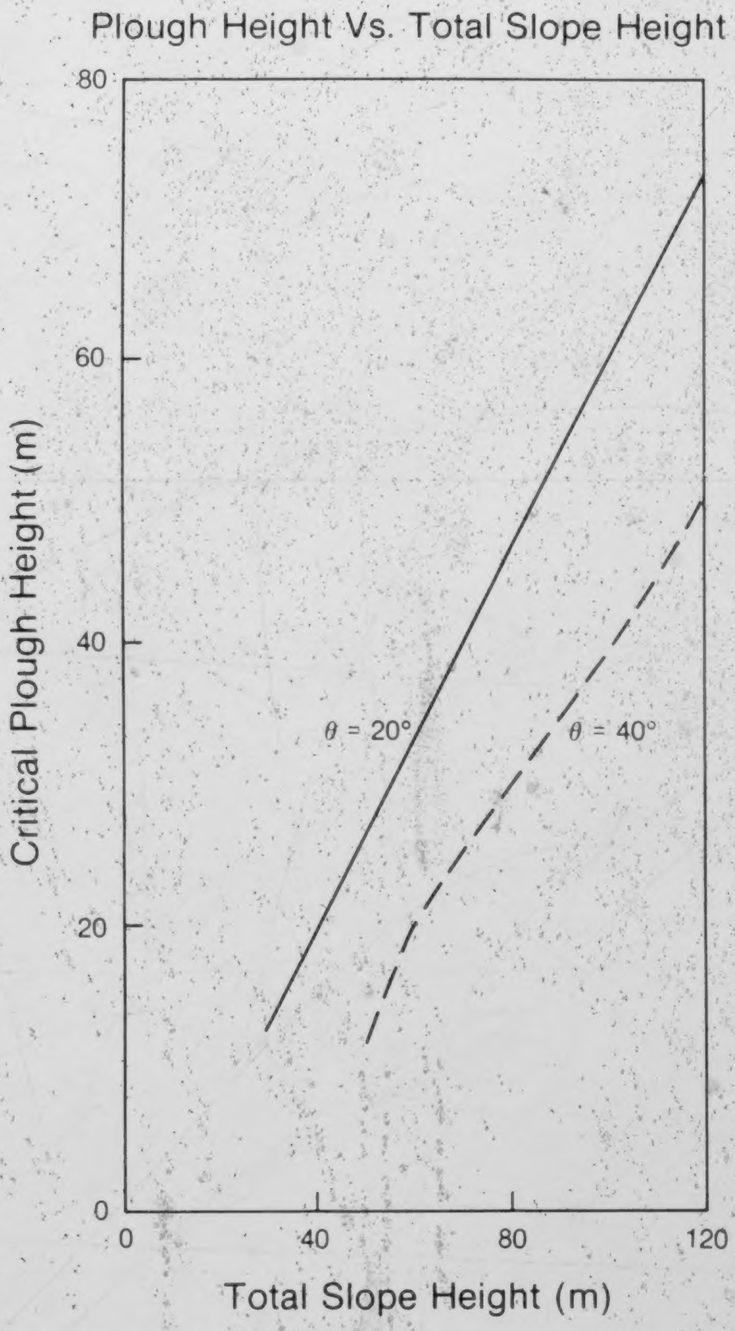

Figure 4.10 Ploughing Failure-Influence of Ploughing Angle (see Table 4.6)

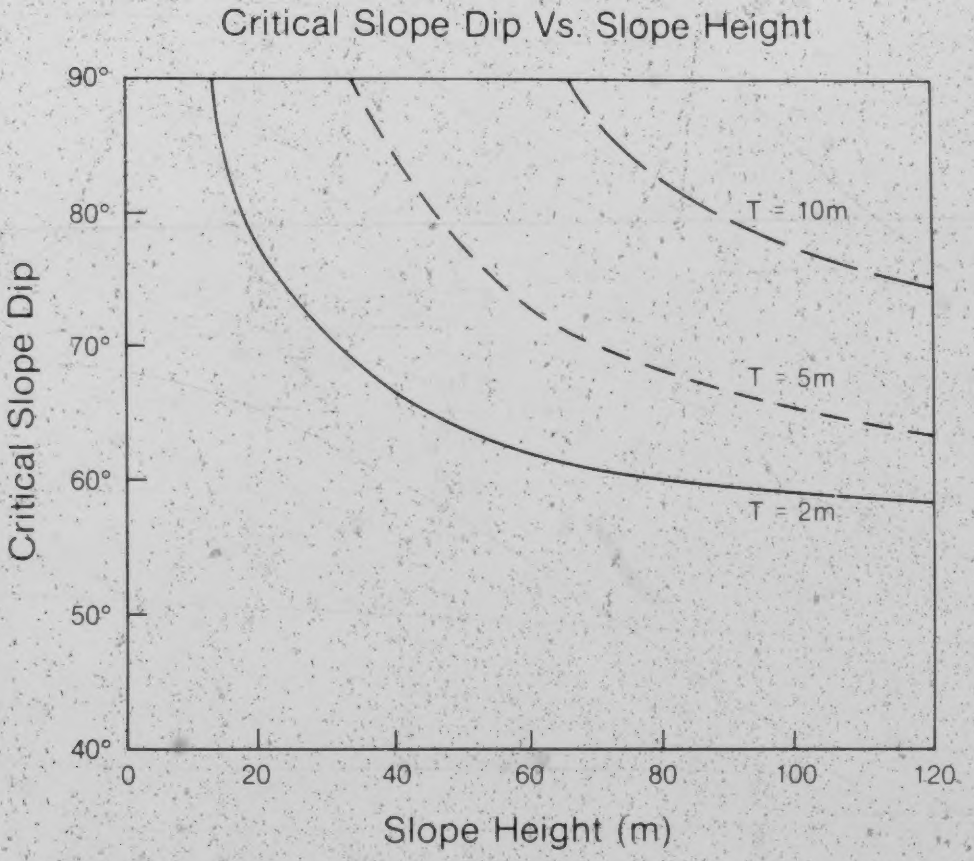

Figure 4.11 **Ploughing Failure – Influence of Slab Thickness (see Table 4.6)**

is that beyond a slab thickness (T) of 5 m only very steep slopes (> 75°) are prone to ploughing instabilities given this range of "average" parameters.

4.4 Buckling Failure

Buckling of thin slabs may theoretically occur on footwall slopes due to high axial stresses in the plane of the slope, high water pressures behind bedding or due to large curvatures. Documented buckling failures take the form of a buckled area near the toe followed by planar slab sliding up-slope of the failed area.

Rock slope buckling failures are commonly analyzed by either assuming pure flexural buckling or by rotational movement of two rigid slabs about three hinge points. Figure 4.12 illustrates these two buckling models and a discussion of each follows.

4.4.1 Flexural Buckling

Flexural buckling analysis incorporates analytical elastic solutions to solve for the critical buckling load (P_{CR}). Normally, the analysis utilizes the two dimensional Euler solution for a weightless continuous column subjected to one dimensional axial loading.

The Euler solution [38] for critical buckling load (P_{CR}) takes the following form:

$$P_{cr} = \frac{K\pi^2 EI}{h_B^2} \qquad (4.9)$$

Where:

K = 1 (column with pinned end)

E = Young's modulus

I = moment of inertia = $\frac{bT^2}{1^2}$ b = unit width; T = slab thickness

h_B = buckled length

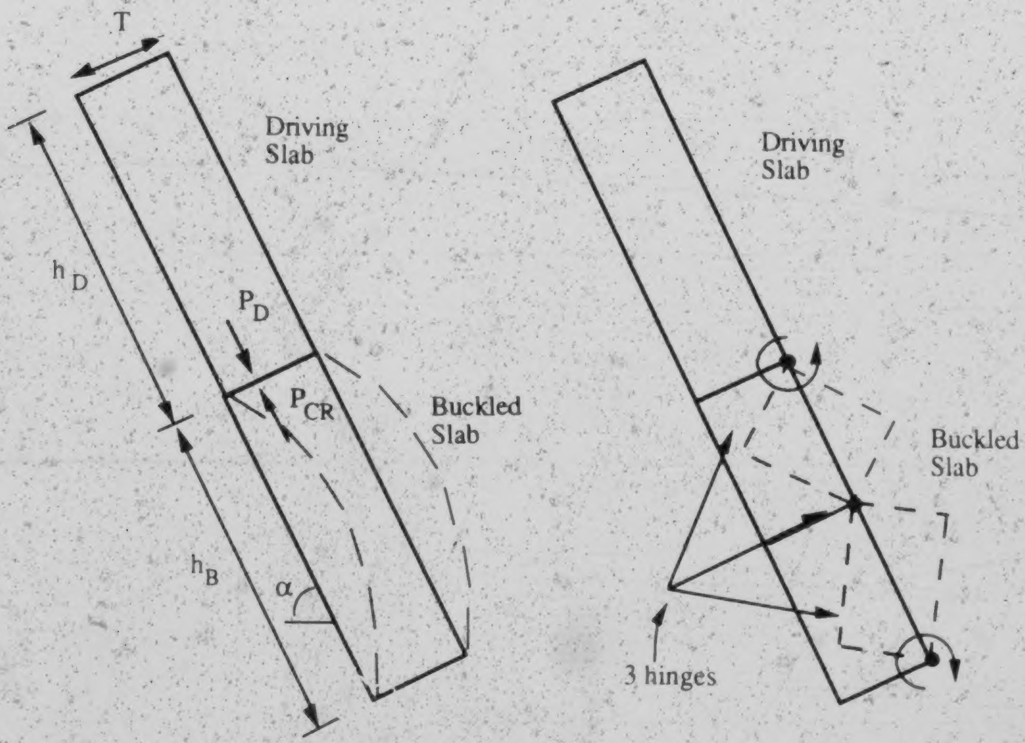
T
h D
Driving Slab
P D
P CR
Buckled Slab
h B
α
Driving Slab
Buckled Slab
3 hinges

A. Flexural Buckling

B. Three Hinge Buckling (after Cavers [40])

Figure 4.12 Buckling Failure Modes

With reference to Figure 4.12.A the disturbing forces P_D parallel to bedding are:

$P_D = W_D(\sin\alpha - \cos\alpha\tan\phi)$

And the factor of safety is expressed as:

$$FS = \frac{P_{CR}}{P_D} \tag{4.10}$$

Assuming that all other slope parameters remain constant, a given total slab length (h) will have a critical pair of driving and buckling slab lengths (h_D and h_B) where the factor of safety is a minimum. Consider the following relationships:

$$\begin{aligned} h &= h_D + h_B \\ h_B &= kh \\ h_D &= h(1-k) \\ W_D &= \gamma Th(1-k) \\ I &= T^3/12 \end{aligned} \tag{4.11}$$

Substituting equations 4.11 into equation 4.10 and solving for the total slab length (h) yields:

$$h^3 = \frac{\pi^2 \cdot E \cdot T^2}{12 \cdot \gamma \cdot FS \cdot k^2(1-k)(\sin\alpha - \cos\alpha\tan\phi)} \tag{4.12}$$

For any given slope (i.e. E, T, γ, α, ϕ = constant) and considering a particular factor of safety (FS) the total slab length, will be a minimum when $k^2(1-k)$ is a maximum. Therefore h = minimum when:

$$\frac{d\left[k^2(1-k)\right]}{dk} = 0$$

$$2k - 3k^2 = 0$$

Then, $k = 2/3$ for minimum h.

Now substituting this critical value of k into equation 4.12 yields the following equation.

$$h^3 = \frac{5{\cdot}55ET^2}{\gamma\, FS \left(\sin\alpha - \cos\alpha \tan\phi\right)} \tag{4.13}$$

Serafin and Pereira [39] have provided a relationship between rock mass modulus (E_{RM}) and rock mass rating (RMR) as follows:

$$E_{RM} = 10^{(RMR - 10)/40}\ \text{GPa} \tag{4.14}$$

Consider the following slope parameters:

Unit Weight (γ) = 25 kN/m^3

Friction Angle (ϕ) = 30°

RMR = 50

Figure 4.13 shows the critical Euler buckling slope height versus slope dip relationships for different slab thicknesses and the above parameters. These are the same parameters used in Figure 4.7 for bilinear slab failure with sliding through the rock mass toe. A comparison of these two figures shows that the Euler buckling model predicts much higher stable slope heights. For example, a 2 m thick slab on a 60° slope shows critical slope heights of about 250 m and 65 m for Euler buckling and bilinear slab failure mechanics respectively. Thus the latter model appears more critical and better representative of maximum slope height for these parameters where unfavorable kinematics are not in evidence. Other combinations of parameters yield similar results. This is not surprising as the modelling of naturally occurring rock slabs as continuously elastic members is not realistic. Nevertheless the flexural buckling approach has been used by many engineers as an indication of maximum attainable slope height. As a result of the preceeding discussion this does not appear to be a good practice.

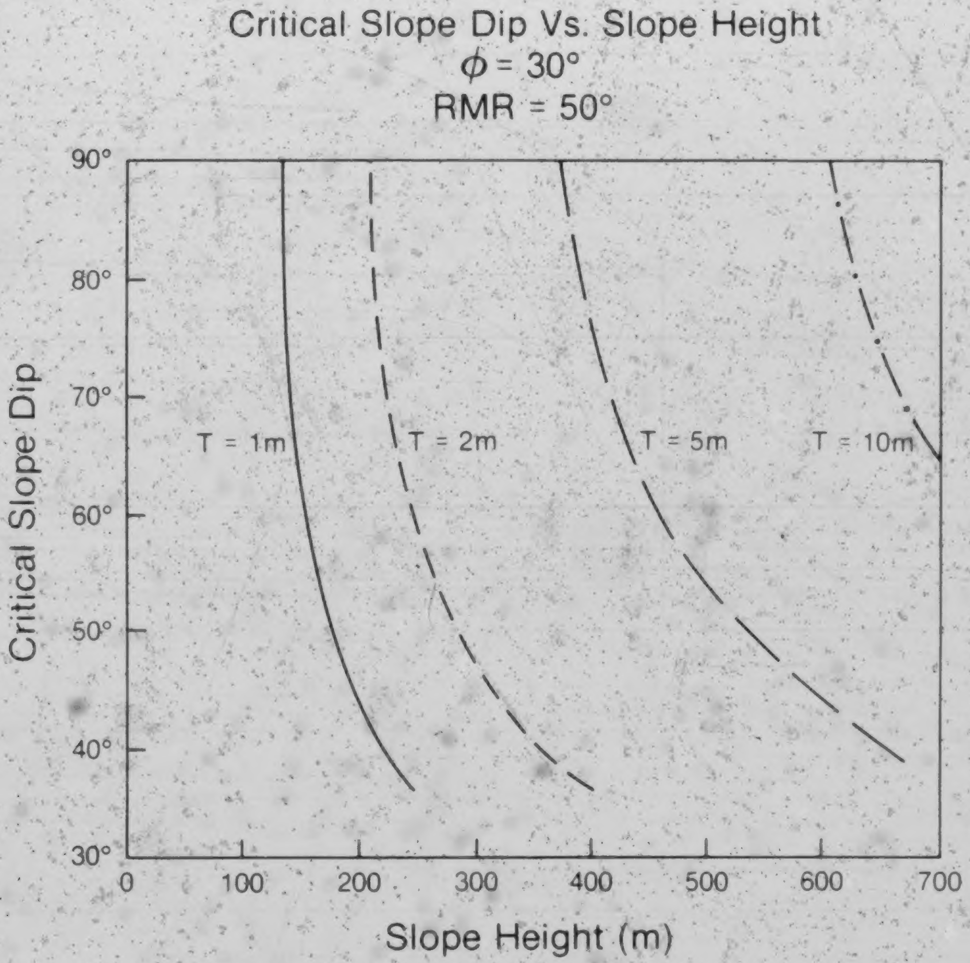

Figure 4.13 Euler-Buckling-Influence of Slab Thickness

4.4.2 Hinge Buckling

Three hinged buckling of planar and curved slopes has been examined and analyzed by Caver [40] and by Hardy Associates [41]. Cavers' three hinged buckling model involves outwards rotational movement of two rigid blocks about three hinge points (Figure 4.12.B). Hard rock slopes are normally separated by cross joints which tend to rationalize the model. Analysis and model testing by Cavers suggests that even if the slab under consideration is dissected by frequent cross joints the upper and lower blocks will still move as units with lengths close to the critical lengths governed by the statics of moment equilibrium.

For planar slab buckling the analysis involves solving force and moment equilibrium for each of the two blocks which results in six equations with six unknowns. For failure of a planar slab to occur it is necessary to invoke a lateral water force which provides the perturbing moment. Western Canadian experience [41] has been for plane buckling to occur only for very thin (few centimeters thick) slabs with low deformation modulus.

Cavers [40, 41] has also extensively examined three hinged buckling for curved footwalls and developed the CURVBUK program for this mode of failure. The program is publicly available along with the Hardy Associates [41] report, however, it was not used for this study. The analysis is similar to the planar case except that the curvature of the slope results in solving nine equations for nine unknowns. Cavers [40] has successfully back analyzed three hinged buckling failure on a thinly bedded (.6 m thick) sandstone footwall where the bedding dips, above and below a roll, are respectively 50 and 70°.

Cavers work and experience in Western Canada suggests the following considerations for three hinged buckling failure mechanics:

i. For planar slopes and those of low curvature where the line of action of the normal forces lies inside the rigid blocks, three hinge failure can only occur through moments created by high water forces. Critical failure mechanics of significantly thick slabs on such slopes is likely dominated by failure mechanisms other than buckling.

ii. For lower radius slopes and isolated rolls, where the line of action of normal forces induces a perturbing moment, consideration of a curved three hinged buckling mode should be given.

Anchoring of footwall rolls prone to buckling may be carried out by reinforcing the slope above the roll, thus effectively reducing the driving force, or by anchoring on the roll itself, thereby directly conteracting the perturbing moment. The former anchoring strategy is preferred as reinforcement can take place before the unstable roll is excavated and the exact roll gometry need not be known.

4.5 Deep Seated Failure

Analysis of deep seated failure in rock slopes is normally carried out considering failure occurring entirely within the rock mass. Thus persistent discontinuities such as bedding joints and faults do not generally influence deep seated failure mechanics, at least as far as the analysis is concerned.

For hard rock slopes such as those pertaining to this study, there is less rotational freedom within the rock mass and planar or multi-planar analyses are more appropriate. Bedding in footwall slopes forms a persistent set of discontinuities and the extent to which failure may occur entirely through the rock mass is limited to the thickness of persistent slabs of rock and the relative strength of bedding joints versus rock mass strength.

Figure 4.14.A shows the geometry of a bedded slope where planar failure occurs entirely through the rock mass. The angle β can be expressed in terms of slab thickness (T), slope height (H), and bedding dip (α) as:

$$\beta = \arctan \left\{ \frac{H \sin \alpha}{H \cos \alpha + T} \right\} \tag{4.15}$$

Figure 4.14.B shows the relationship between critical slope height and slope dip for slab thicknesses of 20 and 50 m assuming failure occurring without the influence of bedding, as shown in Figure 4.14.A. The analyses for Figure 4.14.B is calculated with RMR = 50. This figure can be compared directly with Figure 4.7 for bilinear slab failure with sliding through the rock mass toe. A comparison of the two figures reveals that the bilinear slab mechanism is more critical. Thus for "average" slope conditions bedding has an influence on slope stability up to very large slab thicknesses (> 50 m) and failure is unlikely to occur entirely through the rock mass under these conditions.

4.6 Conclusions

i. The four main failure mechanisms on bedded footwall slopes are planar slab, bilinear slab, ploughing, and buckling. All four modes have been identified in Western Canadian mountain coal mines.

ii. The mechanics of ploughing failure indicates that for "average" conditions failure is limited to slabs less than 5 m thick. The critical plough height is normally 40 to 60% of the total slope height.

iii. Euler buckling does not appear to be a realistic failure mechanism and should not be employed to predict maximum stable slope heights.

iv. In the absence of unfavorably oriented discontinuities dipping out of the footwall slope, bilinear slab failure with sliding through the rock mass toe is normally more critical than failure occurring entirely through the rock mass.

A) Geometry for Rock Mass Failure

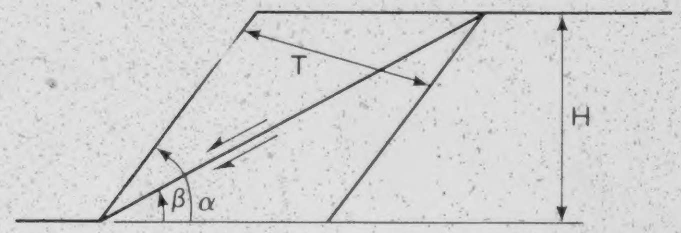

B) Critical Slope Dip Vs. Slope Height

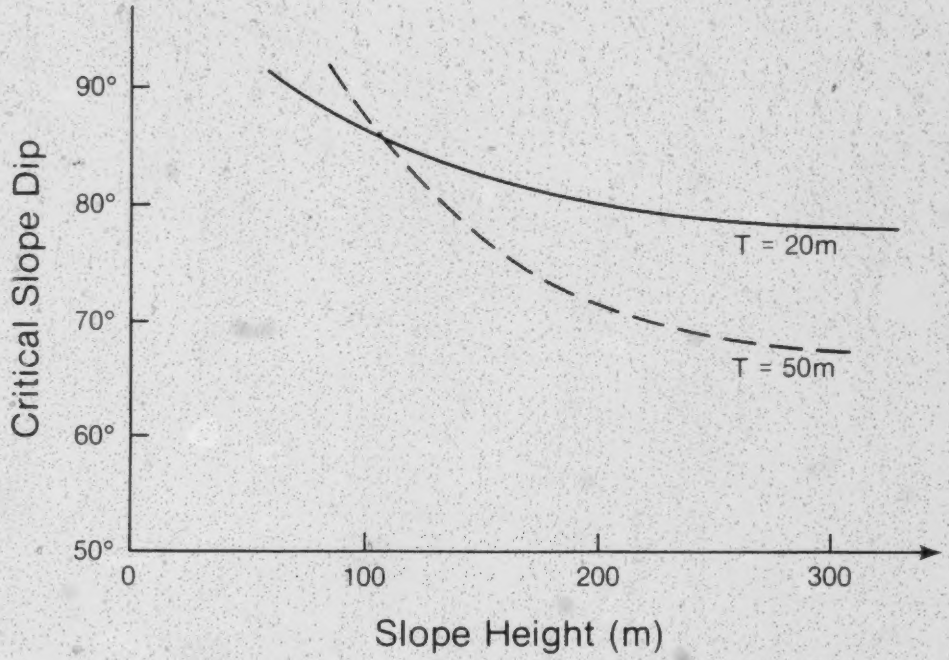

Figure 4.14 Deep Seated Failure Mechanics

v. Anchor reinforcement of bedded footwall slopes should be designed to directly reduce the force of the driving slab rather than to resist the driving slab force by supporting the toe or buckling slabs.

vi. The active factor of safety approach for anchor design is least conservative and most sensitive to uncertainties with regards to selection of design parameters.

5.0 ROCK ANCHOR DESIGN

Mechanical support to stabilize rock slopes can be carried out with rock anchors, shotcrete, wire mesh, buttresses and retaining walls. In footwall slopes the shear strength of bedding joints dominates stability considerations. Anchors offer the most efficient means to mobilize frictional resistance across bedding joints and thus are usually the best means of support. Rock anchors are most commonly made of steel formed into solid bars or wire strands referred to here as bolts or cables respectively.

Rock bolts are anchored to the rock with a mechanical expansion shell, with a resin based grout, or by expansion of a hollow anchor forming a friction bond between the anchor and rock. Where used as active support, rock bolts are pre-stressed after being anchored into the rock and the unanchored portion of the drillhole annulus is then filled with grout to protect against corrosion and lock in the tension. Rock bolts are available in diameters of 15 to 50 mm. Lengths beyond 10 m are difficult to handle and longer lengths may be fastened together with couplings. Hoek and Brown [17] provide a useful summary of different rock bolt systems. Table 5.1 presents some typical properties of high strength steel bars conforming to ASTM.A.722.

Table 5.1 Properties of High Strength Pre-Stressing Steel Bars (After ASTM.A.722)

Nominal Diameter		Nominal Area	
in.	mm	in^2	mm^2
3/4	19	0.44	284
7/8	22	0.60	387
1	25	0.78	503
1 1/8	29	0.99	639
1 1/4	32	1.23	794
1 3/8	35	1.48	955

Ultimate Tensile Strength = 150,000 psi/1035 MPa
Young's Modulus = 2×10^8 kPa

Wire strand cables are normally anchored with grout. Individual strands are normally about one-half inch in diameter. Table 5.2 shows properties for seven wire pre-stressing strand (ASTM.A.779). Multi-strand cables are commonly used to achieve very high capacity loads. Rosengren [42] states that in Australia open pit mine slopes requiring cable support commonly utilize two and four strand cables with ultimate strength of 500 kN and 1,000 kN respectively.

Table 5.2 Properties of Seven Wire Pre-Stressing Steel Strand (after ASTM.A.779)

Type	Nominal Diameter		Nominal Strand Area		Ultimate Tensile Strength	
	in.	mm	in^2	mm^2	10^3 psi	MPa
270	1/2	1.27	0.174	112	270	1860
263	0.6	15.2	0.256	165	263	1815
247	0.7	18.0	0.346	223	247	1705

Young's Modulus = 2×10^8 kPa

Cables for rock slope support provide higher load carrying capacity and are easier to handle for longer installations than solid bar rock bolts. On the other hand, rock bolts are easier to tension and generally less expensive to install. In surface mining, cables are more commonly used as deep passive reinforcing members whereas rock bolts are more common for active support of relatively shallow and well defined slip surfaces. Consequently, rock bolts are normally considered for support of bedded footwall slopes. Anchoring systems for pit slope reinforcement are normally for short term applications (less than two years), amenable to "quick-and-easy" installation, and generally less sophisticated and costly than those common to civil engineering applications. Attention in this section is focussed to those systems which are more easily adopted for mining applications.

5.1 Shear Strength and Active/Passive Systems

The shear strength of bolted rock joints has been studied in the laboratory by Bjurstrom [43], Haas [44], and Ludvig [45]. These workers and others have shown that the additional strength due to anchoring of a cohesionless rock joint is due to the bolt system shearing resistance and the tension within the bolt itself. The resistance to shear of a rock bolt is known as the "dowel effect". Experimental work has shown that the maximum shear resistance is mobilized at large displacements and at lower displacements the bolt tension is of greater importance. Dight [46] has examined the dowel effect of closed discontinuities and developed an analytic approach for design of doweled systems. Unless the reinforcement is being designed strictly as a dowelled system, common practice is to only consider the tension effect of anchor support. This is the approach taken in this study as demonstrated in Section 4.0 where the limit equilibrium analysis for bedded footwall slopes was discussed.

In an active system the anchors are pre-stressed and the limit equilibrium analyses presented in Section 4.0 is statically determinate. For passive reinforcement tension within the anchors only occurs after movement within the slope. Thus, the system is statistically indeterminate and somewhat more difficult to analyze. Rosengren [47] has developed an analytical method to examine the influence of various factors on passive cable bolts. His results show the large effect that dilation angle has on keeping displacements to a reasonable level. This effect is easy to demonstrate by examining the effect of dilation on a passive bolt installed at 90° to the mean joint plane (Figure 5.1.A). The tension in a passive bolt oriented at 90° to the mean joint plane is solely a result of dilation due to the effective roughness on the joint surface. This relationship is expressed as:

$$\tan i = \frac{QL_{AT}}{EA_A\Delta} \tag{5.1}$$

Where: i = effective dilation angle

Q = bolt tension due to roughness

L_{AT} = free stressed length of bolt

E = Young's modulus

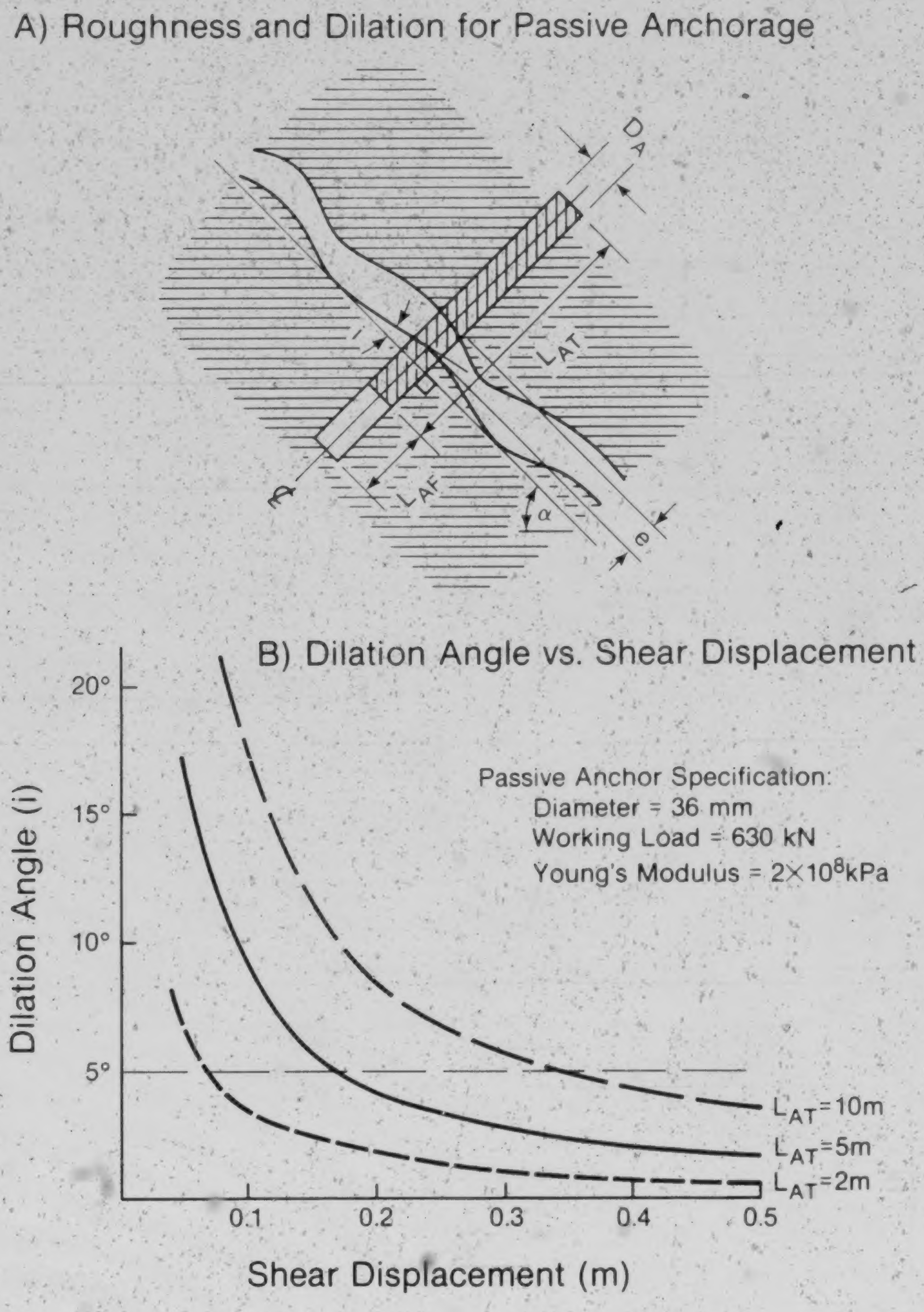

A) Roughness and Dilation for Passive Anchorage

B) Dilation Angle vs. Shear Displacement

Passive Anchor Specification:
Diameter = 36 mm
Working Load = 630 kN
Young's Modulus = 2×10^8kPa

Figure 5.1 Dilation and Passive Bolt Reinforcement

A_A = Effective anchor area

Δ = shear displacement

Now consider a typical 36 mm diameter high strength prestressed steel bar with the following properties:

E = 2 x 10 kPa

A_A = 1018 mm^2

Q = 630 kN (working load)

Figure 5.1.B shows the shear displacement necessary at different roughness angles to fully mobilize the design load on the bolt. This figure shows that at a dilation angle of 5° shear displacements of .08 and .36 m are necessary to fully utilize the design strength of the bolt with free stressed lengths of 2 m and 10 m respectively. These are large strains (≈ 4% which would certainly exceed the peak strength of most bedding joints (≈ 1%). In practice the bolt is normally oriented with an upward component thus increasing axial strain on the bolt and lowering the shear displacement to fully take advantage of the bolt working load. Passive bolting systems should normally only be considered where rock mass dilation is significant (greater than 5°), where bolts are considerably more expensive to pre-stress, or for very stiff anchor systems. None of these criteria are normally applicable to bedded footwall slopes and thus active systems should normally be considered. An exception might be where inexpensive bolting materials, such as used shovel cables, can be used for dowel support of thin slabs (< 1m) on fairly shallow slopes (≈ 40°).

5.2 Design Capacity of Anchor Systems

Once the design anchor load necessary for adequate reinforcing support (see Section 4.0) has been chosen, the capacity of various components of the system must be assessed to determine whether induced stresses set up by the anchors will instigate local failures. A grouted anchor is liable to fail under any of the following modes:

i. steel tendon failure

ii. bond failure

iii. rock mass failure

5.2.1 Steel Tendon Failure

The steel comprising the anchor itself has well defined mechanical characteristics normally conforming to design codes such as ASTM. Littlejohn and Bruce [48] recommend working loads of 50% and 60% of ultimate strength for permanent (greater than two years) and temporary support respectively. In addition, it is common practice to over-pre-stress anchors by about 10% to account for creep and play in the anchor system. Note that for pre-stressed design systems the ultimate strength is the ultimate tensile strength. Whereas for some passive systems (dowels) consideration of shear strength of the anchor might be necessary. The shear resistance of most steels is 55% to 60% of the tensile strength. As discussed in the previous section the anchor shear strength is only fully mobilized at high strains and thus this contribution to overall shearing resistance is normally ignored for most anchor systems.

Corrosion protection must also be considered. Seegmiller [35] has documented a case history where extensive tendon failure developed in partially ungrouted bolts through stress corrosion. Littlejohn and Bruce [48] provide a useful review of corrosion and corrosion protection. For temporary anchors in a non-aggressive groundwater environment fully grouted bolts do not normally require extra protection.

5.2.2 Bond Strength

Bonding of steel anchors to rock is accomplished with cement based grout or polyester resin. Table 5.3 shows advantages and disadvantages of grout versus resin based bonding systems.

Table 5.3 Cement Based Grout versus Polyester Resin Bonding Systems

Grout	Resin
• suitable for wet holes • better suited for weak rocks • better coverage in caved holes • less expensive • better suited for deep cable installations	• anchor zone must be dry • poor bonding in weaker materials • higher load carrying capacity • allows for early load transfer (i.e. quick setting time) • less susceptible to blast damage • better corrosion protection • better suited for shallow pre-stressed installations

In general, for most shallow (3 – 10 m) mining applications resin systems are preferred. Pre-stressed bolts are easily installed by using a quick setting resin (1 – 3 min) in the anchorage zone and a slow setting resin (30 – 60 min) over the free stressed anchor length to lock in the tension. In this fashion, the anchors can be installed, tensioned, and grouted in one pass.

Table 5.4 shows some results of resin bond strength (τ_B) with different rock strengths (σ_c).

Table 5.4 Strength of Polyester Resin With Rock (after Hobst and Zajic [49])

Uniaxial Compressive Strength (MPa)	Bond Strength (MPa)
5	1.2 – 1.6
14	1.6 – 3.0
50	3.0 – 5.0
100	4.0 – 7.0

For design of resin systems it can be assumed that the load bearing capacity of the rock increases uniformly with anchorage length [49]. Thus, the fixed anchorage length can be expressed as:

$$L_{AF} = \frac{Q}{\pi D_D \tau_{Ab}} \tag{5.2}$$

Where: L_{AF} = fixed anchor length
D_D = diameter of borehole
τ_{AB} = bond strength
Q = anchor load

Figure 5.2 shows the fixed anchor length versus bond strength relationship for some commonly used high strength bars. The fixed anchor lengths shown in Figure 5.2 are slightly conservative as the diameter of the bars rather than the borehole diameter was used for the calculations. Dywidag [50] recommends a bond strength of 4MPa for contact with a dry rough drill hole for rock with compressive strength of 40 to 50 MPa. A safety factor of 2 – 3 should be applied to fixed anchor length. Final design should always be based on results of field pull-out tests.

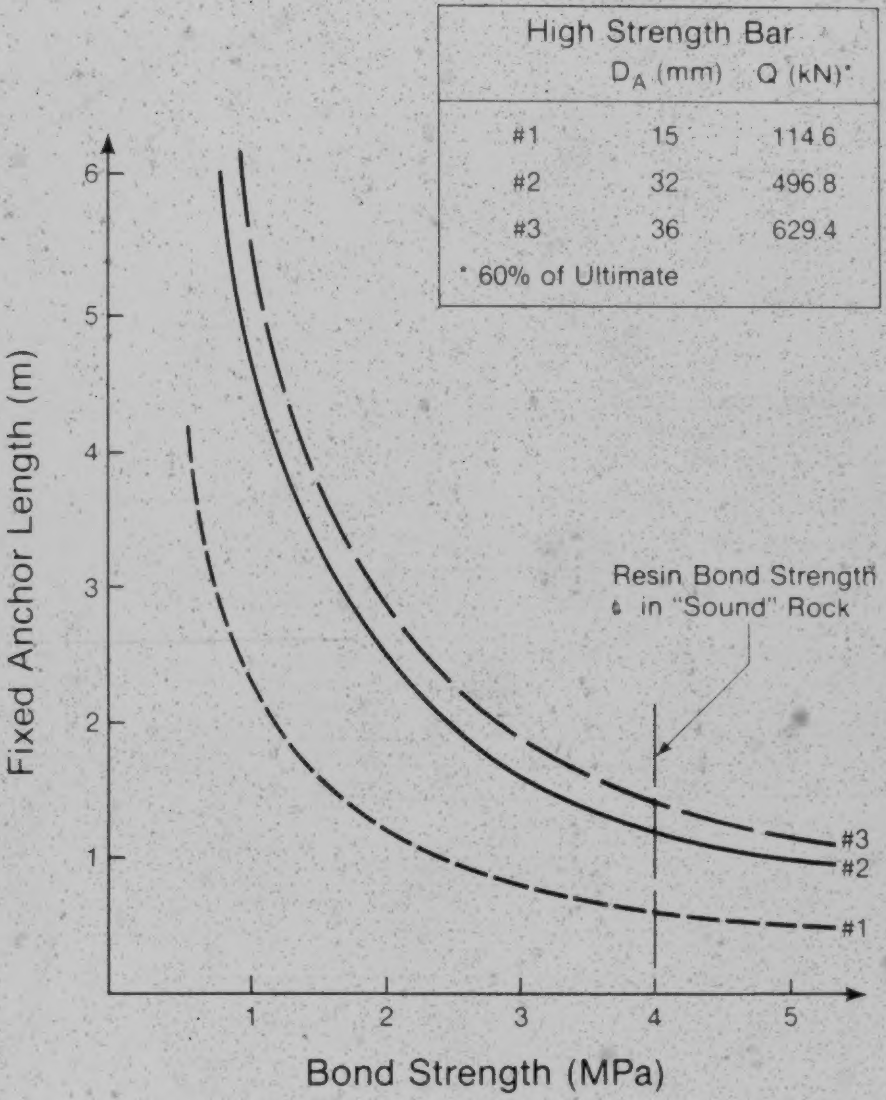

Figure 5.2 Fixed Anchor Length Design Chart (For FS = 1)

5.2.3 Rock Mass Failure

The ability of the rock mass to sustain the load induced by the anchor system depends upon the uplift capacity of the rock mass.

For uplift capacity it is common practice to assume that at failure an inverted cone of rock is pulled out of the rock mass. Littlejohn and Bruce [48] show that a friction angle cone of 60° to 90° (2ϕ) is normally assumed. For mechanical anchors the cone apex is at the end of the anchor and for bonded anchorages the apex is at the center of the fixed anchor length.

Hobst and Zazic [49] recommend formulas for determining allowable anchor loads against uplift (pullout for slopes) in the rock mass.

For a single anchor with a 90° apex pull-out cone:

$$L_{AU} = \sqrt{\frac{Q}{4.44\,\tau_{RM}}} \tag{5.3}$$

For a line of anchors with a 90° pull-out wedge:

$$L_{AU} = \frac{Q}{2.83\tau_{RM}\,L_{AH}} \tag{5.4}$$

Where: L_{AU} = depth of cone or wedge

Q = anchor load

τ_{RM} = rock mass shearing resistance

L_{AH} = horizontal anchor spacing

The rock mass strength can be expressed as:

$$\tau_{RM} = C + \sigma_n' \tan\phi \tag{5.5}$$

During uplift or pull-out the normal stress is tensile and can be assumed to be zero.

Therefore

$$\tau_{RM} \cong C \tag{5.6}$$

From Mohr-Coulomb theory cohesion shear can be expressed in terms of the uniaxial compressive strength (σ_c) and the friction angle as:

$$C = .5\sigma_c \left(\sec \phi - \tan \phi\right) \tag{5.7}$$

Equation 5.7 is not very sensitive to the range of friction angles normally encountered in rock masses (30° – 50°). Thus assuming an average friction angle of 40°:

$$C = 2.3\ \sigma_c \tag{5.8}$$

The rock mass uniaxial compressive strength (σ_{cmass}) derived from the intact value (σ_c) from equation 2.14:

$$\sigma_{cmass} = \sqrt{S}\ \sigma_c \tag{2.14}$$

And from equation 2.16:

$$S = \exp\left(\frac{RMR - 100}{6}\right) \tag{2.16}$$

Therefore:

$$\tau_{RM} \cong C = .23\ \sigma_c \exp\left(\frac{RMR - 100}{12}\right) \tag{5.9}$$

Thus, estimates of τ_{RM} for substitution into equations 5.3 and 5.4 can be obtained given intact σ_c and RMR. Figure 5.3.A shows results of equation 5.3 for single anchor uplift capacity utilizing equation 5.9 for estimating the τ_{RM}. Over the design range for high strength rock bolts commonly used for mining applications sufficient embedment is generally obtained over a wide range of hard rock materials for a minimum pull-out length of 1.5 m. However, in bedded rocks the influence of bedding may result in a different configuration of the pull-out zone. Thus, a factor of safety of 3 is recommended for design against pull-out in bedded strata.

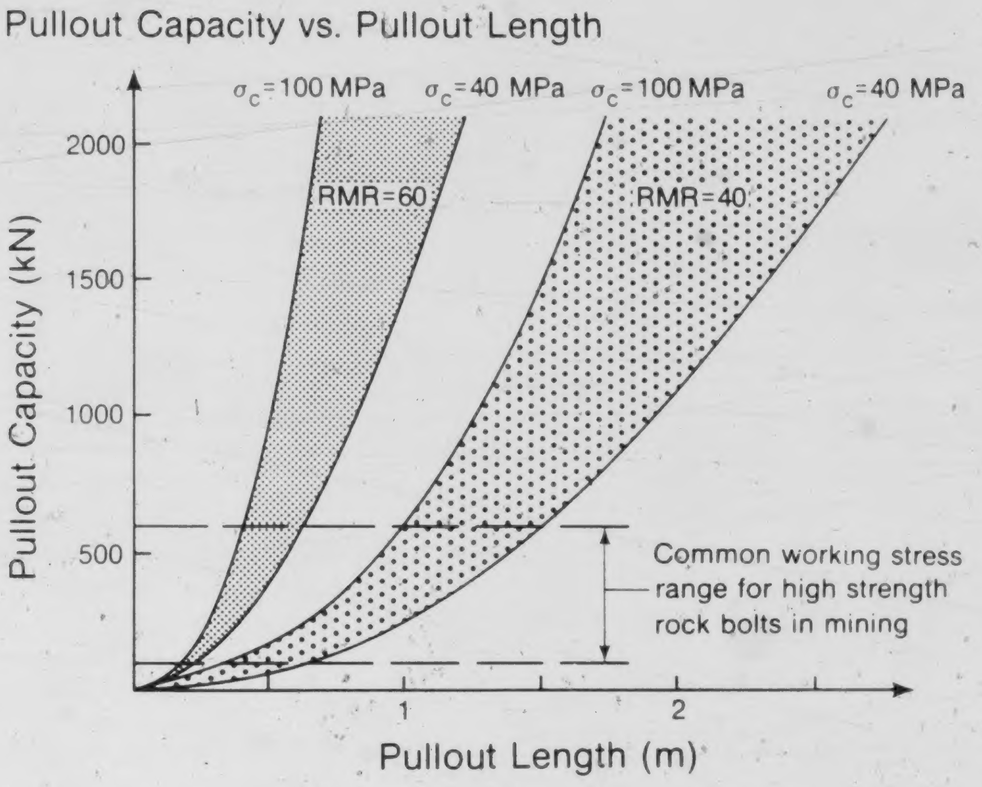

Figure 5.3 Uplift Capacity Design Chart (For FS = 1)

5.3 Anchor Patterns

The manner in which the design loads are distributed through the rock mass will be determined by the anchor pattern. For stresses imposed by a loaded area it is common practice to assume a spread of 2 (vertical) : 1 (horizontal) [51]. Thus, for a point load it can be assumed that the load is spread out over a 90° arc.

Figure 5.4 shows the manner in which the anchor load may be assumed to be distributed on a bedded slope based on the 2:1 rule assuming that the anchorage "point" is approximately twice the thickness of the design slab (in order to accommodate the reaction load). On this basis even coverage of anchor load on an unstable bedding joint can be obtained by defining vertical and horizontal anchor spacing as follows:

$$L_{AV} = \frac{T \sin \alpha}{\sin(135 + \delta - \alpha)\cos(135 + \delta - \alpha)} \tag{5.10}$$

$$L_{AH} = \frac{2T \cos \delta}{\sin(\alpha - \delta)} \tag{5.11}$$

Where: L_{AV} = vertical anchor spacing

L_{AH} = horizontal anchor spacing

T = slab thickness

δ = anchor inclination w.r.t. horizontal

α = bedding dip

As the anchor inclination angle (δ) exceeds ($\alpha - 45^\circ$) the 2:1 rule breaks down as the predicted stress distribution daylights in the slope. Figure 5.5 show results of equations 5.10 and 5.11 for different slope and anchor inclination angles with a unit slab thickness. Figure 5.5.A shows the sensitivity of the vertical spacing to the inclination angle. For most applications it seems reasonable to limit the inclination angle from 0° to 20°. For anchors installed below the horizontal the upslope tension component is lost

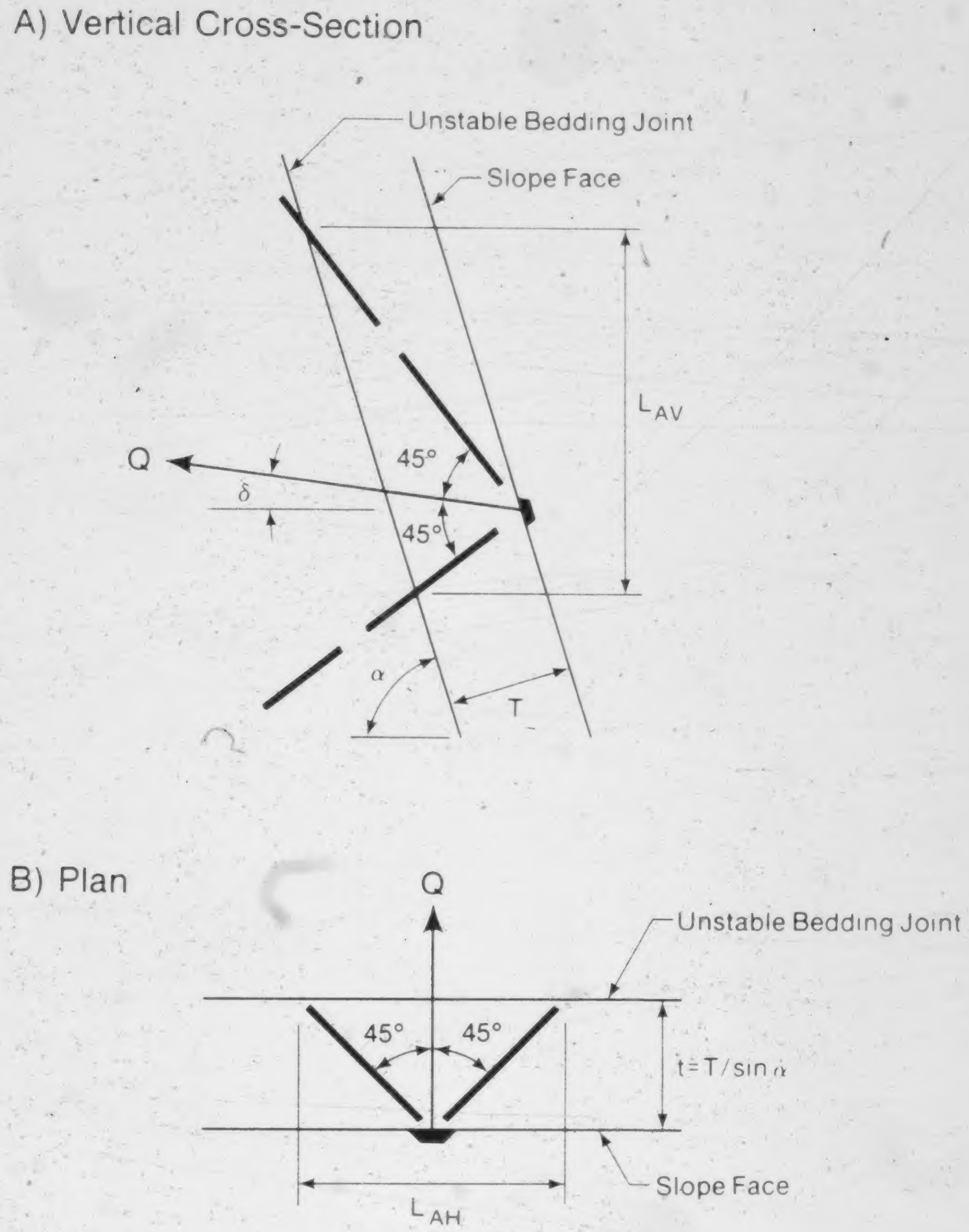
A) Vertical Cross-Section
Unstable Bedding Joint
Slope Face
L_{AV}
Q
45°
δ
45°
α
T
B) Plan
Q
Unstable Bedding Joint
45°
45°
$t = T/\sin\alpha$
Slope Face
L_{AH}

Figure 5.4 Anchor Load Distribution (2:1 Rule)

A) Vertical Spacing

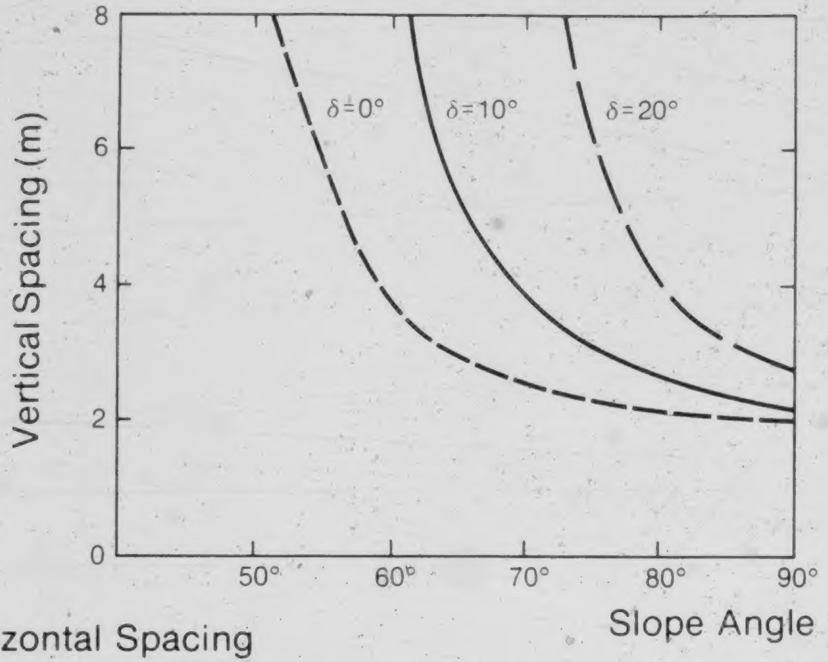

B) Horizontal Spacing

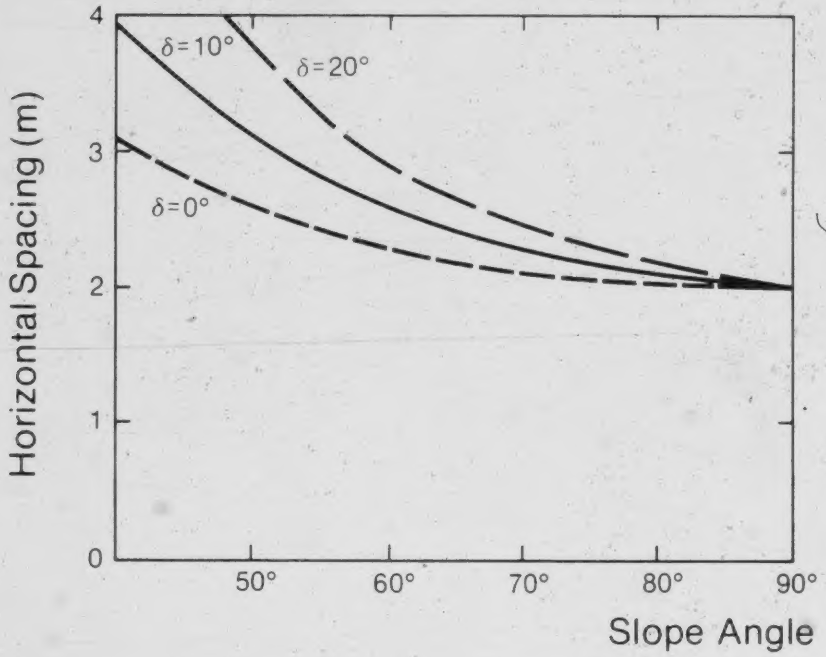

Figure 5.5 **Anchor Spacing Design Charts (for 1 m Slab Thickness)**

and beyond an installation angle of 20° unpredictable stress distributions may result. At any rate installation is logistically difficult beyond $\delta = 20°$.

In most cases achieving an even horizontal distribution of load through adjustment of spacing and anchor tension is not difficult. However, achieving even distribution of vertical load can be a problem where installation is contingent upon sequential excavation and anchor placement. For example, where mining is taking place on benches (vertical lifts) of 15 m, placing anchors at 5 m vertical intervals is costly and inconvenient. In this case the following recommendations are made:

i. Horizontal spacing should be set to distribute the load evenly along bedding strike.

ii. Vertical spacing can be adjusted to suit site conditions, geology, and failure mechanics. However, careful consideration must be taken to avoid setting spacing so that potentially unstable slabs do not occur unsupported between rows of anchors.

Note also that curvilinear shear strength envelopes are sensitive to normal stress (σ_n') variations. Thus an uneven distribution of anchor load might result in local areas of lower effective ϕ values therefore endangering the integrity of the whole slope. It is recommended that design of anchor systems be based on cohesionless linear bedding strength envelopes.

5.4 Conclusions

i. Design of anchor systems on bedded footwall slopes normally requires post-tensioned steel bolts (active support) to limit strains to reasonable levels. Once the anchor loads for reinforcement have been determined from results of limit equilibrium analyses the selection of suitable anchors and anchor patterns should be made based on ability of the rock to sustain the stresses imposed by the anchor system and the failure mechanics.

ii. For many mining applications the design charts in Figures 5.2 and 5.3 can be used to apply suitable safety factors to ensure serviceability.

iii. Table 5.5 lists recommended safety factors to be used for preliminary design in hard rock slopes.

Table 5.5 Recommended Anchor Design Safety Factors for Mining Applications

Failure Mode	Safety Factor	Comments
Anchor Tendon	1.6	63% of ultimate strength
Resin Bond	2.0	Carry out field pull tests for final design
Rock Mass Pullout	3.0	as above

iv. The vertical and horizontal spacing should be selected to ensure a suitable load distribution. Figure 5.5 can be used as an aid in that regard. For most situations, anchorage inclinations of between 0 and 20° to the horizontal are appropriate.

6.0 BEDDED FOOTWALL SLOPES IN WESTERN CANADIAN MOUNTAIN COAL MINES

Western Canada contains vast reserves of high grade coking coal largely located in two belts within the Rocky Mountain Foothills straddling the Alberta/British Columbia border. There are about one billion tonnes of "clean" coking coal reserves [52] situated near existing mining infrastructure (Figure 6.1). Within the reserve areas shown on Figure 6.1 a total of ten producers operate large efficient mines linked with sophisticated rail networks that transport coal mainly to large specialized coal loading ports situated on Canada's west coast. All of the producers operate conventional shovel/truck surface pits. One producer (Smoky River Coal Limited) also operates room-and-pillar underground mines.

During the eighties, Western Canada's coking coal production increased from 13 to 27 million tonnes per year [53]. About half of this increase was due to new production from the northeast British Columbia coal development (Bullmoose and Quintette mines) in 1984. Exports of Western Canadian coking coal comprise about 98% of total production, the majority supplied to Japan. Other export customers include South Korea, Brazil, Taiwan, and the U.S.A.

Surface mineable reserves within the mountain coal mines are located on dip slopes or where the geologic structure has thickened the coal near the surface, creating low strip ratio targets. Footwall slopes in these mines are developed parallel to bedding thus minimizing waste extraction and preventing undercutting of potentially unstable strata. It is therefore desirable to minimize the development of benches beneath the lowermost mineable coal seam. This results in high unbenched footwall slopes. The steeply dipping slopes common to mountain coal mines impose stability restrictions on the extent to which unbenched footwalls can be developed. Rational design of continuous slopes should take into consideration the design approaches discussed thus far in this study.

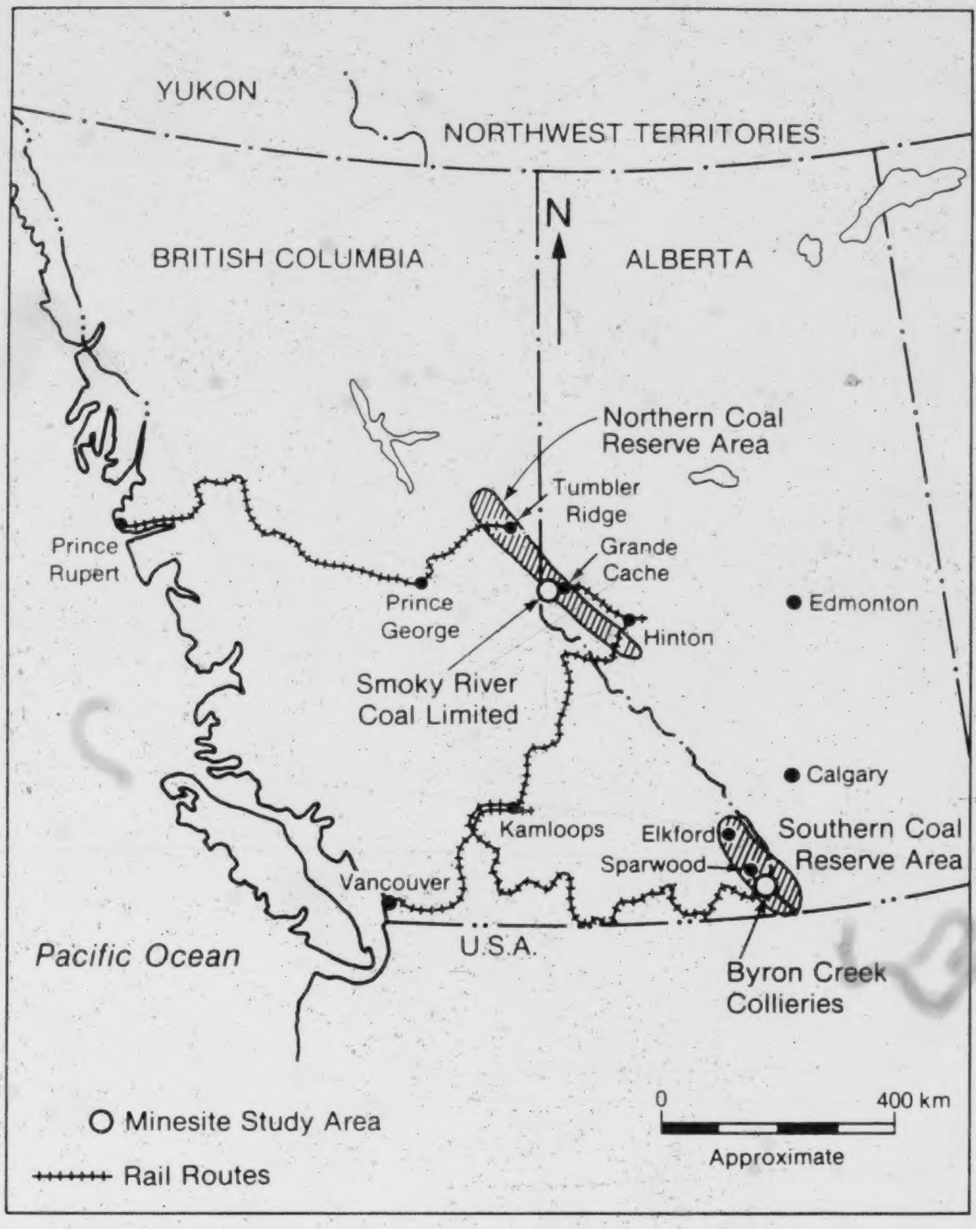
YUKON
NORTHWEST TERRITORIES
N
BRITISH COLUMBIA
ALBERTA
Northern Coal Reserve Area
Tumbler Ridge
Grande Cache
Prince Rupert
Prince George
Edmonton
Hinton
Smoky River Coal Limited
Calgary
Kamloops
Elkford
Southern Coal Reserve Area
Sparwood
Vancouver
Pacific Ocean
U.S.A.
Byron Creek Collieries
0
400 km
Approximate
○ Minesite Study Area
+++++++ Rail Routes

Figure 6.1 Western Canadian Rocky Mountain Coal Mines Reserve Areas

In addition, where anchor reinforcement is being considered, an evaluation of the economics of unsupported versus supported slopes should be carried out.

During the eighties two other studies were performed to examine the design of footwall slopes in Western Canadian mountain coal mines. Hardy Associates [41] examined the footwall at the Line Creek mine in southeastern British Columbia. This study resulted in the development of the analytical method for three hinged buckling analysis previously discussed in Section 4.4. Smoky River Coal Limited and Piteau Associates Engineering Ltd. [54] documented the detailed design, construction, and monitoring of a 100 m high, anchor reinforced, footwall slope at Smoky River Coal in north-central Alberta. During the current investigation these two studies, an extensive literature review, minesite investigations, and recent mining industry experience have been drawn upon to develop a consistent set of guidelines for footwall slopes with particular reference to mountain coal mines. The minesite investigations included field mapping and compilation of available information (from proprietary minesite studies [56]) at Smoky River Coal and Byron Creek Collieries located in the north and south mountain coal reserve areas respectively (see Figure 6.1). In addition three other minesites were visited to assess stability considerations of footwall slopes and assess industry practice. The northeastern British Columbia coal mines were not visited for this study.

In this section results of the site studies are compiled, a review of current footwall design practice is made, and an application of the design concepts discussed in this study are carried out for footwall slopes within the two study areas.

6.1 General Geology

Coal measure strata in the Western Canadian mountain regions are comprised of interbedded sandstone, siltstone, mudstone, and coal. The sandstones and siltstones are generally hard and competent, mudstones are soft and incompetent, and coal is very soft and friable. Mineable coal measures rocks of the Western Canadian mountain regions are contained within Lower Cretaceous strata. Figure 6.2 shows the stratigraphic relationship of coal measures in the northern and southern regions. Although the mineable coal measures strata in the north and south areas are not correlatable, the general lithologic character and engineering properties are markedly similar. This is in sharp contrast to the overlying Upper Cretaceous coal measures strata which is presently being mined in the outer foothills area of north-central Alberta. These Upper Cretaceous rocks are generally much weaker and contain significant amounts of bentonite.

The base of the mineable coal measure strata in both north and south regions is marked by massive marine sandstone units (Torrens Member and Moose Mountain Member) which often form the footwall. Footwalls developed within this basal sandstone unit can attain very high unbenched heights often with little risk of instability.

The predominant structural style of the mountain coal regions consists of thrust sheets separated by complexly folded strata. Thrust faults commonly display a staircase geometry exhibited by wide flats subparallel to bedding joined by narrow ramps oblique to bedding. The flats are often developed in more incompetent strata whereas ramps are generally contained within competent lithologies. Ramps tend to maintain constant angles with respect to bedding of 20 - 40°.

Folding is generally characterized by narrow hinge areas and relatively straight limbs resulting in chevron and box fold geometries. Folding within competent sandstone units is via layer parallel shearing (flexural slip) resulting in polished and slickensided

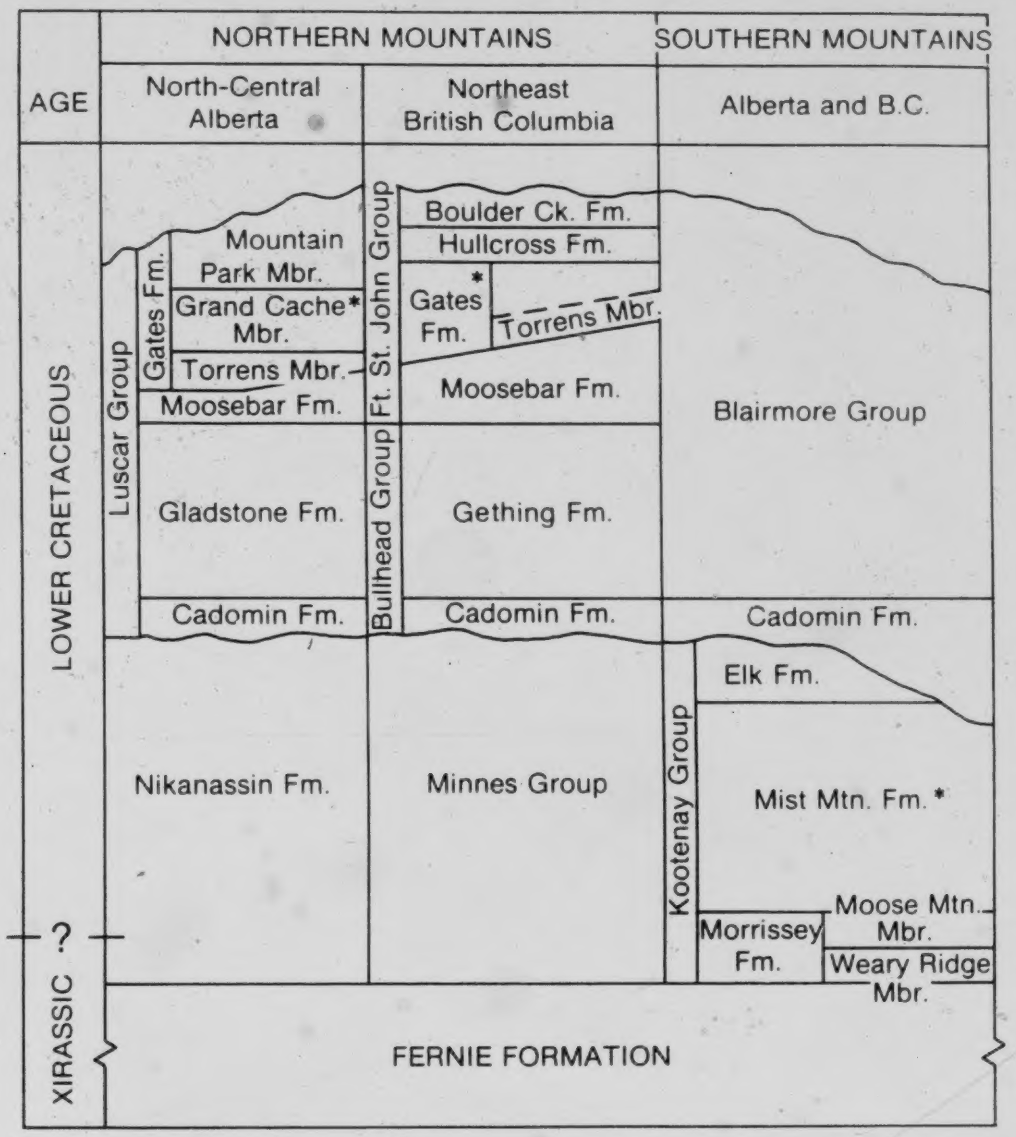
AGE
NORTHERN MOUNTAINS
SOUTHERN MOUNTAINS
North-Central Alberta
Northeast British Columbia
Alberta and B.C.
LOWER CRETACEOUS
XIRASSIC
?
Luscar Group
Gates Fm.
Mountain Park Mbr.
Grand Cache* Mbr.
Torrens Mbr.
Moosebar Fm.
Gladstone Fm.
Cadomin Fm.
Nikanassin Fm.
Bullhead Group
Ft. St. John Group
Boulder Ck. Fm.
Hullcross Fm.
Gates Fm. *
Torrens Mbr.
Moosebar Fm.
Gething Fm.
Cadomin Fm.
Minnes Group
Blairmore Group
Cadomin Fm.
Kootenay Group
Elk Fm.
Mist Mtn. Fm. *
Morrissey Fm.
Moose Mtn. Mbr.
Weary Ridge Mbr.
FERNIE FORMATION

* Producing Coal Bearing Horizons

Figure 6.2 **Coal Measures Stratigraphy of the Western Canadian Rocky Mountains**

bedding planes. Folding within incompetent strata is by simple shear in the hinge areas resulting in completely deformed rock.

6.2 Engineering Geology

Rational design in bedded slopes is best carried out by assigning engineering properties to various lithological units. Thus the four main lithologies common to coal measure strata: sandstone, siltstone, mudstone and coal form useful groupings for engineering purposes even though fairly wide variations and gradations can occur within and between these different lithologies.

Uniaxial compression testing of intact rock is measured directly by compression testing or indirectly from index tests. Table 6.1 presents a summary of the range of uniaxial compressive strengths for the different lithologies derived from minesite reports obtained during this study [56].

Table 6.1 Intact Rock Uniaxial Compressive Strength

Lithology	σ_c (MPa)
Sandstone	80 – 120
Siltstone	40 – 80
Mudstone	20 – 60
Coal	< 10

Table 6.1 shows a wide range in compressive strength reflecting the heterogeneous nature of the rock mass.

Discontinuities are usually of four types:

i. Bedding Joints
ii. Cross Joints
iii. Thrust Faults
iv. "Shear" Faults

Single bedding joints are very persistent, extending for several hundred feet with spacing varying from 0.03 to 1.5 m. Ccarser grained units commonly exhibit greater bedding joint spacing. Due to flexural slip, polished and slickensided bedding surfaces are common, especially at lithological contacts.

Cross joints normally occur in two main mutually orthogonal populations perpendicular to bedding. Cross joint sets can exhibit a fair degree of orientation scatter and less frequent subsets can occur locally. Cross joints generally show spacings of .5 to 1.5 m and are relatively discontinuous, seldom exceeding 3 m in any direction.

Thrusts faults can extend for several hundred metres and, like bedding joints can be considered to be persistent through-going discontinuities. The thrusts generally cut up section at angles of 20 - 40° to bedding dip.

Shears oriented at steep angles to bedding can occur and result in sharp dislocations of bedding planes. These shears can sometimes create serious stability problems by daylighting bedding on footwall slopes.

Hydraulic conductivity is primarily controlled by the discontinuities in the rock mass. An assessment of the data available for this study indicates that the hydraulic conductivity varies from 10^{-8} to 10^{-6} m/sec in a direction parallel to bedding. Hydraulic conductivity normal to bedding is at least one order of magnitude less than that parallel to bedding. As a result natural drainage of footwall slopes is generally poor.

Coal zones are normally the highest permeability stratigraphic units. High water pressures often build up in the coaly strata.

The shear strength of bedding joints is best assessed by considering the weakest bedding planes, as these will control the stability of most footwall slopes. In this regard an assessment of mudstone, coal, and sheared surfaces must be made. Sheared bedding surfaces are caused by the flexural slip mechanism inherent to the folding process. Figure 6.3 shows results of laboratory direct shear tests on bedding planes derived from consultants reports [56] for the two mine site areas. The data has been organized into two groups of bedding plane surfaces:

i. Mudstone Bedding Surfaces
ii. Coal and Carbonaceous Bedding Surfaces

Peak and ultimate strength values are represented by curvilinear and linear strength envelopes respectively for each of the two bedding types. With reference to Figures 6.3.A and 6.3.B the following points are made:

i. The data for each group is bracketed over a narrow range by the peak and ultimate strength values. Most of the bedding joints tested showed evidence of previous movement (i.e. flexural slip).
ii. Peak strength data for Figure 6.3.A and Figure 6.3.B show JRC values of 5 and 7 respectively. If these values are considered to be upperbound values then average peak strength JRC values derived from laboratory direct shear testing are 2.5 and 3.5 for results in Figure 6.3.A and 6.3.B respectively. Applying Barton's empirical correction formula (Equation 2.10), with field to laboratory scale ratios of 10, results in estimated JRC values of about 2 and 3 respectively. From the discussion in Section 2.3.1 these values are close to the 0 to 2 range of JRC values derived from back analyzed results.

A) Mudstone

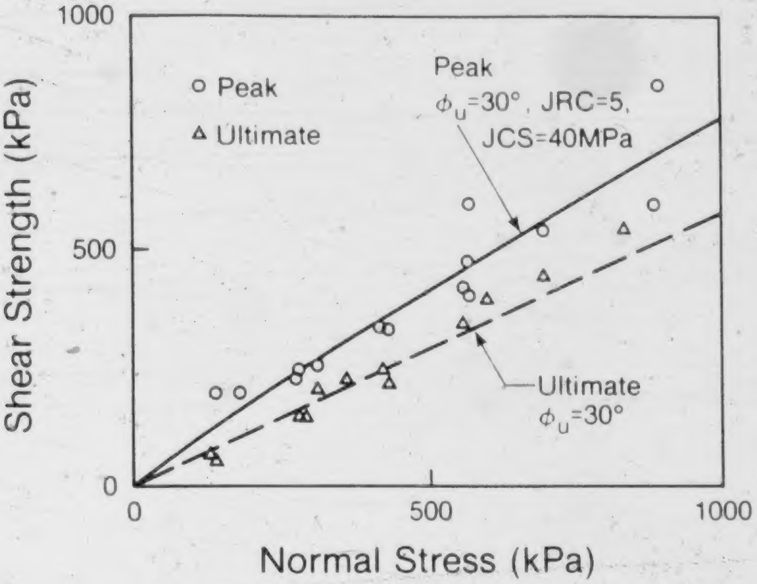

B) Coal/Carbonaceous Laminations

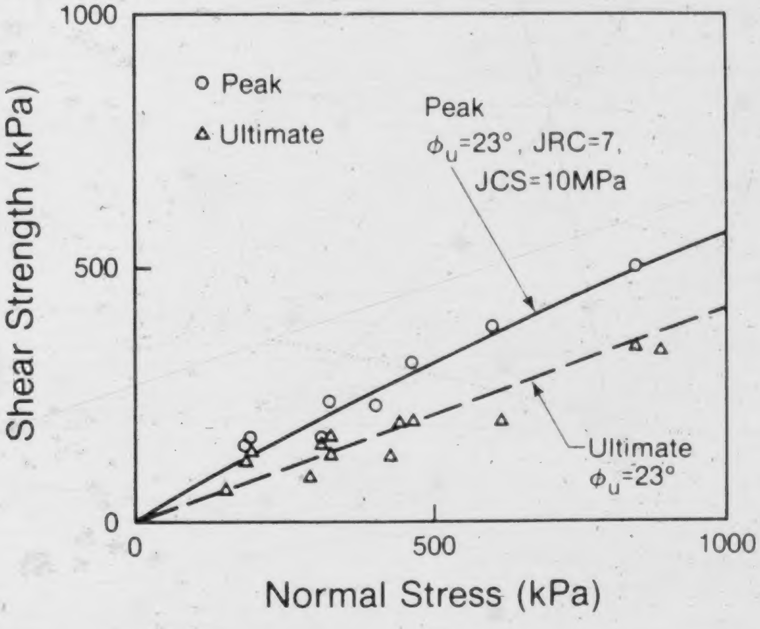

Figure 6.3 **Bedding Joint Direct Shear Test Results**

Table 6.2 summarizes the bedding joint strength parameters recommended for footwall design in Rocky Mountain Coal measures strata.

Table 6.2 Bedding Joint Strength Parameters

	Linear Envelope	Curvilinear Envelope		
	ϕ	ϕ_u	JCS	JRC
Mudstone Bedding	30 – 32°	30°	40 MPA	1 - 2
Coal/Carbonaceous Bedding	23 - 25°	23°	10 MPa	1 - 2

6.3 Design Studies

6.3.1 Smoky River Coal Limited

Smoky River Coal Limited (SRCL) mines high grade metallurgical coal by surface and underground methods in the Rocky Mountains near Grande Cache Alberta. the mine has been in continuous operation since 1970. Coal recovery is mainly from No. 4 Seam which lies 15 to 20 m stratigraphically above the basal Torrens sandstone. No. 4 Seam has a normal unstructured thickness of 6 m but attains thicknesses of up to 30 m in structurally thickened areas.

Surface mining at SRCL takes place on 13.7 m (45 ft.) benches. Waste is blasted and removed with electric cable shovels and loaders. Coal is loaded with loaders and backhoes. Footwall slopes vary from a dip of 30° to near vertical; overturned bedding is not common.

During 1985-1987 SRCL mined steep unbenched continuous footwall slope up to 100 m deep in the Upper East Limb Pit. Rock anchors were used to support daylighted bedding resulting from high angle shears in the slope. The project was unique in

Western Canada as rock anchors had not previously been incorporated for overall pit slope support. The design, mining history, and slope performance of the Upper East Limb footwall slope are well documented in a joint industry/government sponsored report by SRCL and Piteau Associates Engineering Ltd. [54]. Figure 6.4 shows the general geometry of the unbenched footwall slope. Important points drawn from the Upper East Limb study and experience at the minesite are as follows:

i. The slope was continuously supported by 6.1 m (20 ft.) to 9.1 m (30 ft.) long 36 mm (1 3/8 in.) diameter Grade 150 Dywidag threadbar anchors. The anchors were installed on a 3.0 m (10 ft.) horizontal by 4.6 m (15 m) vertical spacing in order to stabilize daylighted bedding within the slope (FS = 1.1). All anchors were post-tension grouted with a combination of fast and slow polyester resin cartridges to a working load of 667 kN (150 kips).

ii. Horizontal drainholes drilled with the airtrac drill (48 mm and 89 mm diameter holes) were effective in reducing high water pressures in the No. 3 coal seam zone about 15 m (50 ft.) behind the footwall slope. Drainholes were spaced at about 30 m (100 ft.) horizontal intervals. No drainholes were installed below the 4245 elevation.

iii. Providing that the footwall was established on bedding planes separating contrasting lithologies, well designed and carefully laid out blasting patterns provided undamaged, clean, and continuous footwall slopes. A 1.5 to 3.0 m standoff distance between the back row toe loads and the design footwalls results in minimum wall damage.

iv. Surveyed movement monitoring prisms proved to be the most practical and reliable means of slope monitoring.

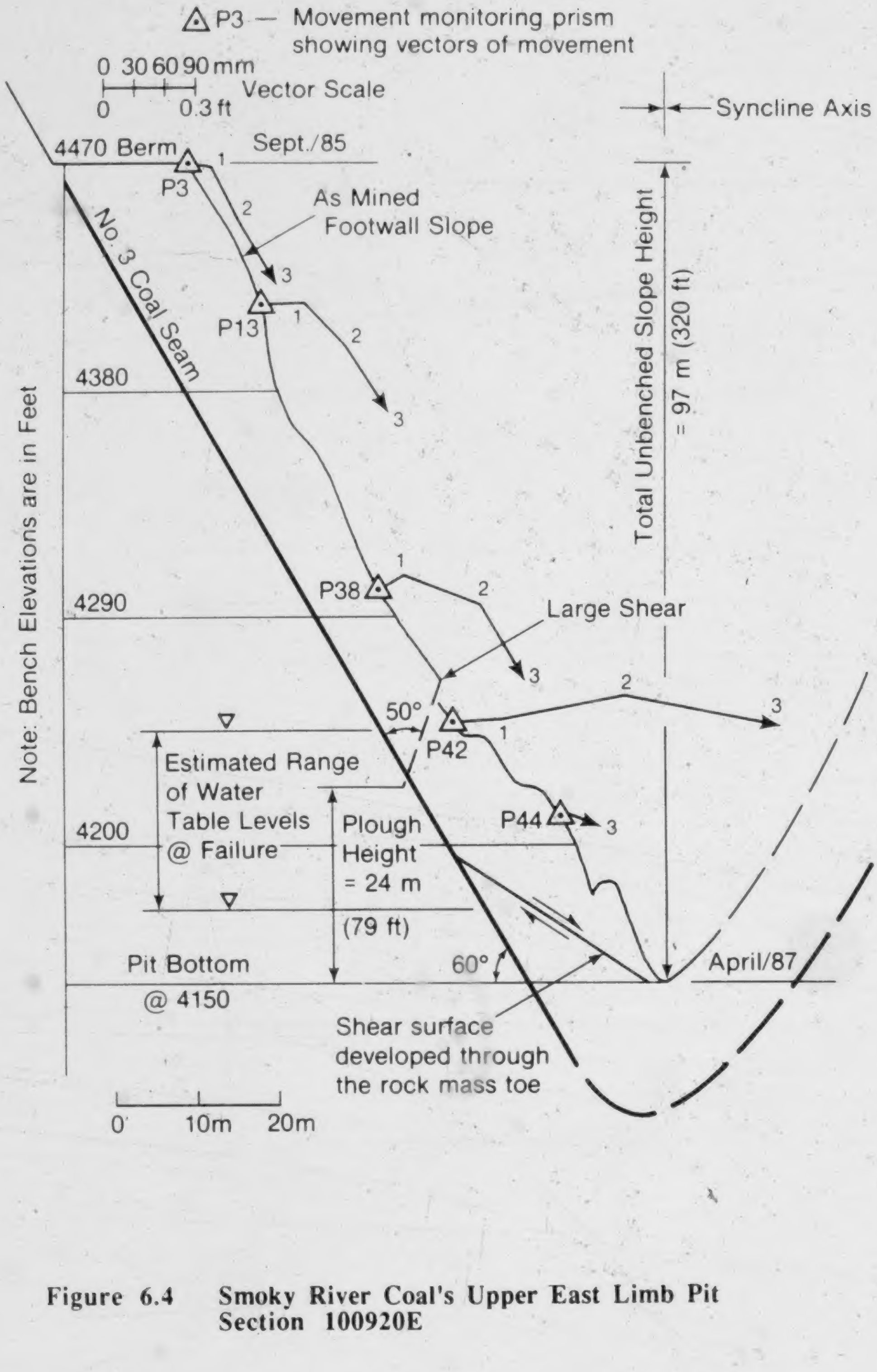
P3 — Movement monitoring prism showing vectors of movement
0 30 60 90 mm
Vector Scale
0 0.3 ft
Syncline Axis
4470 Berm
Sept./85
P3
As Mined Footwall Slope
No. 3 Coal Seam
P13
4380
Total Unbenched Slope Height = 97 m (320 ft)
Note: Bench Elevations are in Feet
P38
4290
Large Shear
50°
P42
Estimated Range of Water Table Levels @ Failure
Plough Height = 24 m (79 ft)
4200
P44
Pit Bottom @ 4150
60°
April/87
Shear surface developed through the rock mass toe
0 10m 20m
1
2
3

Figure 6.4 Smoky River Coal's Upper East Limb Pit Section 100920E

v. Considerable experience was gained in the handling, installation, and general logistics of rock bolting in a surface mining environment. An average cost of about $67.00/m of anchorage was incurred for the project. Estimated savings for the project as against an unsupported alternative were estimated to be about $500,000 or $0.80 per clean tonne of coal recovered from the pit [55]. At the end of the project anchor installation costs were greatly reduced; SRCL now uses a cost of about $50.00/m of anchorage for design and budgeting purposes.

vi. A detailed review of the prism monitoring data was made. Until February, 1987 steady movement rates of about 0.1 mm/day were in evidence. In February and during the spring of 1987 slope movements accelerated. In late March and early April average movement rates increased to greater than 1 mm/day with many prisms having movements greater than 10 mm/day. Mining was carried out only during daylight hours from April 2 until the pit was completed on April 8, 1987. On June 20, 1987 the entire slope over a 244 m (800 ft.) strike length failed back to a thin footwall marker seam (No. 3 Seam); the 100 m high by 12 m thick slab failed behind the anchor supports.

A previous back analysis of the Upper East Limb failure [54] indicated that the slope failed by ploughing along a discontinuous series of shears at about the 4270 elevation (see Figure 6.4). In this study the failure mechanics has been re-examined with consideration given to bilinear slab failure with shearing through the rock mass toe.

Prism trajectories along Section 100920E are shown in Figure 6.4 drawn from the Upper East Limb report [54]. The movement vectors have been sub-divided into three stages of movement.

i. Stage 1: initial outwards movement due to slope relaxation.

ii. Stage 2: slope dilation prior to failure

iii. Stage 3: post peak shear strength movements

Stage 3 reflects the failure mechanics prior to catastrophic collapse. The Stage 3 movements of prisms 3, 13, and 38 are parallel to bedding indicating the down-dip driving slab mechanism. Stage 3 movements for prisms 42 and 44 are much shallower than the upper prisms. These movements are now believed to be due to rock mass shearing near the toe of the slope. Note however that the overall movement for Prism 42 is much larger and generally shallower than all the other prisms. Thus the 4270 shear must be influencing slope displacements to some extent; at least for thin slabs below the shear itself. Whether overall failure developed due to ploughing behind the 4270 shear as compared with bilinear slab failure through the rock mass toe can be debated. Thus an analytical comparison of the two failure modes was undertaken for this study.

Figure 6.5 shows back analyses results of the Upper Limb failure comparing a ploughing versus bilinear slab (failure through the rock mass toe) failure mechanics which incorporates the parameters shown in Table 6.3. Unfortunately an accurate determination of groundwater levels prior to failure was not possible and thus Figure 6.5 shows an estimated range of groundwater levels.

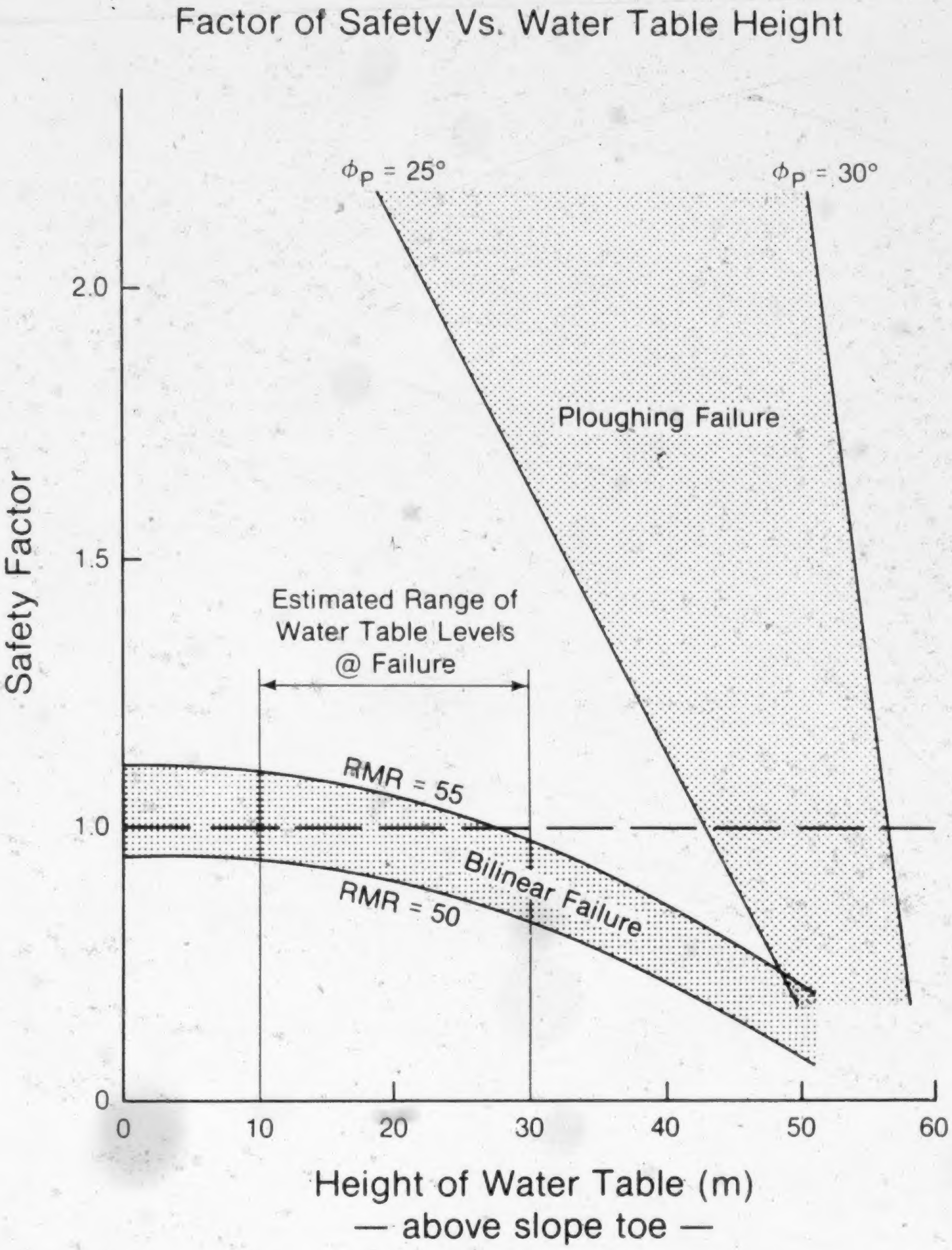

Figure 6.5 Upper East Limb Pit Failure Back Analysis

Table 6.3 Upper East Limb Back Analysis Slope Parameters

Parameter	Ploughing	Bilinear Slab
Slope Height	97 m	97 m
Slope Dip	60°	60°
Unit Wt.	25 kN/m^3	25 kN/m^3
Slab Thickness	12 m	12 m
Bedding Friction Angle (along No. 3 Seam)	25°	25°
Plough Height	24 m	NA
Plough Angle w.r.t. bedding	50°	NA
Plough Friction Angle	25°, 30°	NA
Uniaxial Compressive Strength	NA	60 MPA
Intact m	NA	10
RMR	NA	50°, 55

Results of the analysis shown in Figure 6.5 show that for the slope parameters in Table 6.2 the bilinear slab failure mode is the critical failure mechanism. The bilinear failure mode is far less sensitive to ground water pressure than the ploughing mode and the estimated RMR range fairly represents the strata under consideration. Thus it is concluded that the Upper East Limb slope failure is better represented by consideration for the bilinear slab mechanism, at least as far as the analysis presented in this study is concerned. The actual failure mechanics were probably very complex involving some surface slabbing due to ploughing and a complex development of shear zones near the slope toe. Note that although the slope was adequately supported against failure of daylighting slabs the deeper seated instability was the eventual cause of large catastrophic failure.

In order to compare the rock mass strength with linear envelopes utilizing ϕ and C values, instantaneous friction angle (ϕ_i) and apparent cohesion (C_A) were calculated. The ϕ_i values were calculated by re-arranging equation 4.7 as follows:

$$\phi_i = 2\,(\beta + 45 - \alpha) \tag{4.7}$$

The critical discontinuity angles (β) were obtained from the BILIN program. The C_A values were obtained by first calculating the rock mass uniaxial strength from equation 2.15 and 2.13:

$$S = \exp\left(\frac{RMR - 100}{6}\right) \tag{2.15}$$

$$\sigma_{C\text{mass}} = \sqrt{S}\,\sigma_C \tag{2.13}$$

Once the rock mass uniaxial strength was obtained, the C_A values were calculated from the following relationship:

$$C_A = .5\,\sigma_{C\text{mass}}\left(\sec\phi_i - \tan\phi_i\right) \tag{6.1}$$

A summary of the calculated values is as follows:

Critical Daylighting Shear Surface (β): 34 - 37°

Instantaneous Friction Angle (ϕ_i): 38 - 44°

Apparent cohesion (C_a): 180 - 360 kPa

These values are within the range of rock mass strengths derived from design studies examined for the project [56].

Subsequent to the successful implementation of rock anchor support in the Upper East Limb Pit SRCL has continued to incorporate rock anchors for pit slope design. During this study, consideration was given for rock anchoring on the E-2 Pit footwall in the No. 12 Mine area (see Figure 6.6). Mining of the west end of the pit showed that

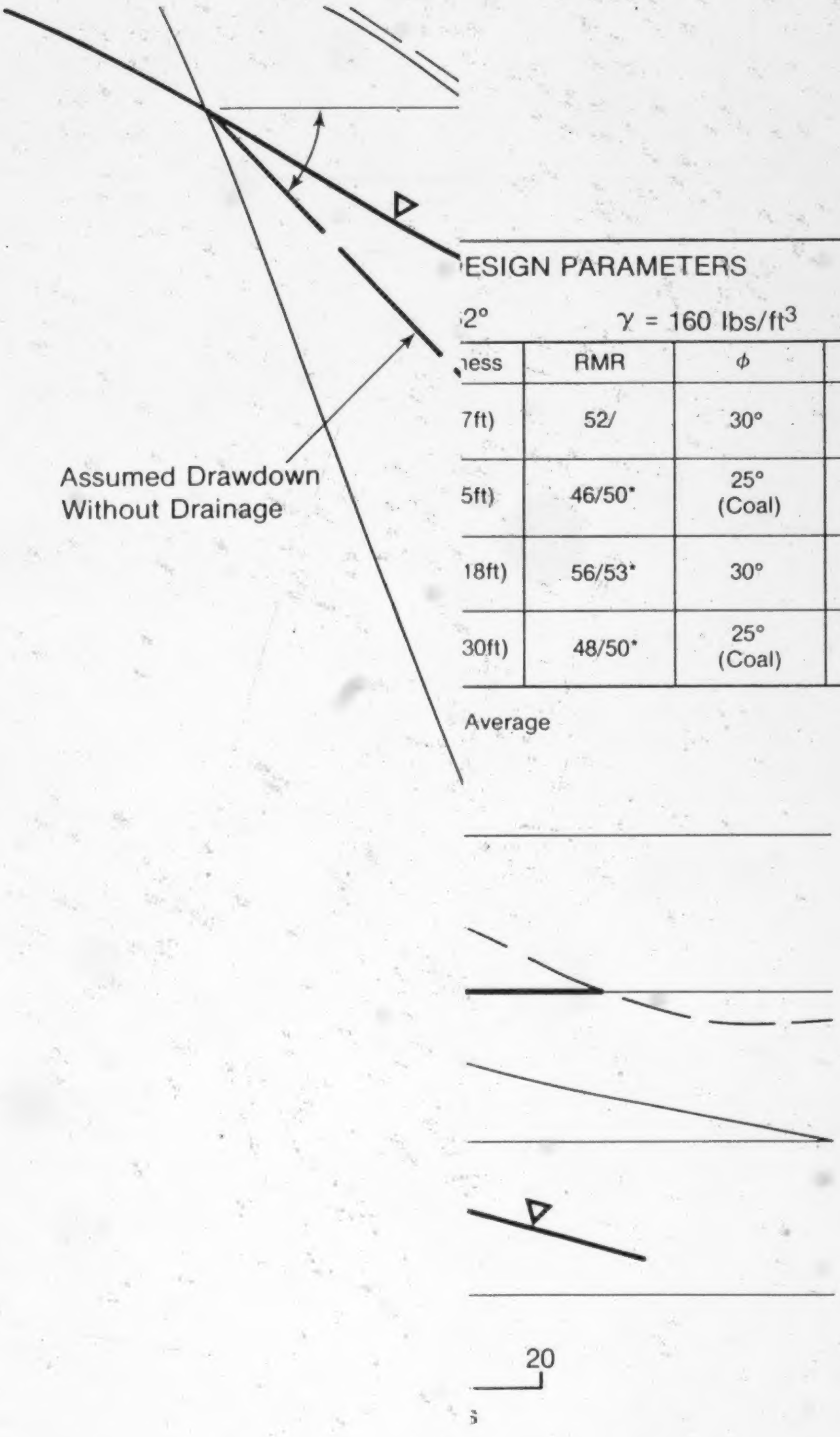
Assumed Drawdown
Without Drainage
20
s

ESIGN PARAMETERS

2° γ = 160 lbs/ft^3

ess	RMR	ϕ	Gc
7ft)	52/	30°	55 MPa (8,000 psi)
5ft)	46/50*	25° (Coal)	20 MPa (3,000 psi)
18ft)	56/53*	30°	70 MPa (10,000 psi)
30ft)	48/50*	25° (Coal)	30 MPa (4,500 psi)

Average

Figure 6.6 Smoky River Coal's E-2 Pit Section 89800E

the footwall A-B siltstone/mudstone unit could be mined as a continuous unsupported footwall up to depths in excess of 27 m (90 ft.). Unlike the Upper East Limit Pit, there were no structures present on the footwall. An evaluation was carried out to determine whether additional unbenched footwall could be feasibly mined as the volumetrics showed that if extra footwall was not required then an additional bench (45 ft./13.7 m) could be economically extracted.

Mining an additional bench involved cutting back the highwall as shown on Figure 6.6. This would result in the release of an additional 60,000 tonnes of coal in the east portion of the pit.

Field mapping was carried out on exposures in the mined out portion of the pit (Appendix F). A kinematic analysis indicated that unfavorably oriented discontinuities were not present and thus it was determined that the stability of the footwall was governed by the bilinear slab mechanism. Figure 6.6 shows the initial versus recommended designs, a summary of the design parameters derived from the field mapping program and experience on the property, and an estimate of the water table drawdown. The cross section shows the footwall stratigraphy to be well defined; this is a necessary component of detailed footwall design. Note also that there are two thin coal seams within the footwall strata.

Results of stability analyses for a dry slope show that the stability of the A-B unit approaches a factor of safety of unity at slope heights in excess of 41 m (135 ft.). Table 6.4 shows results of sensitivity analysis for an unsupported and supported A-B unit footwall slab for the design slope height of 47 m (155 ft.)

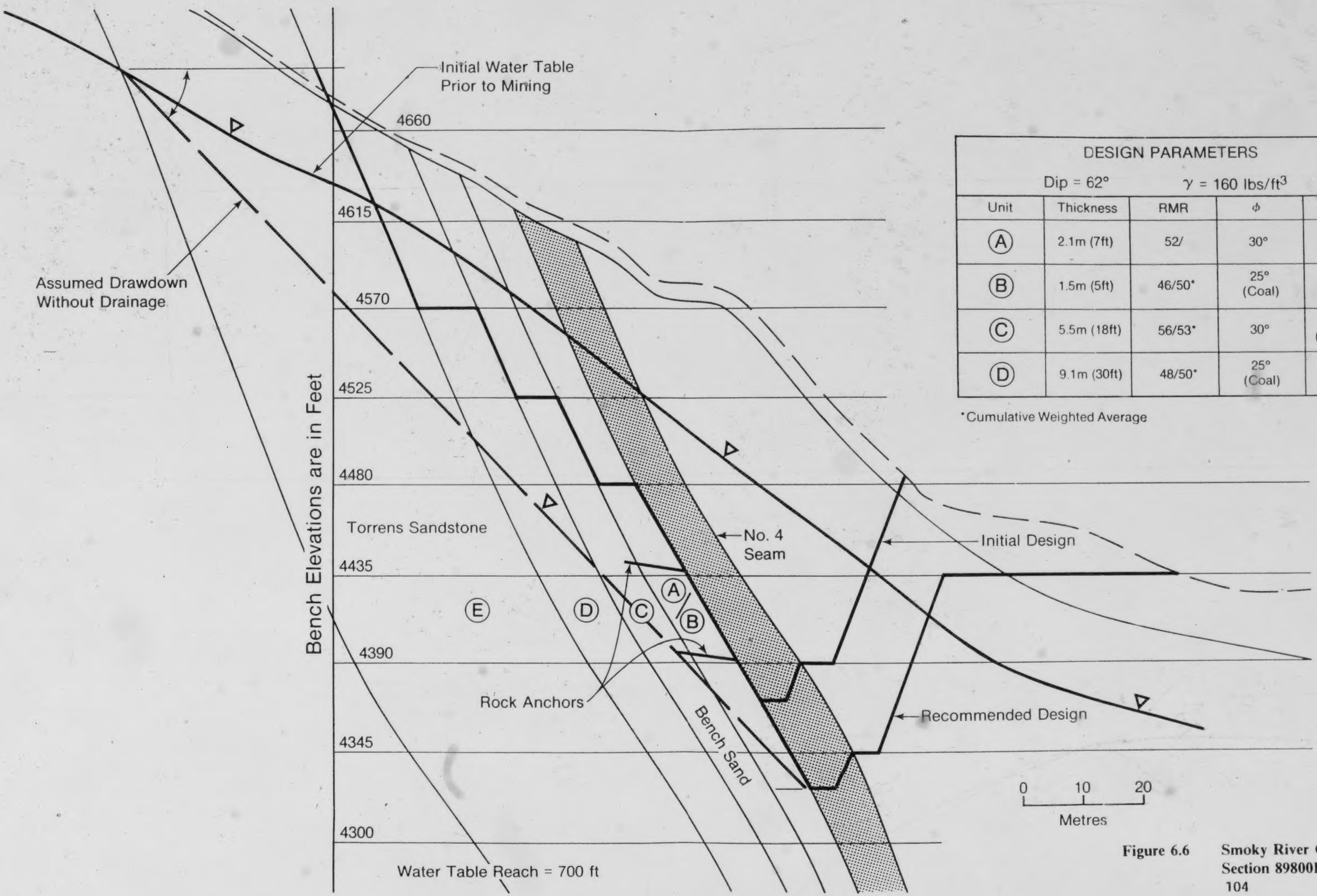
Initial Water Table
Prior to Mining
4660
4615
4570
4525
4480
4435
4390
4345
4300
Assumed Drawdown
Without Drainage
Bench Elevations are in Feet
Torrens Sandstone
No. 4
Seam
Initial Design
Recommended Design
Rock Anchors
Bench Sand
E
D
C
A
B
Water Table Reach = 700 ft
0
10
20
Metres

DESIGN PARAMETERS

Dip = 62° γ = 160 lbs/ft^3

Unit	Thickness	RMR	ϕ	Gc
Ⓐ	2.1m (7ft)	52/	30°	55 MPa (8,000 psi)
Ⓑ	1.5m (5ft)	46/50*	25° (Coal)	20 MPa (3,000 psi)
Ⓒ	5.5m (18ft)	56/53*	30°	70 MPa (10,000 psi)
Ⓓ	9.1m (30ft)	48/50*	25° (Coal)	30 MPa (4,500 psi)

*Cumulative Weighted Average

Figure 6.6 Smoky River Coal's E-2 Pit
Section 89800E

the footwall A-B siltstone/mudstone unit could be mined as a continuous unsupported footwall up to depths in excess of 27 m (90 ft.). Unlike the Upper East Limit Pit, there were no structures present on the footwall. An evaluation was carried out to determine whether additional un[illegible]nched footwall could be feasibly mined as the volumetrics showed that if extra footwall was not required then an additional bench (45 ft./13.7 m) could be economically extracted.

Mining an additional bench involved cutting back the highwall as shown on Figure 6.6. This would result in the release of an additional 60,000 tonnes of coal in the east portion of the pit.

Field mapping was carried out on exposures in the mined out portion of the pit (Appendix F). A kinematic analysis indicated that unfavorably oriented discontinuities were not present and thus it was determined that the stability of the footwall was governed by the bilinear slab mechanism. Figure 6.6 shows the initial versus recommended designs, a summary of the design parameters derived from the field mapping program and experience on the property, and an estimate of the water table drawdown. The cross section shows the footwall stratigraphy to be well defined; this is a necessary component of detailed footwall design. Note also that there are two thin coal seams within the footwall strata.

Results of stability analyses for a dry slope show that the stability of the A-B unit approaches a factor of safety of unity at slope heights in excess of 41 m (135 ft.). Table 6.4 shows results of sensitivity analysis for an unsupported and supported A-B unit footwall slab for the design slope height of 47 m (155 ft.)

Table 6.4 Bilinear Slab Failure Sensitivity Analysis in the E-2 Pit (dry slope)

	Parameter Values		% of Total Variance	
	Mean	Std. Deviation	Unsupported	Supported
Slope Height	47 m	—	—	—
Slope Dip	62°	5°	7.1	10.3
Slab Thickness	3.7 m	0.6 m	0.8	0
Bedding Friction Angle	25°	3°	2.9	4.1
Rock Compressive Strength	55 MPa	5	3.4	3.1
Intact m	10	—	—	—
RMR	50	5	85.8	82.2
Anchor Load	89 kN	9 kN	NA	0.2
Anchor Installation Angle	+ 10°	5°	NA	0.1
Factor of Safety:	Mean		1.13	1.24
	Standard Deviation		0.24	0.27

In order to investigate deeper seated slope stability for thicker slabs beyond the influence of rock anchors an analysis was carried out to assess the stability of the 18 m thick A-D slab which rests on the No. 3 coal seam directly above the massive Torrens basal sandstone unit. Figure 6.7 shows the results of this analysis for different water table elevations above the design slope toe at the 4325 elevation. Results show that measures should be taken to drain the slope down to the 4435-4390 elevation at the No. 3 Seam stratigraphic interval.

As a result of the above analysis the following recommendations were suggested for design:

i. Install tensioned rock anchors to maintain integrity of the A-B unit for 47 m (155

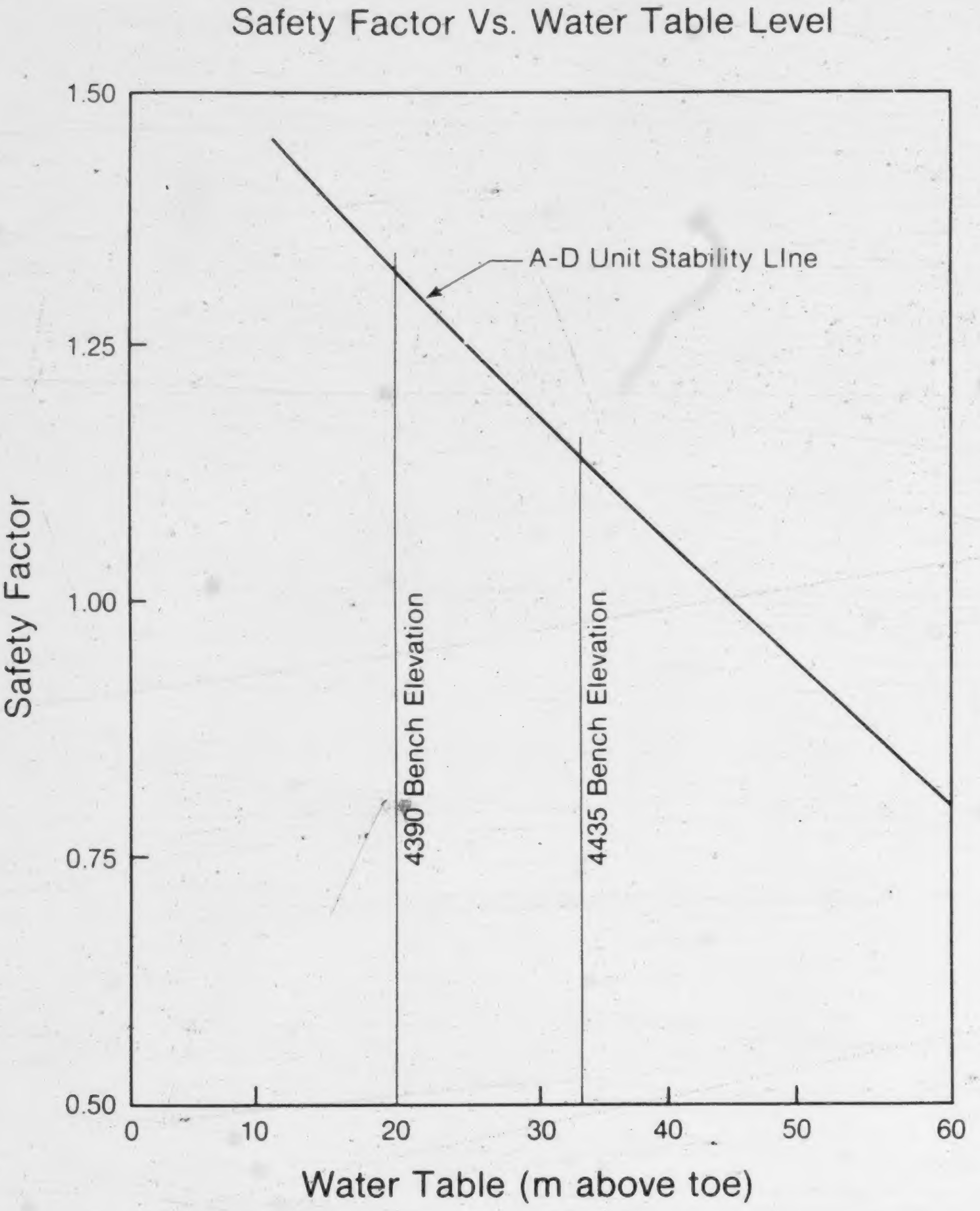

Figure 6.7 **E-2 Pit Deep Seated Design Chart**

ft.) high footwall slope. Require an anchor load of 89 kN per linear meter of slopelength horizontal. Rock anchors should be 10 m long (allowing for 3 m anchorage), tensioned to 667 kN (150,000 kip), and installed at +10° to the horizontal. The anchors can be installed in two rows (4435 and 4390 elevations) at 4.6 m (15 ft.) horizontal spacing.

ii. Maintain water table, through horizontal drainage, below the 4390 elevation and back to the No. 3 seam (base of A-D unit).

iii. Table 6.4 shows that the analysis is very sensitive to small changes in rock quality; a ±5 point difference in RMR attributes 82% of the estimated 0.3 standard deviation for the supported design. Thus, an ongoing mapping program should be carried out focussing on rock quality assessment.

6.3.2 Byron Creek Collieries

Byron Creek Collieries mines thermal and weak coking coal from surface pits located on Coal Mountain near Corbin, British Columbia. Coal mining began on coal Mountain in 1908, however the mine has only been in continuous operation since 1974. Coal recovery is from the "Mammoth" or No. 1 Seam which lies directly on the basal Moose Mountain sandstone. The Mammoth Seam is structurally thickened up to 100 m on Coal Mountain. The pits are characteristically of very low strip ratio however numerous ash partings and rock bands result in a rather high ash run-of-mine product.

The open pits at Byron Creek Collieries are developed on 10 m benches. Waste is excavated with a hydraulic shovel and loaders. Coal is removed with loaders. Footwall slopes vary in dip from 30° to 40° overturned (i.e. 60° past vertical).

During this study footwall slopes in the 51 Pit were evaluated. The 51 Pit contains structurally thickened coal situated in a northwards plunging syncline (Figure 6.8). On

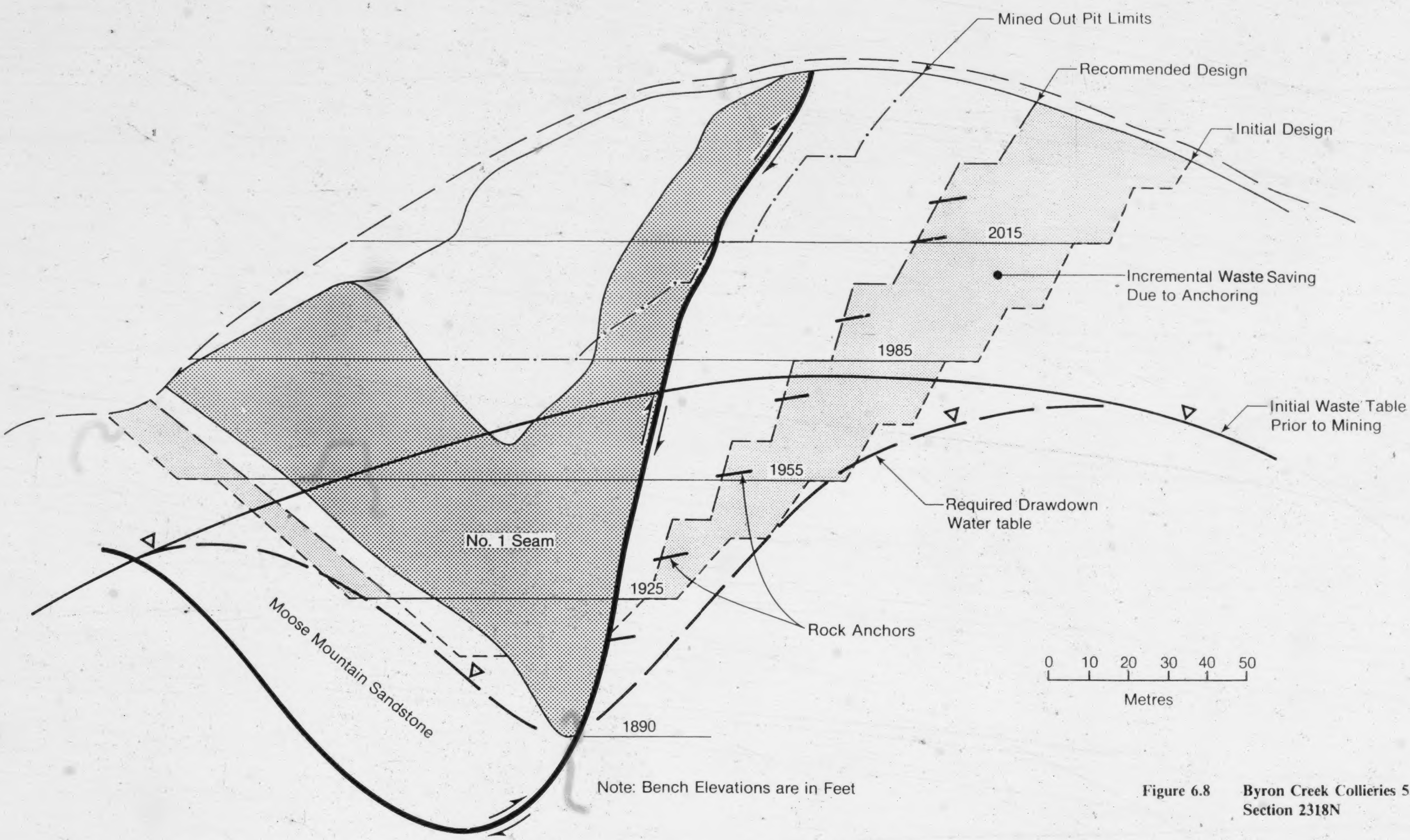
Mined Out Pit Limits
Recommended Design
Initial Design
2015
Incremental Waste Saving Due to Anchoring
1985
Initial Waste Table Prior to Mining
1955
Required Drawdown Water table
No. 1 Seam
1925
Rock Anchors
Moose Mountain Sandstone
1890
0 10 20 30 40 50
Metres
Note: Bench Elevations are in Feet

Figure 6.8 **Byron Creek Collieries 51 Pit Section 2318N**

the west wall of the pit the coal lies relatively undisturbed on the competent Moose Mountain sandstone at dips generally around 40°. On the east wall of the pit the coal seam has been thrust up over thinner bedded and generally weaker coal measure strata and dips generally vary between 50° and 60° on the upper benches. Figure 6.8 shows that below the 1985 elevation bedding dips very steeply around 75°. As shown on Figure 6.7 the pit is partially mined out to the 1985 elevation. In order to mine out the remainder of the coal within the syncline the east wall must be mined back to a stable slope angle. The current design calls for an overall slope angle of about 40°, however experience at Smoky River Coal suggests very strongly that steeper footwall slopes are attainable. Note that the ultimate pit is over 170 m deep; thus, even modest steepening would result in large savings in waste removal.

Results of field mapping on the east footwall (Appendix G) can be summarized as follows:

i. Kinematic analysis indicates that daylighted discontinuities are not present. However, numerous footwall thrusts cutting up section at angles of 20 – 40° to bedding were observed.

ii. Detailed stratigraphic and structural correlations were not possible without additional drillhole information. However, the strata generally consisted of mappable sandstone, siltstone, and mudstone units. The more competent sandstone and siltstone units exhibited bedding joint spacing of 0.3 to 1.0 m.

iii. No coal seams were encountered while traversing the mined out upper benches.

Footwall exposures were not present below the 2015 elevation thus the design for the major portion of the slope follows the existing geological interpretation as shown in Figure 6.8. The overall structural geological setting and analysis indicated that, at the very steep dips under consideration, ploughing failure might be the critical failure mechanism. The latter point is illustrated by comparing Figures 4.7 and 4.11 for ploughing failure and bilinear slab failure respectively. Figure 4.11 shows that for the very steep bedding dips under consideration ($\alpha = 75°$) a 2 m thick slab exhibits a factor of safety of unity when the slope height is 20 m. A sensitivity analysis of ploughing failure for a 2 m thick slab on a 20 m high bench is shown in Table 6.5. Both supported and unsupported conditions are shown.

Table 6.5 Ploughing Failure Sensitivity Analysis in No. 51 Pit (dry slope)

	Parameter Values		% of Total Variance	
	Mean	Std. Deviation	Unsupported	Supported
Bench Height	20 m	—	—	—
Slope Dip	75°	5	33.6	44.3
Slab Thickness	2 m	.2	12.3	6.1
Plough Angle (w.r.t. bedding)	30°	5	32.7	26.7
Plough Height	8 m	—	—	—
Bedding Friction Angle	30°	3	0.7	2.0
Plough Friction Angle	30°	3	20.8	19.7
Anchor Load	200 kN	10	NA	0.3
Anchor Installation Angle	+10°	5	NA	1.0
Factor of Safety:	Mean		1.03	1.49
	Standard Deviation		0.38	0.47

The analysis presented in Table 6.5 reflects the large uncertainties inherent in this conceptual design of the 51 Pit. On this basis anchor support to achieve a factor of safety of 1.5 is recommended at this stage.

The water table prior to mining shown in Figure 6.8 was established from static water levels on borehole geophysical logs. A deep seated bilinear analysis to examine the influence of water pressure on multi-bench stability was also carried out. On this basis it was determined that the footwall slope below the 1985 bench elevation must be effectively drained to about 20 m behind the slope face to achieve a factor of safety of 1.3 against bilinear slab failure. The required water table is shown in Figure 6.8. Above the 1985 Bench drainholes will likely not be required.

From the above discussion the following preliminary design recommendations are made:

i. Establish 20 m double benches incorporating 10 m berms from pit bottom to the 2005 elevation. A row of anchors should be installed at the midpoint of each 20 m high bench in order to stabilize individual benches against ploughing slab failure. For preliminary design 6 m long 36 mm diameter tensioned bolts should be considered. The required bolt horizontal spacing for bolts tensioned to 667 kN (150 KIPS) is 3 m.

ii. Shallower dips are present above 2005 elevation and a 30 m triple bench with similar anchor requirements is recommended for the 2005 to 2035 interval.

iii. The slope should be drained up to 20 m behind the bench faces below the 1985 Bench.

iv. Additional geological and geotechnical studies must be carried out prior to proceeding with final design in order to delineate stratigraphic units and firm up design concepts. It is unlikely that all unstabilizing discontinuities can be located with exploration drilling and ongoing geological mapping and geotechnical evaluations would constitute an important part of the footwall mining and support process. A well designed slope monitoring program would also be required.

This recommended design serves to steepen the overall 51 Pit east wall angle from 40° to 50°. Based on Figure 6.7 the incremental waste saving is estimated to be 3200 BCM per linear meter of pit length. According to the preliminary design discussed above, total anchorage requirements are estimated to be 2.3 bolts per linear meter. The initial pit area follows a strike length of about 500 m. Thus, considering a nominal cost of $50.00/m anchorage installation and $2.50/BCM of waste extraction and haulage this initial evaluation indicates an incremental saving of greater than 3 million dollars if a carefully monitored and controlled slope engineering program is applied. This presents a very significant incentive for consideration of footwall support and initiation of more detailed geotechnical studies in the 51 Pit.

6.4 Conclusions

Rational design methods can be incorporated into the design of footwall slopes in Western Canadian mountain coal mines. In this regard the following points should be noted:

i. Many footwall slopes in Western Canadian mountain coal mines are developed on strong, competent, thickly bedded basal sandstone units. In these situations there is often little requirement for support, except where stratigraphic or structural features serve to daylight bedding.

ii. Where anchor support is warranted there is potential for reducing footwall waste requirements and/or increasing recoverable coal with positive economic returns.

iii. Detailed assessment of footwall stratigraphy and structure are necessary components of the design process. Exploration efforts must be extended beyond the lowermost mineable coal seam in order to satisfy these requirements.

iv. The factor of safety for design must be assessed for each situation according to design parameter variability and uncertainty, the required slope life, and the monitoring program. In this section actual and design studies with factors of safety varying between 1.1 and 1.5 were illustrated.

7.0 DESIGN GUIDELINES

In conclusion, the following guidelines are suggested for rational design of bedded footwall slopes:

i. Footwall stratigraphy and structure must be carefully assessed at the outset of the design process. Most often a footwall can be divided into design sections distinguished by lithology. Variations within these units however must be taken into account.

ii. Shear strength parameters to be incorporated into analyses should be based on an assessment of the strength of continuous bedding joints and a separate assessment of the rock mass strength. Typical parameters for Western Canadian Coal measures strata are contained in Section 6.0.

iii. Where water is present on footwall slopes pressure is likely to be artesian. An assumption of hydrostatic water pressure distribution is not conservative due to the higher hydraulic conductivity parallel to bedding. In most cases, sub-horizontal drains drilled at a slight uphill gradient offer the most economically effective drainage option.

iv. Limit equilibrium techniques provide the best means of stability analysis. Consideration for planar, bilinear, ploughing, and hinged buckling mechanisms may be necessary. Analytical methods for planar, bilinear, and ploughing failure mechanics are contained in this report. Flexural buckling analysis does not appear to be valid. Where unfavorable discontinuities are not present, bilinear slab mechanics with failure through the rock mass toe is the most critical mechanism in most bedded footwalls.

v. For surface mining environments resin anchored tension bars provide the best means of artificial support. As a general rule-of-thumb, anchors should be dimensioned so that the total anchor length is about twice the thickness of the slab under consideration. Horizontal anchor spacing of about 2 to 5 m often provides adequate support and well distributed loads. Vertical spacing should be set according to the failure mechanism under consideration. Installation angles of 0° to 20° to the horizontal are normally appropriate.

vi. The cost of anchor support and drainage requirements should always be compared against the incremental cost of a shallower slope angle. A nominal anchor cost of $50.00/m of anchorage (1990 dollars) can be used for preliminary design.

vi. Design should always take into account the stability of deeper seated slabs behind the thinner anchor supported slabs. An assessment of drainage requirements in this regard should form an integral part of the design process. The analysis contained in this report is useful in this regard.

vii. Provided that sufficient distance is allowed between the design row toe loads, and that the footwall is established on bedding planes separating contrasting lithologies, well designed and carefully laid out blasting patterns should not damage the integrity of footwall slopes.

viii. In surface mining, slope monitoring and ongoing review form an integral part of the design process.

REFERENCES

1. Bishop, A.W., 1960, "The Principle of Effective Stress," Norwegian Geotechnical Institute, Pub No. 32.

2. CANMET, Mining Research Laboratories, 1977, *PIT Slope Manual*, CANMET Report 77-13.

3. Bruce, I.G., Cruden, D.M. and Eaton, T.M., 1989, "Use of a Tilting Table to Determine the Basic Friction Angle of Hard Rock Samples," Canadian Geotechnical Journal, Vol. 26, p. 474-479.

4. Hoek, E. and Bray, J.W., 1981, *Rock Slope Engineering*, The Institution of Mining and Metallurgy, London.

5. Krahn, J., 1974, *Rock Slope Stability with Emphasis on the Frank Slide*, Ph.D. Thesis, University of Alberta, Edmonton.

6. Hassani, F.P. and Scoble, M.J., 1985, "Frictional Mechanism and Properties of Rock Discontinuities," Proceedings of the International Symposium on Fundamentals of Rock Joints, Bjorkliden, p. 185-195.

7. Patton, F.D., 1966, "Multiple Modes of Shear Failure in Rock," Proceedings of the First Congress of the International Society of Rock Mechanics, Lisbon, p. 509-13.

8. Barton, N. 1976, "The Shear Strength of Rock and Rock Joints," International Journal of Rock Mechanics and Mining Science, Vol. 13, p. 255-279.

9. Ladanyi, B. and Archambault, G., 1969, "Simulation of Shear Behavior of a Jointed Rock Mass," Eleventh Symposium on Rock Mechanics, p. 105-125.

10. Denby, B., Hassani, F.P. and Scoble, M.J., 1983, "Shear Strength of Weak Zones in Coal Measures Slopes," Second Surface Mining and Quarrying Symposium, Institute of Mining and Metallurgy, p. 171-181.

11. Barton et al., 1978, "Suggested Methods for the Quantitative Description of Discontinuities," International Journal of Rock Mechanics and Mining Sciences, Vol. 15, p. 319-368.

12. Tse, R. and Cruden, D.M., 1979, "Estimating Joint Roughness Coefficients," International Journal of Rock Mechanics and Mining Science, Vol. 16, p. 303-307.

13. Bandis, S, Lumsden, A.C. and Barton, N.R., 1981, "Experimental Studies of Scale Effects on the Shear Behavior of Rock Joints", International Journal of Rock Mechanics and Mining Science, Vol. 18, p. 1-21.

14. Rengers, N., 1970, "Influence of Surface Roughness on the Friction Properties of Rock Planes," Proceedings of the Second Congress of the International Society of Rock Mechanics, Belgrad, Vol. 1, p. 229-234.

15. Barton, N.R. and Bandis, S., 1982, "Effect of Block Size on the Shear Behavior of Jointed Rock," 23rd Symposium on Rock Mechanics, p. 739-760.

16. Barton, N.R., Bandis, S. and Bakhtar, K., 1985, "Strength Deformation and Conductivity Coupling of Road Joints," International Journal of Rock Mechanics and Mining Science, Vol. 22, p. 121-140.

17. Hoek, E. and Brown, E.T., 1980, *Underground Excavations in Rock*, Institution of Mining and Metallurgy, London.

18. Hoek, E. and Brown, E.T., 1988, The Hoek-Brown Failure Criterion - a 1988 Update," 15th Canadian Rock Mechanics Symposium, University of Toronto, p. 1-38.

19. Bieniawski, Z.T., 1989, *Engineering Rock Mass Classifications*, John Wiley and Sons, New York.

20. Romana, M., 1985, "New Adjustment Ratings for Application of Bieniawski's Classification to Slopes," Proceedings of the International Symposium on Rock Mechanics in Excavations, Mining, and Civic Works, ISRM, Mexico City, p. 59-68.

21. Dershowitz, W.S. and Einstein, H.H., 1988. Characterizing Rock Joint Geometry with Joint System Models," Rock Mechanics and Rock Engineering, Vol. 21, p. 21-51.

22. James, P.M., 1986, "Slopes in Rock: A Design Philosophy," Proceedings of the International Symposium on Engineering in Complex Rock Formations, Beijing, China, p. 422-429.

23. McMahon, B.K., 1985, "Some Practical Considerations for the Estimation of Shear Strength of Joints and Other Discontinuities," Proceedings of the International Symposium on Fundamentals of Rock Joints, Bjorkliden, p. 475-485.

24. Author's personal files.

25. Jennings, J.E., 1970, "A Mathematical Theory for the Calculation of the Stability of Slopes in Open Cast Mines," Planning Open Pit Mines, Johannesburg, p. 87-102.

26. Brawner et al., 1971, "Stability Studies of a Footwall Slope in Layered Coal Deposit," 13th U.S. Symposium on Rock Mechanics, p. 329-365.

27. Hoek, E., 1983, "Strength of Jointed Rock Masses," Géotechnique, Vol. 33, p. 187-223.

28. Ladanyi, B. and Archambault, G., 1972, "Evaluation de la Resistance au Cisaillement d'un Massive Rocheux Fragmente," Proceedings of the 24th International Geology Congress, Montreal, p. 249-260.

29. Sharp et al., 1972, "Influence of Groundwater on the Stability of Rock Masses," Transactions of the Institution of Mining and Metallurgy, Vol. 81, p. A13-A20 and p. A113-A120.

30. Robert et al., 1977, "Groundwater Flow Systems and Slope Stability," Canadian Geotechnical Journal, Vol. 14, p. 466-476.

31. Patton, F.D., 1979, "Groundwater Instrumentation for Mining Projects," Proceedings of the First International Mine and Drainage Symposium, Denver, p. 123-153.

32. Seegmiller, B.L., 1979, "Horizontal Drains - Their Use in Open Pit Mine Dewatering," Proceedings of the First International Mine Drainage Symposium, p. 258-274.

33. Hawley, P.M., Martin, D.C. and Acott, C.P., 1985, "Failure Mechanics and Design Considerations for Footwall Slopes," 87th Annual General Meeting of the CIM, Vancouver.

34. Jaeger, J.C., 1971, "Friction of Rocks and Stability of Rock Slopes," Géotechnique, Vol. 21, p. 97-134.

35. Seegmiller, B.L., 1982, "Artificial Support of Rock Slopes," 3rd International Conference on Stability in Surface Mining, Vancouver, p. 249-288.

36. Stimpson, B. and Robinson, K.E., 1982, "A Computer Program for Footwall Slope Stability Analysis in Steeply Dipping Bedded Deposits," 3rd International Conference on Stability in Surface Mining, Vancouver, p. 437-455.

37. Dawson, R. and Sheehan, P., 1988, "Geotechnical and Mine Planning Considerations in Structurally Thickened Coal Deposits at Smoky River Coal Limited, Alberta," International Journal of Surface Mining, Vol. 2, p. 135-142.

38. Popov, E.P., 1976, "Mechanics of Materials," Prentice Hall, New Jersey.

39. Serafim, J.L. and Pereira, J.P., 1983,"Considerations of the Geomechanics Classification of Bieniawski," Proceedings of the International Symposium on Engineering Geology in Underground Construction, Lisbon, Vol. 1, p. II33-II42.

40. Cavers, D.S, 1981, "Simple Methods to Analyze Buckling of Rock Slopes," Rock Mechanics, Vol. 14, p. 87-104.

41. Hardy Associates (1978) Ltd. 1986, "Development of Design Criteria for Steeply Dipping Footwall Stability in Mountain Regions, DSS File Number 075Q 23440-5-9221.

42. Rosengren, K.J., 1986, "Wall Reinforcement in Open Pit Mining," The Aus IMM/IE Australian Newman Combined Group Large Open Pit Mining Conference, p. 257-265.

43. Bjurstrom, S., 1974, "Shear Strength of Hard Rock Joints Reinforced by Grouted Untensioned Bolts," Proceedings of the 3rd Congress of the ISRM, Vol. 2, p. 1194-1199.

44. Haas, C.J., 1981, "Analysis of Rock Bolting to Prevent Shear Movement in Fractured Ground," Mining Engineering, Vol. 33, p. 698-704.

45. Ludvig, B., 1983, "Shear Tests on Rock Bolts," Proceedings of the International Symposium on Rock Bolting, Abisko, p. 113-123.

46. Dight, P.M., 1982, *Improvement to the Stability of Rock Walls in Open Pit Mines*, Ph.D. Thesis, Monash University, Australia.

47. Rosengren et al., 1987, "Preplaced Cable Bolts for Slope Reinforcement in Open Cut Mines," Proceedings of the 6th Congress of ISRM, Montreal, Vol. 1, p. 491-495.

48. Littlejohn, G.S. and Bruce, D.A., 1977, "Rock Anchors State of the Art," Foundation Publications Ltd., Essex, England.

49. Hobst, L. and Zazic, J. 1983, *Anchoring in Rock and Soil*, Elsevier Scientific Publishing Company, New York.

50. Dywidag Systems International, Company brochure entitled "DYWIDAG Anchor Systems".

51. Canadian Geotechnical Society, 1985, *Canadian Foundation Engineering Manual.*

52. Romaniuk, A.S. and Naidu, M.G. 1986, *Coal Mining in Canada*, CANMET Report 87-3E, September, 1987.

53. Energy, Mines and Resources Canada, 1989, *Statistical Review of Coal in Canada.*

54. Smoky River Coal Limited and Piteau Associates Engineering Ltd., 1987, Upper East Limb Open Pit Rock Anchoring and Slope Monitoring Project.

55. Fawcett et al., 1987, Footwall Anchoring at Smoky River Coal Limited, 89th Annual General Meeting of the CIM, Toronto.

56. List of proprietary minesite studies made available for this project:

    A. Smoky River Coal Limited:

        i. R.M. Hardy & Associates Ltd., 1973, Report of Subsoil, Stability, Drainage and Erosional Factors Relevant to Design of Mine No. 9.

        ii. R.M. Hardy & Associates Ltd., 1976, Report on geotechnical and Hydrological Factors Relative to Proposed No. 9 Mine Extension.

        iii. Piteau Associates Engineering Ltd., 1985. Summary of Geotechnical Assessments and Design of Footwall Slopes in the Upper East Limb Open Pit.

iv. Hardy Associates (1978) Ltd., 1985, Review of Proposed Anchor Stabilization of Footwall of Upper East Limb Pit.

v. Piteau Associates Engineering Ltd., 1986, No. 12 Mine Preliminary Geotechnical and Hydrogeological Assessments.

B. Byron Creek Collieries:

i. Hardy Associates (1978) Ltd., 1982, Report on Phase I Geotechnical Investigations Related to Pit Wall Design.

ii. Golder Associates, 1982, Stability Assessment for Pit Wall Designs.

iii. Piteau Associates Engineering Ltd., 1984, Geotechnical and Hydrogeological Assessments for the Design of Open Pit Slopes at Coal Mountain.

iv. Piteau Associates Engineering Ltd., 1984, Reassessment of the Design of Open Pit Slopes of Coal Mountain for Bench Heights in Increments of Ten Metres.

v. Piteau Associates Engineering Ltd., 1986, Geotechnical and Hydrogeological Assessments for the Five Year Mine Plan for the 12 Pit and 14 Pit Areas.

57. Hamilton, R.W., 1990, *Dragline Pit Design and Sensitivity Analysis*, M.Sc. Thesis, University of Alberta, Edmonton.

58. Ang, A.H. and Tang, W.H., 1975, *Probability Concepts in Engineering Planning and Design, Volume 1, Basic Principles*, John Wiley & Sons, New York.

59. Rowe, P.W., 1962, The Stress-Dilatancy Relation for Static Equilibrium of an Assembly of Particles in Contact, Procedures of the Royal Society, Vol. 269, No. 1339, p. 500-527.

60. Morgenstern, N.R. and Sangrey, D.A., 1978, "Methods of Stability Analysis," Chapter 7 in Landslides Analysis and Control, Special Report No. 176, Transportation Research Board, National Academy of Sciences, Washington, D.C., p. 155-171.

APPENDIX A
SENSITIVITY ANALYSIS

In geotechnical engineering the natural parameters that control the physical processes upon which design decisions are based can often only be bracketed within fairly large limits due to uncertainties and natural variation. In fact this lack of certainty, common to geotechnical design problems sets the field apart from the other engineering disciplines. As a result of these recognized variations and uncertainties has emerged the observational method and various probabilistic design techniques. Before proceeding with these approaches it is necessary to consider which parameters actually control the design. Testing and monitoring efforts can then be directed at these parameters. The influence of geotechnical parameters on design is assessed via a sensitivity analysis. In this study sensitivity analysis is achieved through the use of the VARSIM computer code developed by Professor W.H. Griffin and graduate student R.W. Hamilton of the Department of Mining, Metallurgical and Petroleum Engineering at the University of Alberta. The program is fully documented in the M.Sc. thesis by Hamilton [57] and a brief explanation of the concepts along with a worked example follows.

A.1 Random Variables

A particular variable which can be assigned a set of possible values is known as a random variable. Such a variable (denoted by capital X) and its associated values (denoted by small x) may be represented by a frequency or probability distribution. If the values of a random variable are continuous then it may be described by a real valued functional relationship, $f_X(x)$, which completely defines it. An example is the Normal or Gaussian distribution which has a characteristic bell shape. The expected value of a probability distribution is known as the mean (μ_X) and the measure of dispersion about the mean is defined by the variance $\left(\sigma_X^2\right)$: The square root of the variance is known as the standard deviation (SD_X) of the random variable.

For independent identically distributed normal data, the dispersion about the mean exhibits an approximate distribution as follows:

1 SD — 68% of data

2 SD — 95% of data

3 SD — virtually all data

As a further approximation, the above relationships may be extended to any fairly symmetric "mound shaped" data distribution thus forming a useful set of guidelines for sensitivity analysis.

Ang and Tang [58] show that the mean and variance of a function of a single random variable, y = g (X), are as follows:

$$\mu_Y = E\left[g(X)\right] = \int_{-\infty}^{\infty} g(x)\, f_X(x)\, dx \qquad \text{(A.1)}$$

$$\sigma_Y^2 = E\left[g(X) - \mu_X\right]^2 = \int_{-\infty}^{\infty} \left[g(x) - \mu_X\right]^2 f_X(x)\, dx \qquad \text{(A.2)}$$

Equations (1) and (2) may be solved numerically by expanding g (X) in a Taylor's series about the mean. Ang and Tang [58] show that the first order approximation of equations A.1 and A.2 results in the following expressions:

$$\mu_Y \approx g(\mu_X) \qquad \text{(A.3)}$$

$$\sigma_Y^2 \cong \sigma_X^2 \left(\frac{dg}{dx}\right)^2 \qquad \text{(A.4)}$$

For linear functions, equations A.3 and A.4 yield very good approximations of the exact moments. For non-linear functions these approximations are usually adequate for many practical purposes. More importantly, equation A.4 is a simple but powerful tool for evaluating sensitivity of a function to variations about its estimate.

For functions of more than one statistically independent random variable,

$$y = (X_1, X_2, \ldots X_n),$$

the first order approximation of mean and variance are as follows [58]:

$$\mu_X \cong g(\mu_{X_1}, \mu_{X_2} \cdot \cdot \mu_{X_n}) \tag{A.5}$$

$$\sigma_y^2 \cong \sum_{i=1}^{N} \sigma_{X_i}^2 \left(\frac{\partial g}{\partial X_i}\right)^2 \tag{A.6}$$

Equation A.6 is the basis for propagation of error analysis and also forms the basis for sensitivity analysis incorporated into the VARSIM program. In addition to the variance component (σ_Y^2), the VARSIM program also calculates the BIAS term defined as:

$$\text{BIAS}[g(X_1, X_2 \ldots X_n)] = \sum_{i=1}^{n} \frac{1}{2} \sigma_{X_i}^2 \frac{d^2 g}{dX_i^2}$$

The bias is derived from a second approximation of the mean and provides an indication about the mean.

A.2 Using VARSIM

The VARSIM program analyses random variables of a user defined function which is referred to by the program as the double precision function REC [X (I), N]; where X(I) is an array containing N random variables to a maximum of N = 20. The REC function must be written by the user in FORTRAN 77 source code, compiled to object code, and linked with the VARSIM.LIB libraries.

Initial values of X(I) are set by the user in the REC (X_x, N) subprogram. Following the above procedure, the executable VARSIM program (execute file name defined by the user during the compiling operation) may be used for variance/bias analysis and for Monte Carlo simulation as described below.

A.2.1 Variance/Bias Analysis

Once the executable VARSIM program containing the user defined REC function has been initialized, a variance and bias component analysis table is written to the screen. An estimated mean and standard deviation value for each random variable is input and the program calculates the mean, variance, and bias of REC (X (I)) as follows:

(i) The mean or expected value of the function is calculated as REC (X (I)) where the X (I) represents the estimated value of the random variables.

(ii) The variance of the REC function is calculated as:

$$\text{VAR REC}(X(I)) = \sum_{I=1}^{N} \text{VAR}(x(I)) \left[\frac{d\,\text{REC}(x(I))}{dX(I)}\right]^2 \tag{A.7}$$

This is a first order approximation as per equation (17). The program calculates the partial derivatives with the IMSL subroutine DDERIV.

(iii) The bias is calculated as:

$$\text{BIAS } X(I) = \sum_{I=1}^{N} \frac{1}{2} \text{VAR } X(I) \frac{d^2\,\text{REC}(X(I))}{d\,X(I)^2} \tag{A.8}$$

The VARSIM program calculates the individual variance and bias terms for each variable. The sum of each of these terms is the estimated variance and bias for the function. The percentage contribution of the individual variance and bias terms to the totals for each parameter is written alongside the estimated mean and standards deviation values. This provides the user with an indication of the sensitivity of each parameter to the calculated result.

A.2.2 Monte Carlo Simulation

After performing the variance/bias analysis discussed above the VARSIM program allows the user to proceed with Monte Carlo simulation. Although a knowledge of the frequency distribution function is not necessary for the sensitivity analysis, Monte Carlo simulation requires that the distribution be defined. VARSIM allows the random variables to be assigned to normal or log-normal distributions. After receiving an initial value for the pseudo-random number generator the program obtains 1,000 Monte Carlo samples of REC (X (I, N)) writing each sample to a file in double precision list directed format. The simulation file may then be displayed with any external graphics package. Monte Carlo simulation has not been used in this study.

A.2.3 Sensitivity Analysis Example

In order to demonstrate the application of the VARSIM program for variance/bias analysis and to compare analytically derived values with those of the program, an example using the SLAB function is given. SLAB calculates the factor of safety of a planar slab with respect to sliding on a rock slope using simple rigid body static equilibrium principles. Assuming a linear Mohr Coulomb failure envelope (i.e. JRC = 0) the safety factor is expressed as:

$$FS = \tan \phi_u \left[\cot \alpha - \frac{.5\, H_W^2\, \gamma_W}{T\, \gamma\, H_X} \right] \tag{A.9}$$

Development of the limit equilibrium analyses and explanation of the variables is contained in Appendix B.

Assume typical mean and standard deviation values as follows:

Table A.1 Example Parameters

Random Variable	Mean	Standard Deviation
ϕ_u	30°	3
α	25°	3
H	30 m	3
H_w	10 m	1
T	3 m	.3
γ	25.5 KN/m^3	3
γ_w	9.81 KN/m^3	0

For the purposes of this example the standard deviation is chosen to be equal to about 10% of the mean. For sensitivity analysis it is not necessary to have an accurate knowledge of the standard deviation in a statistical sense; engineering judgement should be used to estimate the range within which the majority of values are expected to be. In the case of nearly symmetric distributions (mound-shaped) about 65 - 70% of the data will lie in this range. Substituting the above estimates of the most expected random variables (i.e. the mean) into equation 21 yields:

$$FS = 0.9462$$

Analytic solution of equation (A.7) results in the following table of values:

Table A.2 Analytic Solution of Example Variance

Random Variable	$\frac{dF}{dX\,(I)}$ @ $\mu_{X\,(I)}$	$\sigma^2_{X(I)}$	$\sigma^2_{X(I)}\left[\frac{dF}{dX\,(I)}\right]^2$
ϕ_υ	2.1851	.00274*	.0131
α	2.6064	.00274*	.0186
H	0.0097	9	.0008
H_W	– 0.0584	1	.0034
T	0.0973	.09	.0009
γ	0.0115	9	.0012
γ_W	– 0.0298	0	0

* Converted to radians

VAR (FS) = 0.0380
SD (FS) = 0.1949

Analytic solution of equation (A.8) for the BIAS term results in the following table of values:

Table A.3 Analytic Solution of Example Bias

Random Variable	$\frac{d_2^{FS}}{dX\,(I)^2}$ @ $\mu_{X\,(I)}$	$\sigma^2_{X\,(I)}$	$\frac{1}{2}\,\sigma^2_{X\,(I)}\,\frac{d^2\,F}{dX\,(I)^2}$
ϕ_υ	1.2615	.00274*	.0017
α	9.0254	.00274*	.0124
H	– 0.0006	9	– 0.0027
H_W	– 0.0058	1	– 0.0029
T	0.0002	.09	0
γ	– 0.0009	9	– 0.0041
γ_W			

* Converted to radians

BIAS (F) = 0.0044

Output from the SLAB program with the same mean and standard deviation values is as follows:

Table A.4 VARSIM Solution of Example Variance and Bias

Variable Name	Mean	Standard Deviation	% Bias	% Variance
1. Variable Dip	25.00	3.00	267.37	49.00
2. Slope Height	30.00	3.00	–52.31	2.24
3. Slab Thickness	3.00	.30	–52.31	2.24
4. Height of Water Table	10.00	1.00	–52.31	8.97
5. Rock Unit Weight	25.50	3.00	–72.40	3.10
6. Water Unit Weight	9.81	0	0.00	0.00
7. Ultimate Friction Angle	30.00	3.00	61.96	34.44

Total Bias in Safety Factor	.0056
Estimated Safety Factor	.9462
Standard Deviation of Safety Factor	.1950

The analytically derived and program values compare as shown below:

	Analytic	Program
Mean	0.9462	0.9462
Standard Deviation	0.1949	0.1950
Bias	0.0044	0.0056

Thus the mean and standard deviation compare favorably (4 and 3 decimal places respectively) whilst the bias differs by 25%. The latter difference is due to the inherent inaccuracies in the numerical second partial differentiation process. Consequently the bias should only be used as a relative indication of skewness about the mean.

The results of the program output indicate the relative degree to which the individual variance components contribute to the total variance (% VAR column). This is the most useful part of the variance analysis and indicates where efforts to better define certain random variables should be focussed. Note that the most significant variables are the dip of the slope and the friction angle. This is not surprising as the factor of a slab without water pressures is expressed simply as:

$$FS = \frac{\tan \phi}{\tan \alpha}$$

APPENDIX B
PLANAR SLAB FAILURE MECHANICS

B.1 General Geometry

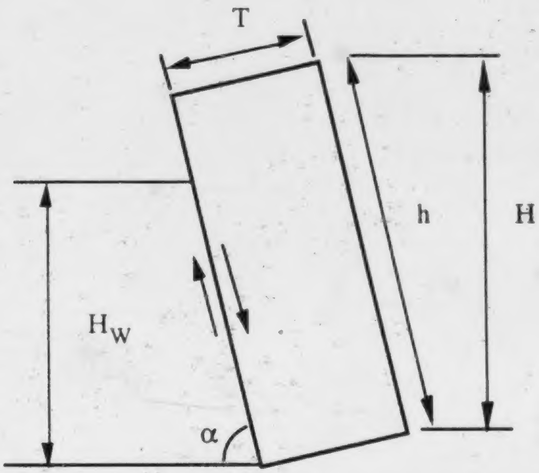

Input Parameters:

- γ = unit weight of rock
- γ_W = unit weight of water
- H = slab height
- H_W = ground water height
- T = slab thickness
- α = slope dip
- Q = anchor force
- δ = anchor installation angle

B.2 Force Equilibrium (along bedding)

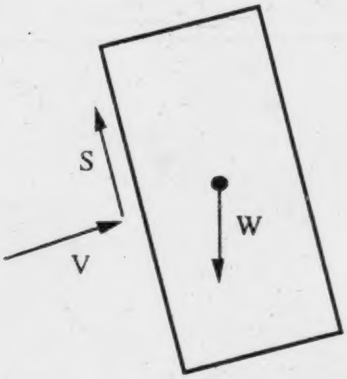

- weight of slab (W) = $\dfrac{T\gamma H}{\sin\alpha}$
- water force (V) (See B.3)
- normal force on bedding (N) = $W\cos\alpha - V$

B.3 Water Table Profile

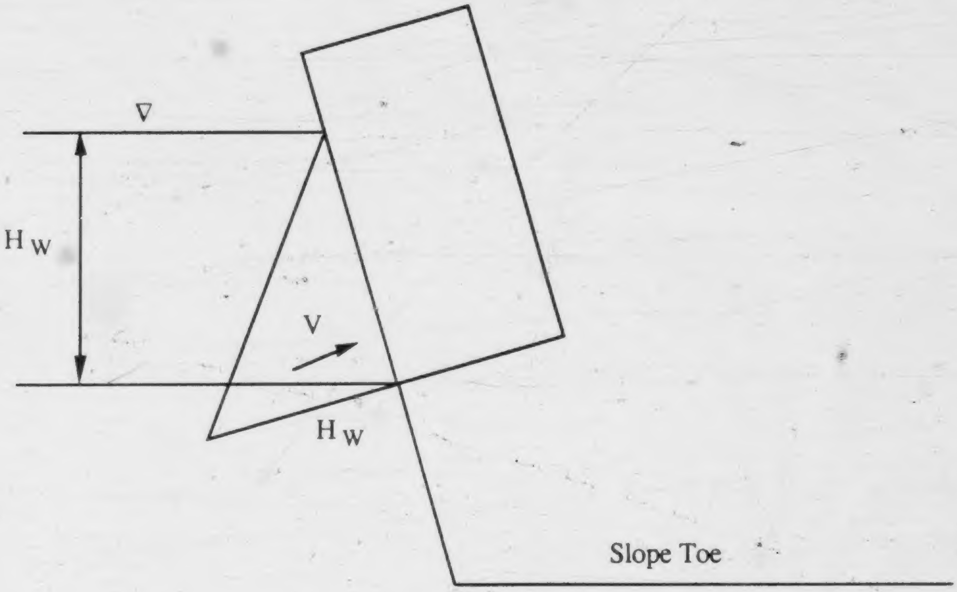

The water force distribution on the daylighted bedding plane surface assumes that the slab behavior is an impermeable barrier to seepage. Thus the maximum water pressure ($H_W \gamma_W$) occurs at the base of the slab. This is a conservative assumption, however it emphasizes the highly unstable effects that groundwater will have on slopes containing daylighted bedding. The water force (V) is expressed as follows:

$$V = \frac{\gamma H_W^2}{2 \sin \alpha}$$

- shear strength of bedding (S)

$$= N \tan\left[\phi_U + JRC \log\left(\frac{h \cdot JCS}{N}\right)\right]$$

After Barton [8] where:

ϕ_U = ultimate angle of shearing resistance

JRC = Barton's Joint Roughness Coefficient

JCS = bedding plane surface compressive strength

- factor of safety (FS)

$$= \frac{\text{Resisting Forces}}{\text{Disturbing Forces}} = \frac{S}{W \sin \alpha} \qquad \text{(B.1)}$$

B.4 Anchor Reinforcement

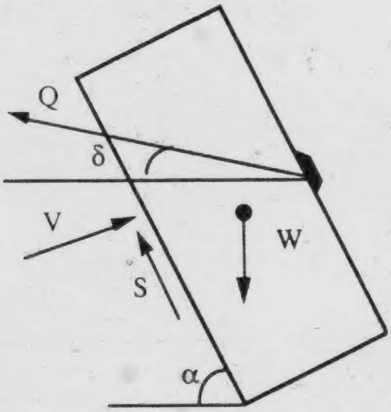

δ = anchor installation angle measured from the horizontal ('+' = upwards; '–' = downwards)

$N = W \cos \alpha - V + Q\,(\sin \alpha - \delta)$

- passive support:

$$FS_P = \frac{S + Q\cos(\alpha - \delta)}{W \sin \alpha} \qquad \text{(B.2)}$$

- active support:

$$FS_A = \frac{S}{W \sin \alpha - Q\cos(\alpha - \delta)} \qquad \text{(B.3)}$$

- excess shear support:

$$FS_{ES} = \frac{Q\left[\cos(\alpha - \delta) + \sin(\alpha - \delta)\tan\left(\phi_U + JRC \log \frac{(h \cdot JCS)}{N}\right)\right]}{W \sin \alpha - S} \qquad \text{(B.4)}$$

B.5 SLAB SUB-PROGRAM SOURCE CODE

```
       DOUBLE PRECISION FUNCTION REC(X,N)
C   TO CALCULATE SAFETY FACTOR OF A BEDDED FOOTWALL SLOPE AGAINST
C   PLANAR SLAB FAILURE
C  ***************************************************************
C
C   INPUT: "X" IS A REAL*8 VECTOR OF LENGTH 11 WHOSE COMPONENTS ARE:
C
C   X(1)= dip of footwall
C   X(2)= height of slope
C   X(3)= thickness of slab
C   X(4)= height of water table
C   X(5)= unit weight of rock
C   X(6)= unit weight of water
C   X(7)= ultimate friction angle of bedding
C   X(8)= joint roughness coefficient
C   X(9)=joint compressive strength
C   X(10)= anchor application angle
C   X(11)= anchor load
C
C   N IS A INTEGER*2 VARIABLE SET BY THE FIRST ENTRY TO REC AT 11
C
C **************************************************************
C
C  OUTPUT= INPUT IS SET BY FIRST CALL TO THIS ROUTINE AND IS UNCHANGED
C          THEREAFTER.
C
C   THE FUNCTION RETURN IN THE FORM "Y=REC(X,N)" GIVES THE
C   FACTOR OF SAFETY.
C
C ***************************************************************
C
C ERRORS: ALL VALUES MUST BE > 0.
C
C
C    USER BEWARE AS NO ERROR CHECKING IS DONE.
C ****************************************************************
      REAL*8 X(*),A,H1,W,V,N1,S
      INTEGER*2 N
      CHARACTER*28 FACT(20)
      CHARACTER*15 FRNM
      CHARACTER*7 FRUNTS
      COMMON /FUNC/FRNM,FRUNTS,FACT
      LOGICAL*4 SW
      DATA SW/.FALSE./
      DATA A/.01745329252D0/
      IF(SW)GO TO 1
      FRNM='safety factor'
      FRUNTS='no dim.'
      FACT(1)='dip of footwall in degrees'
      FACT(2)='height of slope'
      FACT(3)='thickness of slab'
      FACT(4)='height of water table'
      FACT(5)='unit wt of rock'
      FACT(6)='unit wt of water'
      FACT(7)='ultimate friction angle'
      FACT(8)='joint roughness coefficient'
      FACT(9)='joint comp. strength'
      FACT(10)='anchor application angle'
      FACT(11)='anchor load'
      X(1)=60.D0
      X(2)=10.D0
      X(3)=2.D0
      X(4)=00.D0
      X(5)=25.0D0
      X(6)=9.81D0
      X(7)=30.0
      X(8)=0.D0
      X(9)=100000.D0
      X(10)=0.D0
      X(11)=350.D0
      N=INT2(11)
      SW=.TRUE.
    1 H1=X(2)/SIN(A*X(1))
      W=X(3)*X(5)*H1
      V=(X(4)**2)*X(6)/(2*SIN(A*X(1)))
      N1=W*COS(A*X(1))
      S=N1*TAN(A*X(7))
      REC=(S)/(W*SIN(A*X(1))-X(11)*COS(A*(X(1)-X(10))))
      RETURN
      END
```

APPENDIX C
BILINEAR SLAB FAILURE MECHANICS

C.1 General Geometry

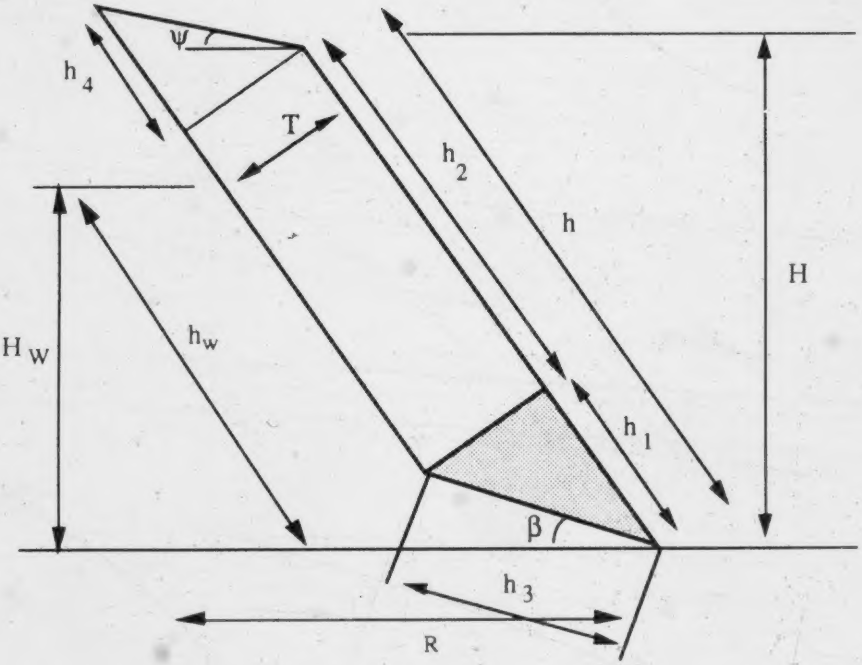

Input Parameters:

γ = unit weight of rock
γ_w = unit weight of water
H = slope height
H_W = height of water table
T = slab thickness
α = slope dip.
β = dip of secondary discontinuity set
Q = anchor tension

δ = anchor installation angle
ψ = upper slope angle
ϕ_U = ultimate angle of frictional resistance
JCS = Joint Compressive Strength
JRC = Joint Roughness Coefficient
RMR = Rock Mass Rating
m_I = intact m coefficient
σ_C = intact rock compressive strength

- $h = \dfrac{H}{\sin \alpha}$
- $h_1 = \dfrac{T}{\tan(\alpha - \beta)}$
- $h_2 = h - h_1$
- $h_w = \dfrac{H_w}{\sin \alpha}$
- $h_3 = \dfrac{h_1}{\cos(\alpha - \beta)}$
- $h_4 = T \cot(\alpha - \psi)$

C.2 General Forces

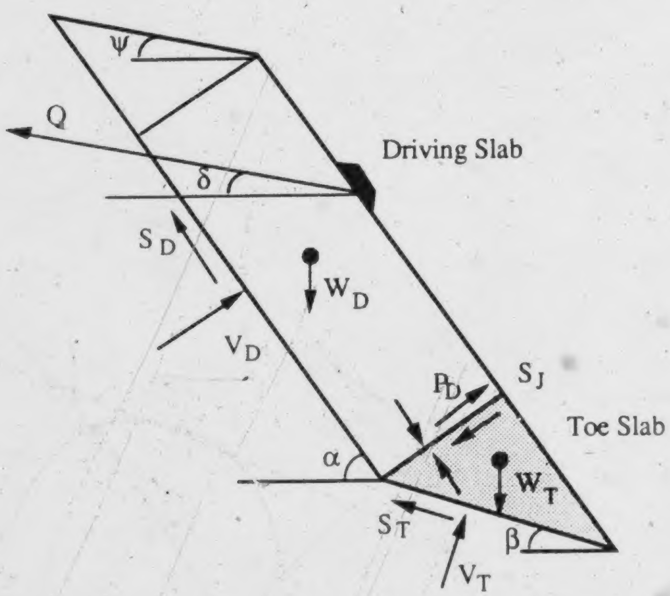
ψ
Q
δ
Driving Slab
S_D
W_D
V_D
P_D
S_J
Toe Slab
α
W_T
S_T
β
V_T

- weight of Driving Slab (W_D)
  $= T\gamma\,(h_2 + 1/2\ h_4)$
- weight of Toe Slab (W_T)
  $= 1/2\ T\gamma h_1$
- V = Water Forces – see C.3
- S = Shearing Resistances – see C.4
- Q = Anchor Load
- α = bedding dip
- β = secondary discontinuity failure angle
- δ = anchor installation angle

C.3 Water Force Distribution

Case (A): Water Table above toe slab

$$H_W > \frac{T \sin \beta}{\sin(\alpha - \beta)}$$

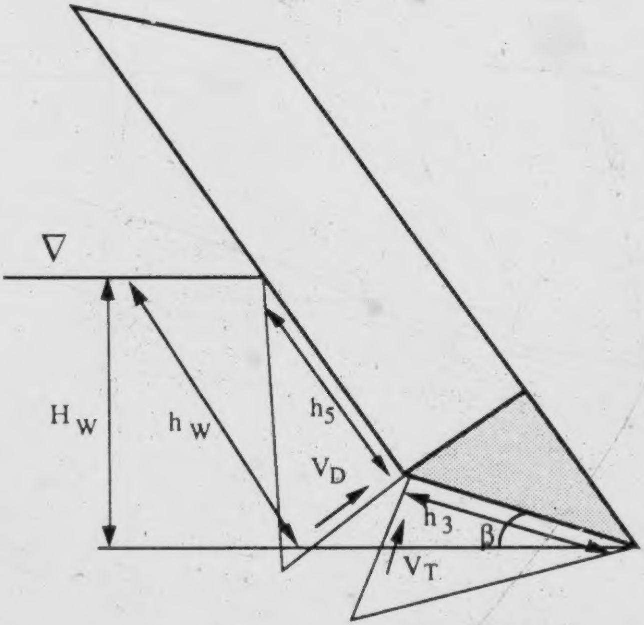

$$h_5 = h_W - \frac{T \sin \beta}{\sin \alpha \sin(\alpha - \beta)}$$

$$V_D = \frac{1}{2} \gamma_W h_5^2 \sin \alpha$$

$$V_T = \frac{1}{2} \gamma_W h_5 h_3$$

Case (B): Water table below toe slab

$$h_6 = \frac{H_W}{\sin \beta}$$

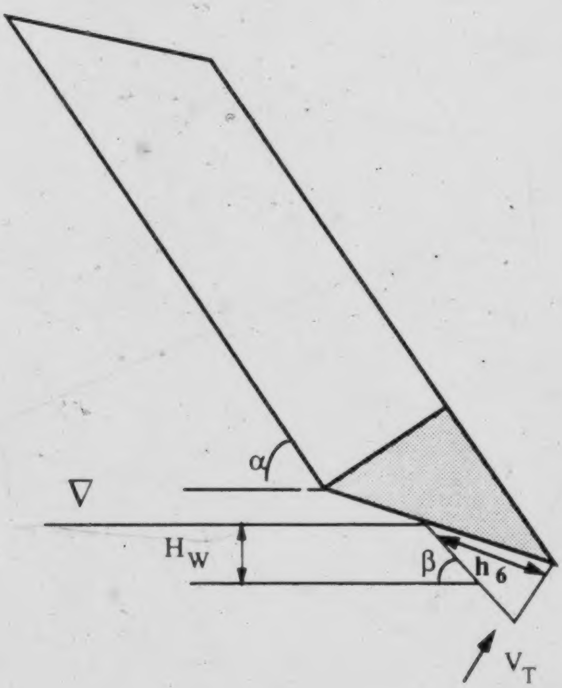

$$h_6 = \frac{H_W}{\sin \beta}$$

$V_D = 0$

$V_T = 1/2\ \gamma_W H_W h_6$

C.4 Force Equilibrium of Driving Slab

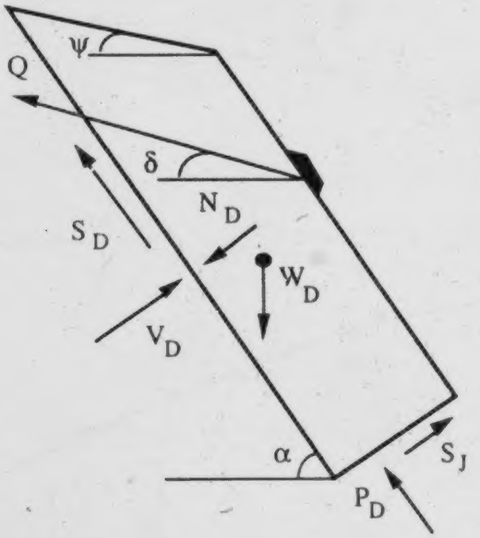

- normal force on driving slab bedding (N_D)

  $= W_D \cos\alpha - V_D + Q \sin(\alpha - \delta)$

- shear resistance of driving slab (S_D)

  $= N_D \tan\left[\phi_U + \mathrm{JRC}\log\frac{\mathrm{JCS}\,(h_2 + h_4)}{N_D}\right]$

  After Barton [8]

- excess shear force parallel to bedding (P_D)

  $= W_D \sin\alpha - S_D$

- shear resistance of driving slab cross-joint (S_J)

  $= P_D \tan\phi_J$

Anchor Load accounted for in safety factor equation.

C.5 Force Equilibrium of Toe Slab

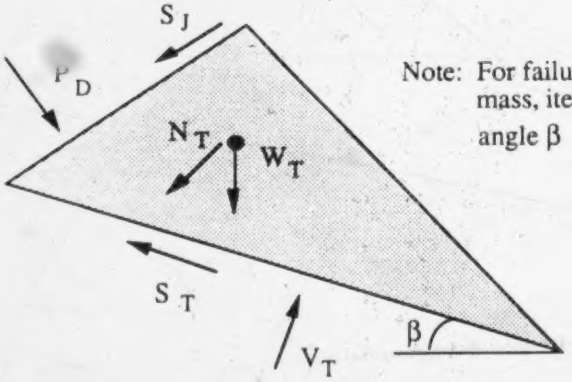

Note: For failure through the rock mass, iterate to find critical angle β

- Normal force on toe slab failure plane (N_T)

  $= W_T \cos\beta + \cos P_D (\alpha - \beta) - V_T$

- shearing resistance of toe slab failure plane (S_T)

  i. For failure along pervasive daylighting discontinuity

  $$S_T = N_T \tan\left[\phi_U + JRC \log\left(\frac{JCS \cdot h_3}{N_T}\right)\right]$$

  ii. For failure thru rock mass

  $$S_T = \frac{m \cdot \sigma_c \cdot h_3}{8}\left(\cot\phi_i - \cos\phi_i\right)$$

  After Hoek [18]

  Where: $\phi_i = \mathrm{Arctan}\left[\frac{1}{\sqrt{4\, y \cos^2 \Omega - 1}}\right]$

  $$\Omega = 1/3\left(90^\circ + \arctan\frac{1}{\sqrt{y^3 - 1}}\right)$$

  $$y = 1 + 16\left(\frac{mN_T + S\sigma_c h_3}{3m^2 \sigma_c h_3}\right)$$

  m = Hoek's cofficient for rock mass strength

$$= m_I \cdot \exp\left(\frac{RMR - 100}{14}\right)$$

After Hoek [18]

s = Hoek's s coefficient for rock mass strength

$$= \exp\left(\frac{RMR - 100}{6}\right)$$

After Hoek [18]

- Factor of Safety (FS)

i. Passive Support

$$FS_P = \frac{S_T + S_J \sin(\alpha - \beta) + Q \sin(\alpha - \delta)}{P_D \cos(\alpha - \beta) + W_T \sin\beta} \tag{B.1}$$

ii. Active Support

$$FS_A = \frac{S_T + S_J \sin(\alpha - \beta)}{P_D \cos(\alpha - \beta) + W_T \sin\beta - Q \cos(\alpha - \delta)} \tag{B.2}$$

iii. Excess Shear Support

$$FS_{ES} = \frac{Q\left[\cos(\alpha - \delta) + \sin(\alpha - \delta)\tan\left(\phi_U + JRC \log \frac{JCS\,(h_2 + h_4)}{N_D}\right)\right]}{P_D \cos(\alpha - \beta) + W_T \sin\beta - S_T} \tag{B.3}$$

C.6 BILIN SUB-PROGRAM SOURCE CODE

```
        DOUBLE PRECISION FUNCTION REC(X,N)
C   TO CALCULATE SAFETY FACTOR OF A BEDDED FOOTWALL SLOPE AGAINST
C   BILINEAR SLAB FAILURE
C   ****************************************************************

C   INPUT: "X" IS A REAL*8 VECTOR OF LENGTH 15 WHOSE COMPONENTS ARE:
C
C   X(1)= dip of footwall
C   X(2)=dip ofdaylighting discontinuity
C   X(3)= height of slope
C   X(4)= thickness of slab
C   X(5)= height of water table
C   X(6)= unit weight of rock
C   X(7)= unit weight of water
C   X(8)= ultimate friction angle of bedding
C   X(9)= joint roughness coefficient
C   X(10)= joint compressive strength
C   X(11)= rock compressive strength
C   X(12)= intact m coefficient
C   X(13)= rock mass rating
C   X(14)= angle of upper slope
C   X(15)= anchor application angle
C   X(16)= anchor force
C
C   N IS A INTEGER*2 VARIABLE SET BY THE FIRST ENTRY TO REC AT 13
C
C ****************************************************************
C
C  OUTPUT= INPUT IS SET BY FIRST CALL TO THIS ROUTINE AND IS UNCHANGED
C         THEREAFTER.
C
C   THE FUNCTION RETURN IN THE FORM "Y=REC(X,N)" GIVES THE
C   FACTOR OF SAFETY.
C
C *****************************************************************
C   USER BEWARE AS NO ERROR CHECKING IS DONE.
C ******************************************************************
      DOUBLE PRECISION X(*),A,M,S,ST1,B,H,H1,H2,H3,H4,H5,H6,HW,WD
      DOUBLE PRECISION H7,SJ,BMAX,C
      DOUBLE PRECISION WT,VD,VT,ND,SD,FD,NT,E,QI,ST,Z,Y,K
      INTEGER*2 N
      CHARACTER*28 FACT(20)
      CHARACTER*15 FRNM
      CHARACTER*7 FRUNTS
      COMMON /FUNC/FRNM,FRUNTS,FACT
      COMMON /BET/B
      COMMON /BM/BMAX
      LOGICAL*4 SW
      DATA SW/.FALSE./
      DATA A/.01745329252D0/
      OPEN(12,FILE='OUT')
      IF(SW)GO TO 1
      FRNM='safety factor'
      FRUNTS='no dim.'
      FACT(1)='dip of footwall'
      FACT(2)='dip of daylighting discont.'
      FACT(3)='height of slope'
      FACT(4)='thickness of slab'
      FACT(5)='height of water table'
      FACT(6)='unit wt of rock'
      FACT(7)='unit wt of water'
      FACT(8)='ultimate friction angle'
      FACT(9)='joint roughness coefficient'
      FACT(10)='joint comp. strength'
      FACT(11)='rock comp. strength'
      FACT(12)='intact m coefficient'
      FACT(13)='rock mass rating'
      FACT(14)='angle of upper slope'
      FACT(15)='anchor application angle'
      FACT(16)='anchor force'
      FACT(17)='inter-slab friction angle'
      X(1)=60.D0
      X(2)=0.D0
      X(3)=60.D0
      X(4)=2.D0
      X(5)=00.D0
      X(6)=25.D0
      X(7)=9.81D0
      X(8)=30.0
      X(9)=0.D0
      X(10)=60000.D0
      X(11)=60000.D0
      X(12)=10.D0
      X(13)=50.D0
      X(14)=0.D0
      X(15)=0.D0
      X(16)=0.D0
      X(17)=00.D0
      N=INT2(17)
      SW=.TRUE.
C  CALCULATE HOEKS COEFFICIENTS
1     M=X(12)*DEXP((X(13)-100.D0)/14.D0)
      S=DEXP((X(13)-100.D0)/6.D0)
C  CHANGE ANGLES TO RADIANS
      X(1)=X(1)*A
      X(2)=X(2)*A
      X(8)=X(8)*A
      X(14)=X(14)*A
      X(15)=X(15)*A
      X(17)=X(17)*A
C  DETERMINE WHETHER FAILURE THRU ROCK MASS OR ALONG DAYLIGHTED DISC'Y
       IF (X(2).EQ.0.D0) THEN
C  SET STARTING TOE RESISTANCE AND FAILURE ANGLE THRU ROCK MASS
        ST1=1000000000
        B=0.08726646D0
C  SET X(2)=B FOR SLIP ALONG DISCONTINUITY
      ELSE
        B=X(2)
      ENDIF
C  CALCULATE GEN'L GEOMETRY
      H=X(3)/DSIN(X(1))
2     H1=X(4)/DTAN(X(1)-B)
      H2=H-H1
      H3=H1/DCOS(X(1)-B)
      H4=-X(4)*1/DTAN(X(14)-X(1))
      H5=X(5)
      HW=X(5)/DSIN(X(1))
      H6=HW-X(4)*SIN(B)/(SIN(X(1))*SIN(X(1)-B))
      H7=X(5)/SIN(B)
C  CALCULATE SLAB WEIGHTS
      WD=X(6)*X(4)*(H2+.5D0*H4)
      WT=.5D0*X(6)*X(4)*H1
C  CALCULATE WATER FORCES
C  CASE A
      IF (X(5).GT.X(4)*SIN(B)/SIN(X(1)-B)) THEN
                VD=X(7)*H6**2*SIN(X(1))/2
                VT=X(7)*H6*H3/2
      ELSE
C  CASE B
                VD=0.D0
                VT=X(7)*X(5)*H7/2
      ENDIF
      ND=WD*DCOS(X(1))-VD+X(16)*DSIN(X(1)-X(15))
      IF (ND.LE.0.D0) THEN
           SD=0.D0
           GO TO 10
      ENDIF
C  CALCULATE SHEARING RESISTANCE OF DRIVING SLAB
      IF (H2.LT.0.D0) THEN
         SD=0.D0
         GO TO 10
      ENDIF
      SD=ND*DTAN(X(8)+X(9)*DLOG10(X(10)*(H2)/ND))
 10   FD=WD*DSIN(X(1))-SD
      IF (FD.LT.0.D0) FD=0.D0
      SJ=FD*DTAN(X(17))
      NT=WT*DCOS(B)+FD*DSIN(X(1)-B)-VT
      IF (NT.LE.0.D0) THEN
           ST=0.D0
           GO TO 20
      ENDIF
      IF (X(2).EQ.0.D0) THEN
C  CALCULATE SHEARING RESISTANCE OF ROCK MASS
          Z=16*(M*NT+S*X(11)*H3)
          Y=3*M**2*X(11)*H3
          K=1.D0+Z/Y
          E=.52359878D0+DATAN(1.D0/DSQRT(K**3-1.D0))/3.D0
          QI=DATAN(1.D0/(DSQRT(4.D0*K*DCOS(E)**2-1.D0)))
          ST=(1.D0/DTAN(QI)-DCOS(QI))*M*X(11)*H3/8.D0
C  CHECK FOR MINIMUM ST
            IF (ST.LT.ST1)  THEN
               ST1=ST
               B=B+.01745329D0
               GO TO 2
            ENDIF
      ELSE
C  CALCULATE SHEARING RESISTANCE OF DAYLIGHTED DISCONTINUITY
          ST=NT*DTAN(X(8)+X(9)*DLOG10(X(10)*(H3)/NT))
      ENDIF
C  CALCULATE ACTIVE SAFETY FACTOR
 20   REC=(ST+SJ*DSIN(X(1)-B))/(FD*DCOS(X(1)-B)+WT*DSIN(B)-X(16)*
     #  DCOS(X(1)-X(15)))
      X(1)=X(1)/A
      X(2)=X(2)/A
      X(8)=X(8)/A
      X(14)=X(14)/A
      X(15)=X(15)/A
      X(17)=X(17)/A
      B=B*57.2957795D0
      C=X(3)/TAN(A*X(1))+X(4)/SIN(A*X(1))
      BMAX=ATAN(X(3)/C)/.01745329252D0
      WRITE(12,*)B,C,BMAX
      RETURN
      END
```

APPENDIX D
PLOUGHING SLAB FAILURE MECHANICS

D.1 General Geometry

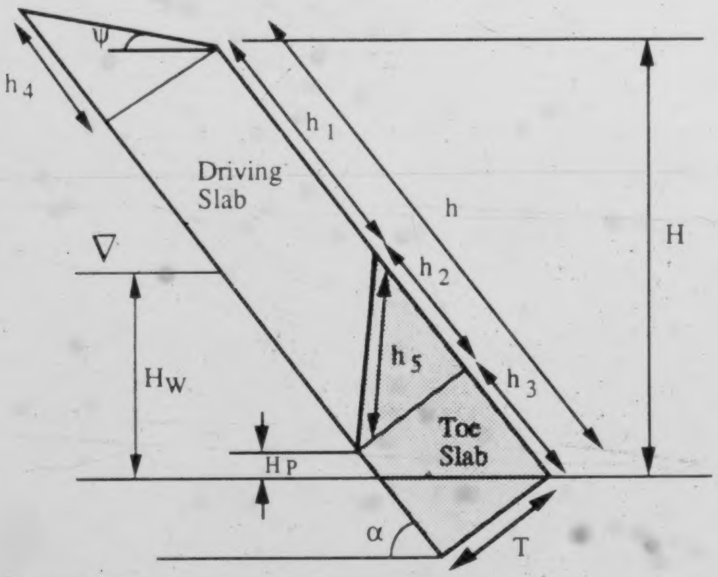

Input Parameters:

γ = total unit weight

γ_w = unit weight of water

α = slope dip

ψ = upper slope angle

θ = plow angle w.r.t. bedding

H = slope height

H_W = height of water table

H_P = height of plow discontinuity (at base of slab)

JRC = joint roughness coefficient

JCS = joint compressive strength

T = slab thickness

ϕ_U = ultimate friction angle

Q = anchor load

δ = anchor installation angle

$h = H/\sin\alpha$

$h_1 = T/\tan\alpha + H_P/\sin\alpha$

$h_2 = T/\tan\theta$

$h_3 = h - h_2 - h - h_1$

$h_4 = -T\cot(\psi - \alpha)$

$h_5 = T/\sin\theta$

$h_w = H_W/\sin\alpha$

D.2 General Force Diagram

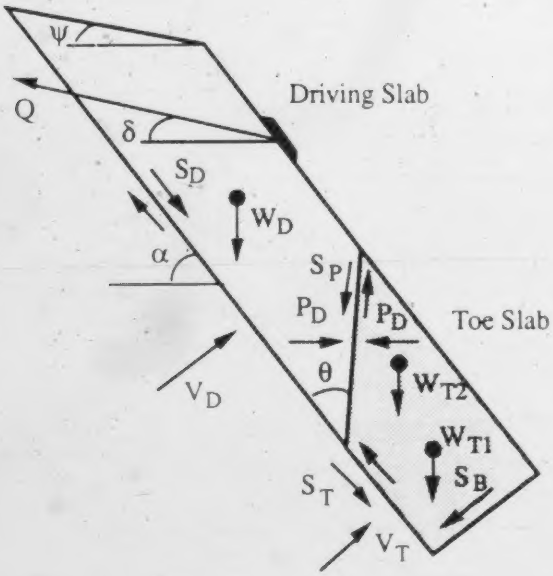
ψ
Q
δ
Driving Slab
S_D
W_D
α
S_P
P_D
P_D
Toe Slab
θ
V_D
W_{T2}
W_{T1}
S_B
S_T
V_T

W = slab weights

V = water forces (see D.3)

S = shear resistances

F_D = excess shear force of driving slab

θ = anchor load applied at an angle δ to the horizontal

- weight of Driving Slab (W_D)
  $= \gamma T \, (h_3 + 1/2 \, h_2 + 1/2 \, h_4)$
- weight of Toe Slab (W_T)
  $W_{T1} = Th_1 \gamma$; $W_{T2} = 1/2 \, h_2 T\gamma$

D.3 Water Force Distribution

Case (A) Water Table Above Plough $H_W > H_P$

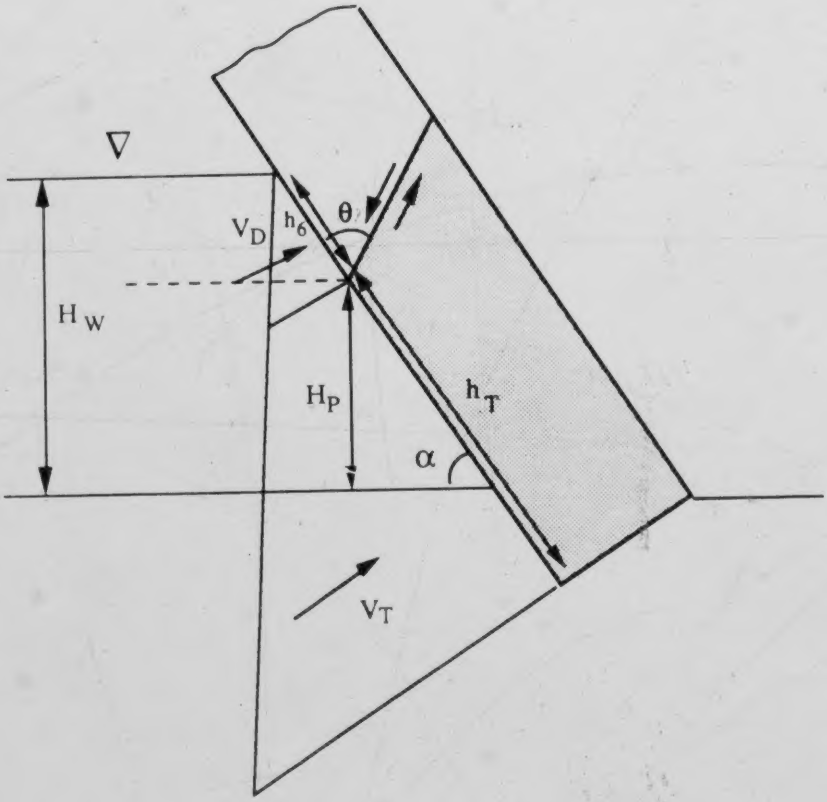

∇
V_D
h_6
θ
H_W
H_P
h_T
α
V_T

$$h_6 = \frac{H_W - H_P}{\sin \alpha} \qquad h_7 = h_1$$

$$V_D = 1/2\ \gamma_w h_6 (H_W - H_P)$$

$$V_T = 1/2\ \gamma_w (h_1 - h_6)^2 \sin \alpha - V_D$$

Case (B) Water Table Below Plough

$H_W \leq H_P$

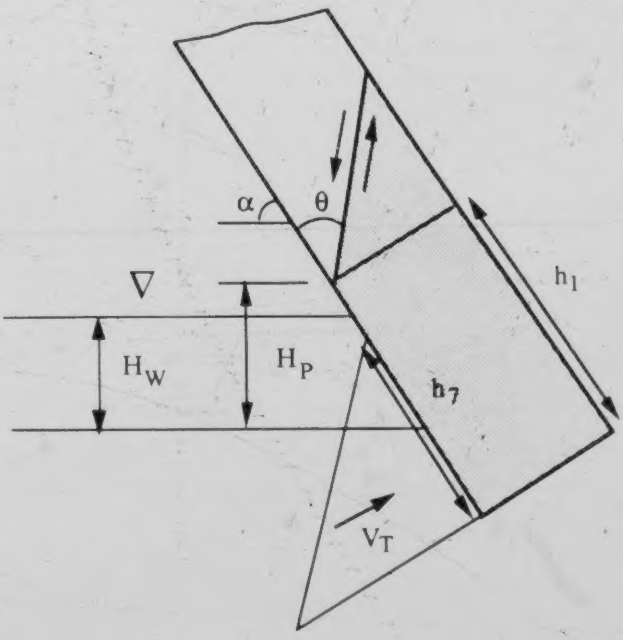
α
θ
∇
h_1
H_W
H_P
h_7
V_T

$$h_7 = h_1 - \frac{(H_P - H_W)}{\sin \alpha}$$

$V_D = 0$

$V_T = 1/2\, \gamma_w\, h_7^2 \sin \alpha$

D.4 Moment Arms on Toe Slab

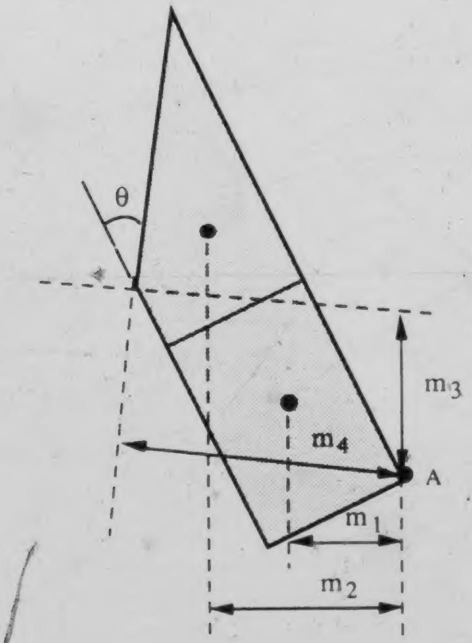

$$m_1 = \frac{T}{2} \sin \alpha \frac{h_1}{2} \cos \alpha$$

$$m_2 = \left(\frac{h_2}{3} + h_1\right) \cos \alpha + \frac{T}{3} \sin \alpha$$

$$m_3 = h_1 \cos \theta - T \sin \theta$$

$$m_4 = (h_1 + h_2) \sin \theta$$

D.5 Force Equilibrium of Toe Slab

(Resolved 11 to S_B)

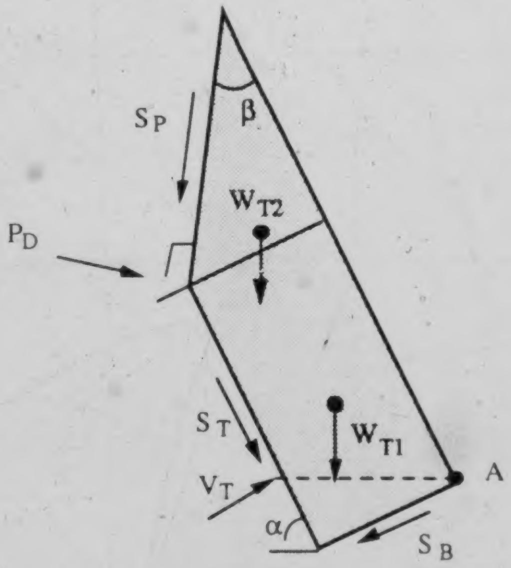

$$V_T + P_D \cos\beta = S_P \sin\beta + S_B + W_{T1} \sin\alpha + W_{T2} \sin\alpha$$

Where: $S_B = P_D \tan\phi_P$

$$S_T = W_{T1} \cos\alpha + W_{T2} \cos\alpha + P_D \sin\theta$$

Solve for P_D

$$P_D = \frac{(\cos\alpha \tan\phi_P + \sin\alpha)(W_{T1} + W_{T2}) - V_T}{\cos\theta - 2\tan\phi_P \sin\theta}$$

D.6 Moment Equilibrium of Toe Slab

Moments about A (See D.5)

$$m_1 W_{T1} + m_2 W_{T2} + m_4 S_P + TS_T = \frac{h_7}{3} V_T + P_D (m_3 + xh_5)$$

Where: x = fractional distance along h_5 of pt. of application of F_D

$$S_P = P_D \tan \phi_P$$

$$S_T = [(W_{T1} + W_{T2}) \cos \alpha - V_T] \tan \phi$$

Solve for P_D:

$$P_D\, m_4 \tan \phi_P - P_D (m_3 + xh_5) = \frac{h_7}{3} V_T - m_1 W_{T1} - m_2 W_{T2} - TS_T$$

$$P_D = \frac{h_7 V_T - m_1 W_{T1} - m_2 W_{T2} - T[(W_{T1} + W_{T2}) \cos \alpha - V_T] \tan \phi_B}{m_4 \tan \phi_P - (m_3 + xh_5)}$$

$$P_D = \frac{V_T\left(\frac{h_7}{3}\right) + \tan \phi_B - W_{T1}\left(m_1 + T \cos \alpha \tan \phi_B\right) - W_{T2}\left(m_2 + T \cos \alpha \tan \phi_B\right)}{m_4 \tan \phi_P - (m_3 + xh_5)}$$

D.7 Forces on Driving Slab

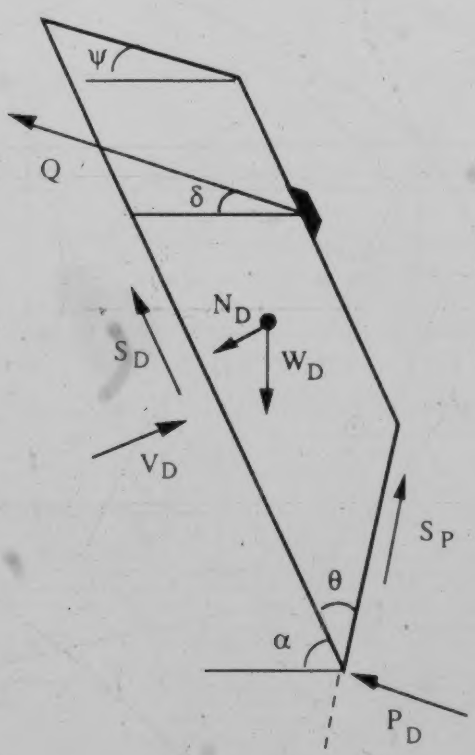

N_D = net normal force on bedding plane

$$S_D = N_D \tan\left[\phi_U + \text{JRC} \log \frac{\text{JCS } h_2}{N_D}\right]$$

$$N_D = W_D \cos \alpha - V_D + Q \sin(\alpha - \delta)$$

D.8 Force Equilibrium of Driving Slab

Resisting Force (R)

$$R = S_D + P_D \sin\theta \; S_P \cos\theta$$

Note: For ploughing P_D is derived from moment equilibrium (D.6). However, in some situations where water pressures are high and ploughing discontinuity is near the slope toe force equilibrium may be more critical (D.5).

Disturbing Force (D)

$$D = W_D \sin\alpha$$

Factor of Safety (FS)

i. Passive Support

$$FS_P = \frac{R + Q\cos(\alpha - \delta)}{D} \qquad \text{(D.1)}$$

ii. Active Support

$$FS_A = \frac{R}{D - Q\cos(\alpha - \delta)} \qquad \text{(D.2)}$$

iii. Excess Shear Support

$$FS_{ES} = \frac{1}{D - R} Q\left[\cos(\alpha - \delta) + \sin(\alpha - \delta)\right] \cdot \left[\tan\left(\phi_U + JRC \log JCS \frac{(h_2 + h_3 + h_4)}{N_D}\right)\right] \qquad \text{(D.3)}$$

D.9 PLOW SUB-PROGRAM SOURCE CODE

```
      DOUBLE PRECISION FUNCTION REC(X,N)
C   TO CALCULATE SAFETY FACTOR OF A BEDDED FOOTWALL SLOPE AGAINST
C   PLOWING SLAB FAILURE
C  *****************************************************************
C
C   INPUT: "X" IS A REAL*8 VECTOR OF LENGTH 16 WHOSE COMPONENTS ARE:
C
C   X(1)= dip of footwall
C   X(2)= height of slope
C   X(3)= thickness of slab
C   X(4)= height of water at bedding discontinuity
C   X(5)= height of water at plough discontinuity
C   X(6)= height of plough discontinuity
C   X(7)= point of applicaton of driving force
C   X(8)= unit weight of rock
C   X(9)= unit weight of water
C   X(10)= ultimate friction angle of bedding
C   X(11)= joint roughness coefficient
C   X(12)= joint compressive strength
C   X(13)= angle of upper slope
C   X(14)= ploughing angle with bedding
C   X(15)= anchor installation angle
C   X(16)= anchor load
C *****************************************************************
C   USER BEWARE AS NO ERROR CHECKING IS DONE.
C ******************************************************************
      DOUBLE PRECISION X(15),H,H1,H2,H3,H4,H5,M1,M2,M3,M4,HP,R1
      DOUBLE PRECISION WT1,WT2,WD,VD,ND,SD,D,A,W,Y,Z,U
      DOUBLE PRECISION H6,H7,FS,FDM,FDF,SPM,SPF
      INTEGER*2 N
      CHARACTER*28 FACT(20)
      CHARACTER*15 FRNM
      CHARACTER*7 FRUNITS
      COMMON/FUNC/FRNM,FRUNITS,FACT
      COMMON/HEIGHT/HP,FS
      LOGICAL*4 SW
      DATA SW /.FALSE./
      DATA A /.01745329252D0/
      OPEN(UNIT=10,FILE='FORCE.OUT')
      IF(SW)GO TO 1
      FRNM='saftey factor'
      FRUNITS='no dim'
      FACT(1)='dip of slope'
      FACT(2)='angle of upper slope'
      FACT(3)='ploughing angle w.r.t. bdg.'
      FACT(4)='slope height'
      FACT(5)='height of plough'
      FACT(6)='slab thickness'
      FACT(7)='height of water table'
      FACT(8)='rock unit weight'
      FACT(9)='water unit weight'
      FACT(10)='basic friction angle'
      FACT(11)='joint roughness coeff.'
      FACT(12)='joint comp. strength'
      FACT(13)='anchor installation angle'
      FACT(14)='anchor load'
      FACT(15)='plow friction angle'
      FACT(16)='moment arm factor'
      X(1)=60.D0
      X(2)=0.D0
      X(3)=20.D0
      X(4)=60.D0
      X(5)=10.D0
      X(6)=2.D0
      X(7)=0.D0
      X(8)=25.D0
      X(9)=9.81D0
      X(10)=30.D0
      X(11)=0.D0
      X(12)=60000.D0
      X(13)=0.D0
      X(14)=0.D0
      X(15)=30.D0
      X(16)=0.D0
      N=INT2(16)
      SW=.TRUE.
C   CONVERT ANGLES TO RADIANS
    1 X(1)=X(1)*A
      X(2)=X(2)*A
      X(3)=X(3)*A
      X(10)=X(10)*A
      X(13)=X(13)*A
      X(15)=X(15)*A
C   SET PLOW HEIGHT
      IF (X(5).EQ.0.D0) THEN
         HP=5.D0
      ELSE
         HP=X(5)
      ENDIF
C   DEFINE SLAB GEOMETRY
      H=X(4)/SIN(X(1))
    2 H1=HP/SIN(X(1))+X(6)/TAN(X(1))
      H2=X(6)/TAN(X(3))
      H3=H-H2-H1
      H4=-X(6)*1/TAN(X(2)-X(1))
      H5=X(6)/SIN(X(3))
      H6=(X(7)-HP)/SIN(X(1))
      HW=X(7)/SIN(X(1))
C  CALCULATE MOMENT ARMS ON TOE SLAB
      M1=X(6)/2*SIN(X(1))+H1/2*COS(X(1))
      M2=(H2/3+H1)*COS(X(1))+X(6)/3*SIN(X(1))
      M3=H1*COS(X(3))-X(6)*SIN(X(3))
      M4=(H2+H1)*SIN(X(3))
C  CALCULATE SLAB WEIGHTS
      WT1=X(6)*H1*X(8)
      WT2=.5D0*H2*X(6)*X(8)
      WD=X(6)*X(8)*(H3+H2/2+H4/2)
C  CALCULATE WATER FORCES
C  CASE A
      IF (X(7).GT.HP) THEN
        H7=H1
        VD=X(9)*H6*(X(7)-HP)/2
        VT=(X(9)*(H1+H6)**2*SIN(X(1))/2.D0)-VD
      ELSE
C  CASE B
          H7=H1-(HP-X(7))/SIN(X(1))
```

```
            VD=0.D0
            VT=X(9)*H7**2*SIN(X(1))/2.D0
      ENDIF
C  MOMENT EQUILIBRIUM OF TOE SLAB
      W=VT*(H7/3+TAN(X(10)))
      Y=WT1*(M1+X(6)*COS(X(1))*TAN(X(10)))
      U=WT2*(M2+X(6)*COS(X(1))*TAN(X(10)))
      Z=M4*TAN(X(15))-(M3+X(16)*H5)
      FDM=(W-Y-U)/Z
      IF (FDM.LE.0.D0) REC=0.D0
C  FORCE EQUILIBRIUM OF TOE SLAB
      FDF=((COS(X(1))*TAN(X(15))+SIN(X(1)))*(WT1+WT2)-VT)
     # /(COS(X(3))-2*TAN(X(15))*SIN(X(3)))
C  SHEAR RESISTANCE OF TOE SLAB ALONG PLOW DISCONTINUITY
      SPM=(FDM)*TAN(X(15))
      SPF=(FDF)*TAN(X(15))
C  FORCES ON DRIVING SLAB
      ND=WD*COS(X(1))+X(14)*SIN(X(1)-X(13))-VD
      IF (ND.GT.0.D0) THEN
            SD=ND*TAN(X(10)+X(11)*LOG10(X(12)*(H2+H3)/ND))
      ELSE
            SD=0.D0
      ENDIF
C  RESISTING FORCES
      RM=SD+FDM*SIN(X(3))+SPM*COS(X(3))
      RF=SD+FDF*SIN(X(3))+SPF*COS(X(3))
C  DISTURBING FORCES
      D=WD*SIN(X(1))
      IF (X(5).EQ.0.D0) THEN
C  FIND MIN. R
          RM=MIN(RM,RF)
          IF ((RM.LT.D).OR.(HP.GT.X(4))) THEN
             HP=HP+.5D0
             GO TO 2
          ENDIF
      ENDIF
C  DISTURBING FORCES
C  ACTIVE SAFETY FACTOR
      FS=RF/(D-X(14)*COS(X(1)-X(13)))
      REC=RM/(D-X(14)*COS(X(1)-X(13)))
      X(1)=X(1)/A
      X(2)=X(2)/A
      X(3)=X(3)/A
      X(10)=X(10)/A
      X(13)=X(13)/A
      X(15)=X(15)/A
      RETURN
      END
```

APPENDIX E
DIGITAL FOOTWALL MODELLING

During June, 1990, Douglas Curran of Prometric Technologies conducted detailed surface modelling of a footwall bedding plane surface at Byron Creek Collieries, near Sparwood, British Columbia. The modellng involved shining a grid of light on the footwall, and utilizing precise digital photogrammetric techniques, surveying the grid points. The work was carried out at two different grid sizes: 1.0 m and 4.8 m, each having a grid density of 21 x 21 nodes. Figure E.1 shows a photograph of the 1.0 m digital grid. The data was presented as a 3-D coordinate file for each grid size. Following receipt of the raw data the SURFER (Golden Software Inc.) program was used to create a contoured plan in the plane of the footwall surface.

Figure E.2 shows the results of the 1.0 m grid size. Grid node spacing is 0.05 m and is meant to represent the smaller scale roughness for a typical block size. The grid node spacing is 5% of the grid size and is meant to approximate the base length of "critical asperities" affecting peak strength. The photograph (Figure E.1) shows several bedding dislocations where small slabs have fallen off the footwall. These are indicated as dashed lines on the profiles. Where bedding is continuous, the profiles are relatively planar.

Figure E.3 shows the results of the 4.8 m grid size. The larger grid node spacing (0.24 m) is meant to reflect the deviations from planarity apparent over several block lengths. The profiles show that for a block size of 1 m the upslope and downslope waviness angles practically cancel each other out.

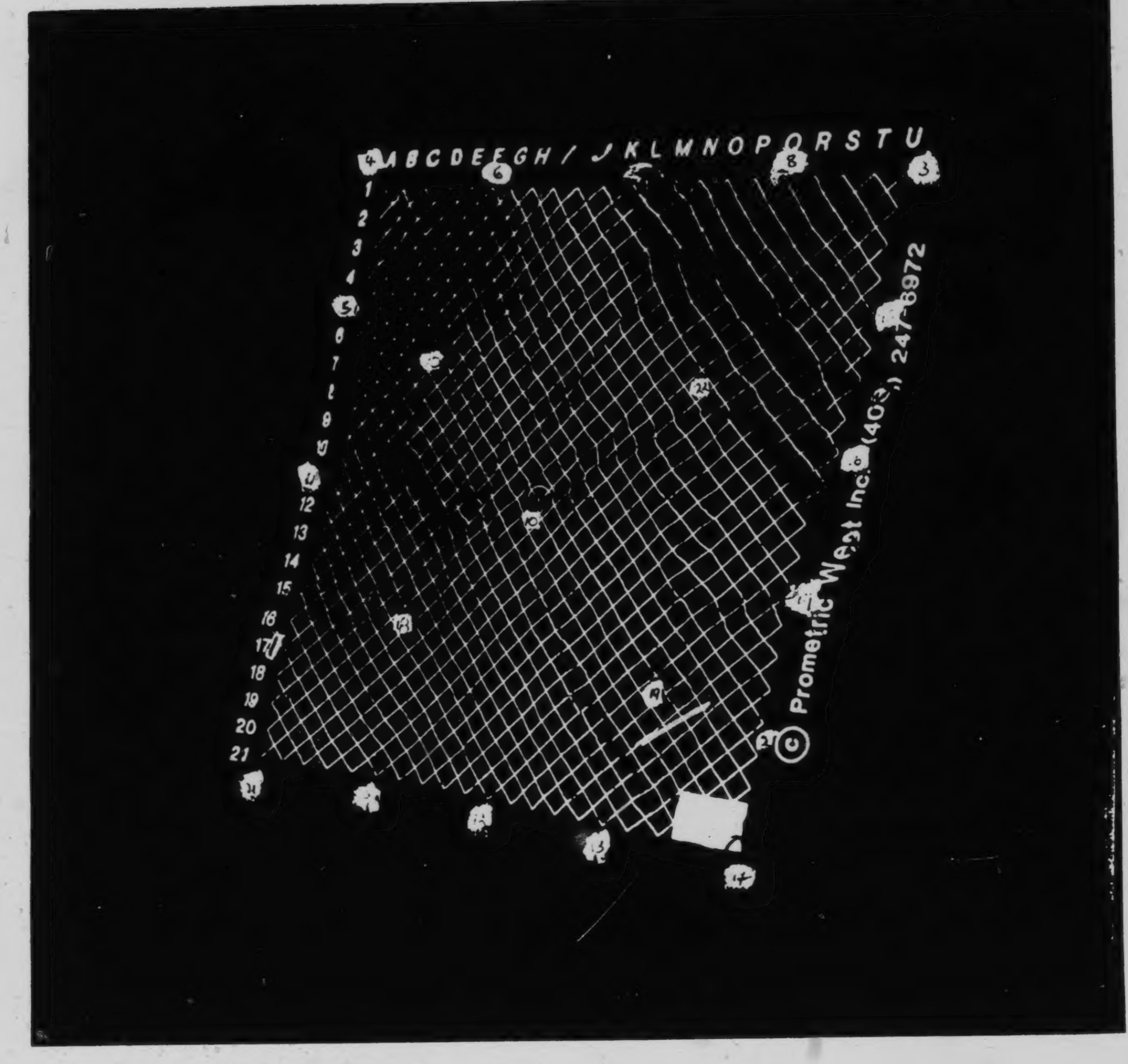
A B C D E F G H I J K L M N O P Q R S T U
1 2 3 4 5 6 7 8 9 10 11 12 13 14 15 16 17 18 19 20 21
© Prometric West Inc. (403) 247-6972

Figure E.1 Photograph of the 1.0 m Digital Grid

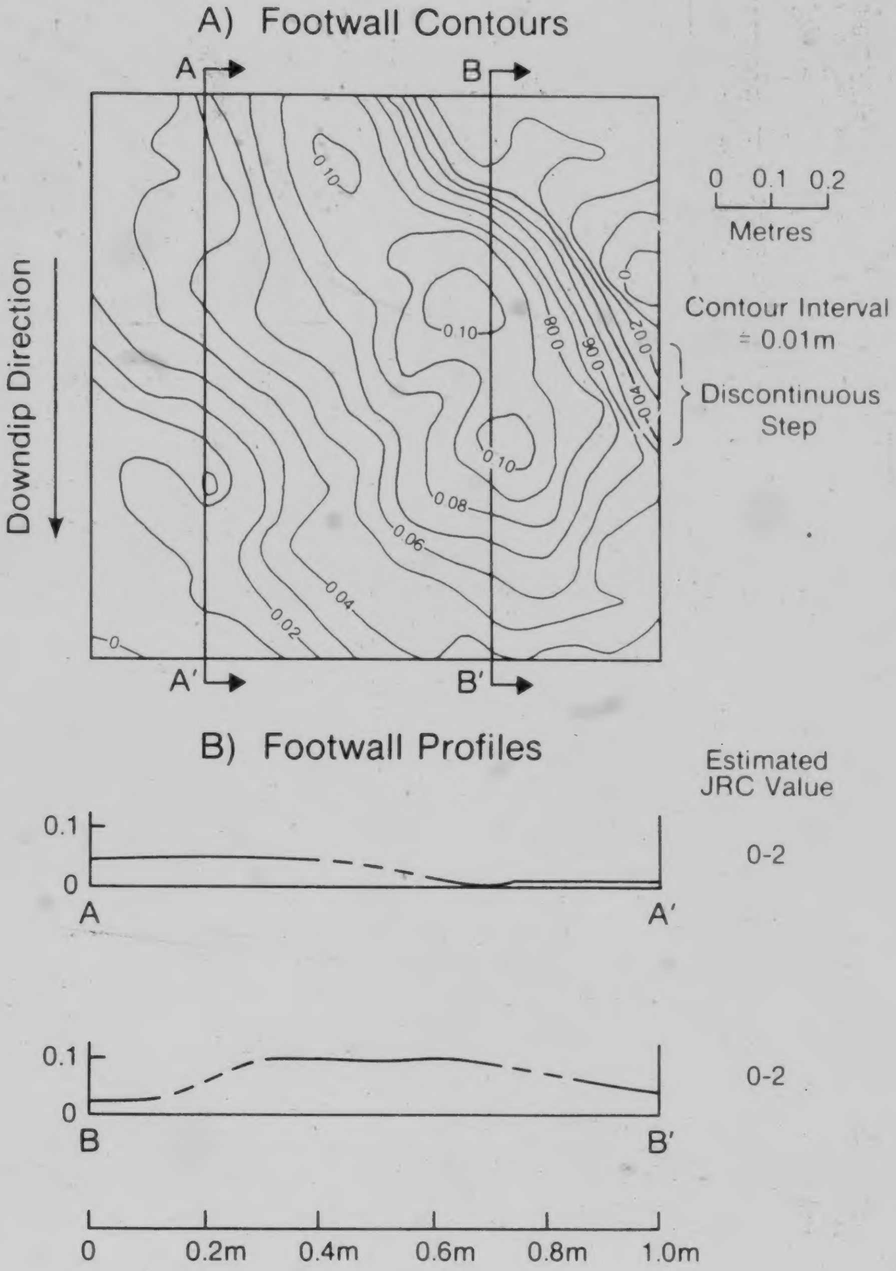
A) Footwall Contours
A
B
A'
B'
Downdip Direction
0 0.1 0.2
Metres
Contour Interval
≐ 0.01m
Discontinuous
Step
0.10
0.10
0.10
0.08
0.06
0.04
0.02
0
0.08
0.06
0.04
0.02
0
B) Footwall Profiles
Estimated
JRC Value
0.1
0
A
A'
0-2
0.1
0
B
B'
0-2
0
0.2m
0.4m
0.6m
0.8m
1.0m

Figure E.2 1.0 m Grid Footwall Surface

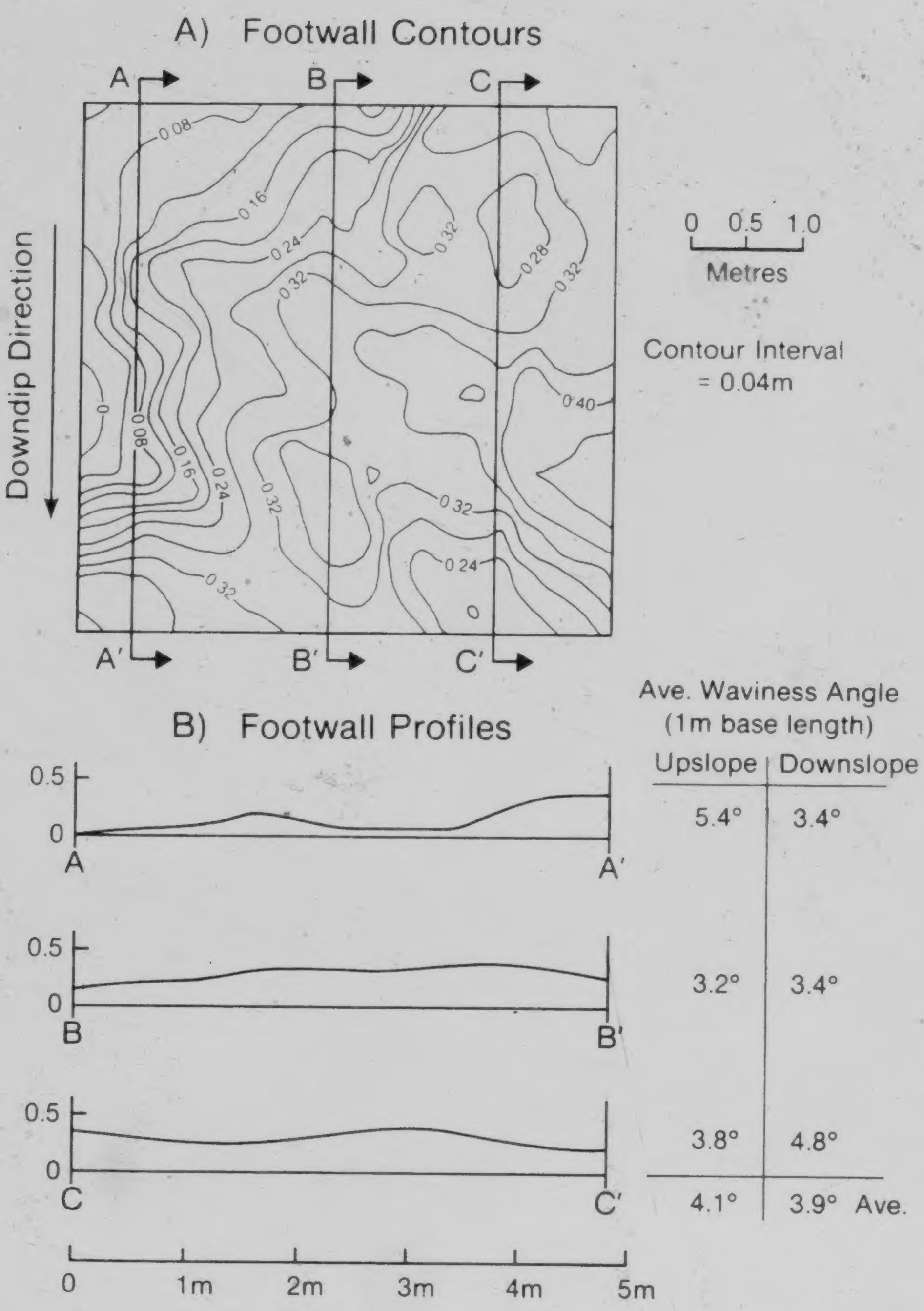

Ave. Waviness Angle
(1m base length)

	Upslope	Downslope
A–A'	5.4°	3.4°
B–B'	3.2°	3.4°
C–C'	3.8°	4.8°
Ave.	4.1°	3.9°

Figure E.3 **4.8 m Grid Footwall Surface**

APPENDIX F
SMOKY RIVER COAL LIMITED FIELD STUDY

During May 1990 field work was carried out to assess the footwall stability within the E-2 Pit at Smoky river Coal Limited, near Grande Cache, Alberta. Assistance was provided by Alex Bagnell of Smoky River Coal Limited. The field work involved collecting orientation data (dip direction and dip) and mapping a 18.3 m (60 ft.) stratigraphic thickness of exposed footwall section within the pit.

Figures F.1 and F.2 show equal area stereographic projection and the resulting kinematic analysis respectively of the orientation data. The equal area projection contours are derived from the ORIENT computer program developed by Dr. H.A.K. Charlesworth in the Department of Geology at the University of Alberta.

Results of the footwall mapping are contained in Table F.1. Note that the footwall above the massively bedded Torrens sandstone unit is broken down into four stratigraphic units for design purposes. The thin coal seams below the B and D units account for the major bedding weaknesses in the footwall strata. Thus the A-B and A-D units form the slabs on which the analysis is based.

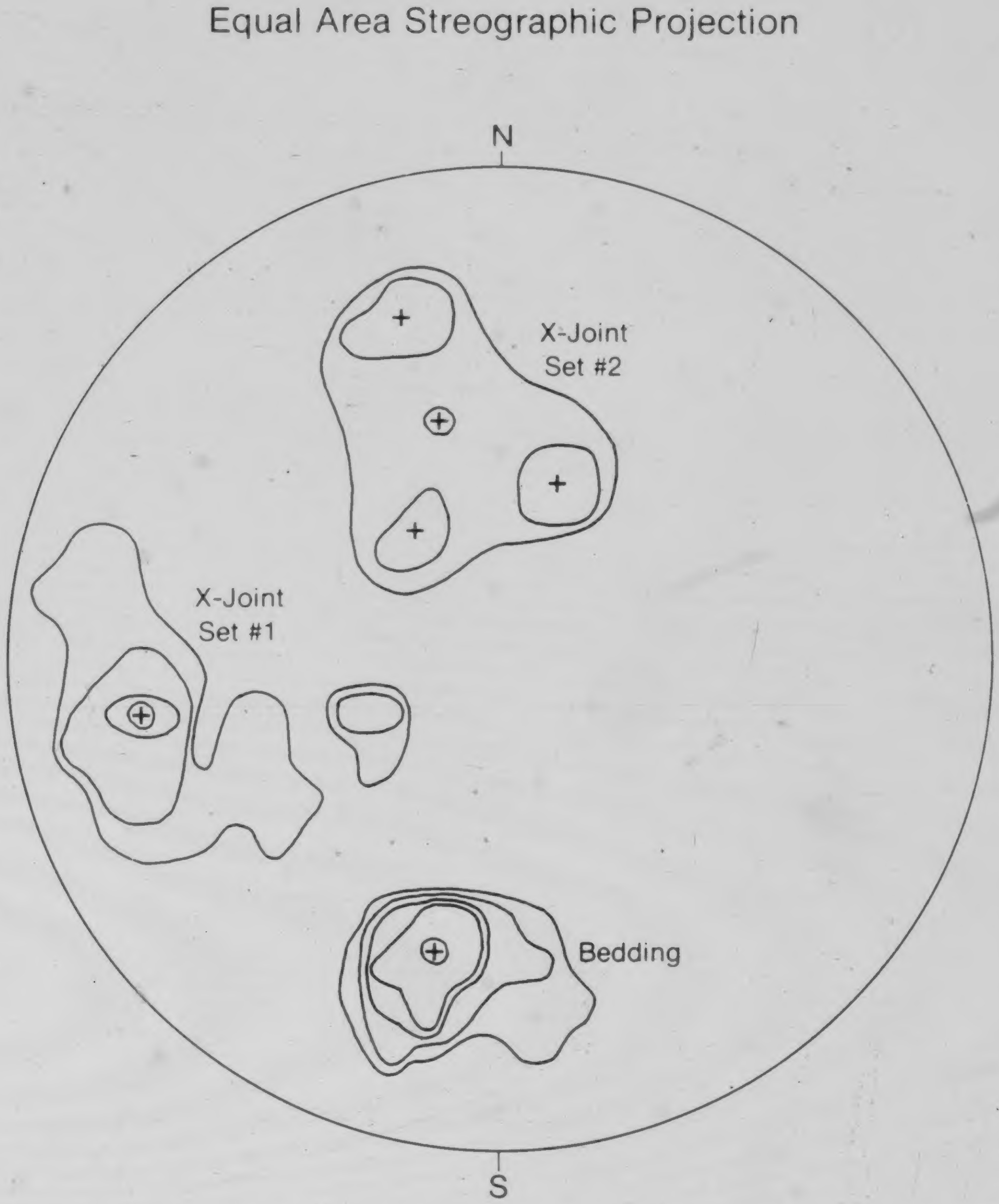

Figure F.1 E-2 Pit Discontinuities

Streographic Projection

	Dip Direction	Dip
Bedding	12°	62° ± 10°
X-Joint #1	82°	72° ± 10°
X-Joint #2	166°	53° ± 20°

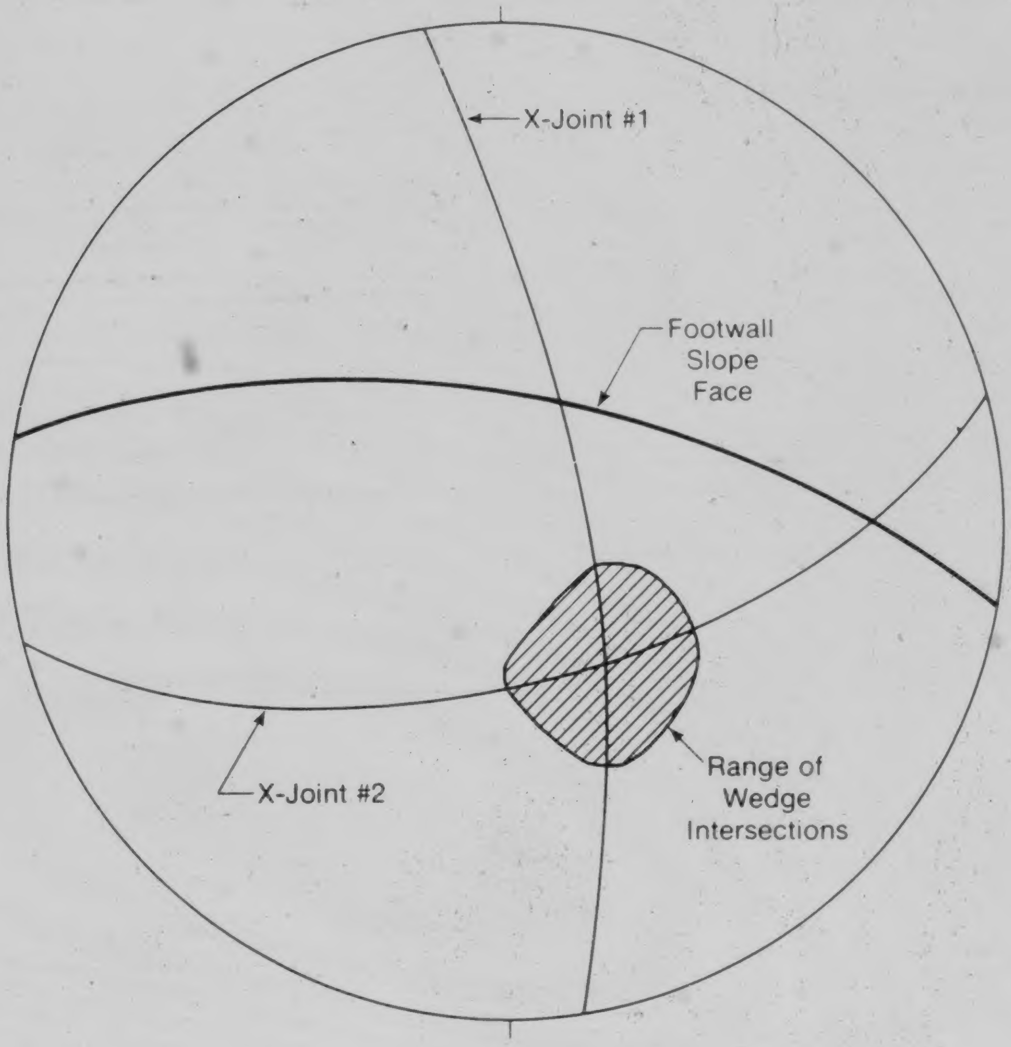
X-Joint #1
Footwall Slope Face
X-Joint #2
Range of Wedge Intersections

Figure F.2 E-2 Pit Footwall Kinematics

Table F.1 E-2 Pit Engineering Geology Footwall Slopes

Unit	Lithology	Thickness	σ_c	X Joint Spg.	Bldg. Joint Spg.	RQD	Joint Condition	Ground Water	RMR
(A)	Sandy siltstone (No. 4 Seam footwall)	7 ± 1	8,000 psi (55 MPa)	2 – 3 ft. (.76 m)	.3 – 1.3 ft. (.24 m)	90			52
		RMR	6		8	18	10	10	
(B)	Mudstone with marker coal seam at base	5 ± .5	3,000 psi (20 MPa)	1 – 1.5 ft. (.38 m)	.2 – 1.0 ft. (1.8 m)	80			46
		RMR	3		7	16	10	10	
(C)	Medium sandstone (Bench Sand)	18 ± 1	10,000 psi (68 MPa)	1.5 – 3.0 ft. (.68 m)	.5 – 2.0 ft. (.38 m)	100			56
		RMR	7		9	20	10	10	
(D)	Mudstone with #3 Seam at base	30 ± 2	4,500 psi (30 MPa)	1 – 1.5 ft. (.38 m)	.5 – 1.0 ft. (.23 m)	90			48
		RMR	4		6	18	10	10	
(E)	Torrens sandstone	Massive Bedded Basal Sandstone Unit							55 – 60

APPENDIX G
BYRON CREEK COLLIERIES FIELD STUDY

During May, 1990 field work was carried out to assess the footwall stability within the 51 Pit at Byron Creek Collieries, near Sparwood, British Columbia. Assistance was provided by Bill Shaw and Greg Cave of the Coal Division, Esso Resources Canada Limited. The field work involved collecting orientation data, mapping of discontinuity spacing, and general reconnaissance within the pit.

Figure G.1 and G.2 show equal area stereographic projection and the resulting kinematic analysis respectively of the orientation data. The equal area projection contours are derived from the ORIENT computer program developed by Dr. H.A.K. Charlesworth in the Department of Geology at the University of Alberta.

Figure G.3 shows results of the discontinuity spacing data.

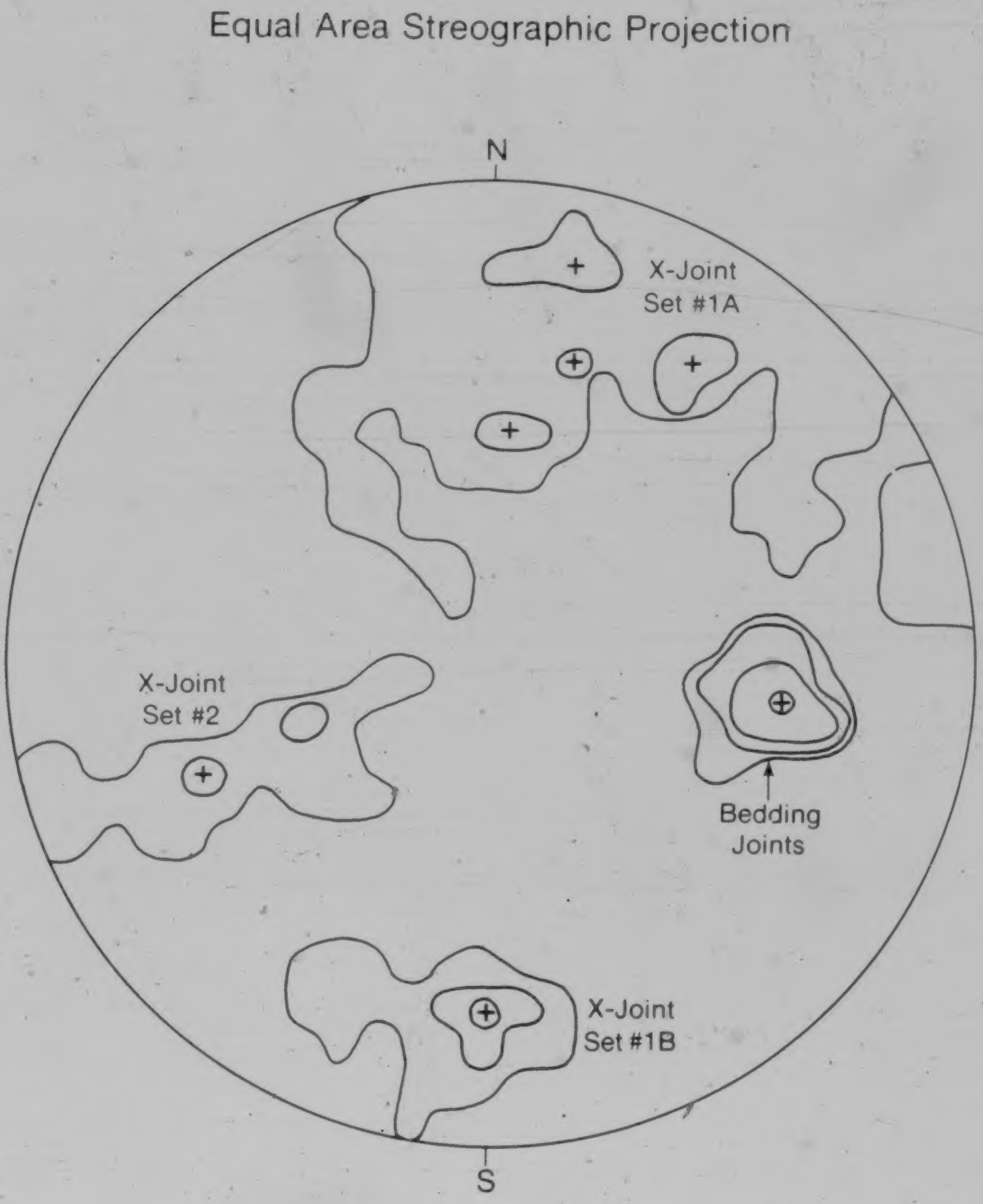
Equal Area Streographic Projection
N
X-Joint Set #1A
X-Joint Set #2
Bedding Joints
X-Joint Set #1B
S

Figure G.1 51 Pit Discontinuities

Streographic Projection

	Dip Direction	Dip
Bedding	97°	55°~75°
X-Joint #1A	196°	52° ± 15°
X-Joint #1B	0°	64° ± 10°
X-Joint #2	67°	54° ± 10°

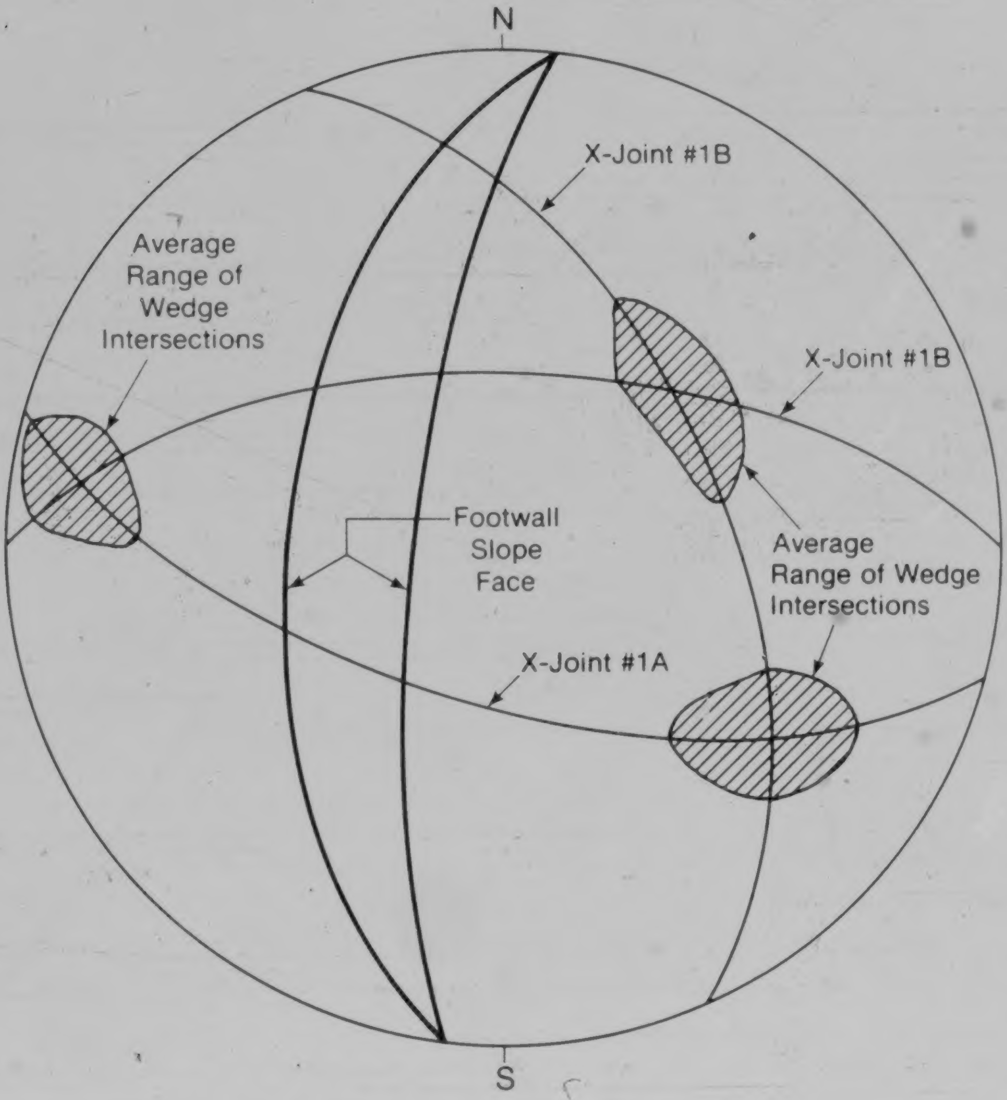
N
X-Joint #1B
Average Range of Wedge Intersections
X-Joint #1B
Footwall Slope Face
Average Range of Wedge Intersections
X-Joint #1A
S

Figure G.2 51 Pit Footwall Kinematics

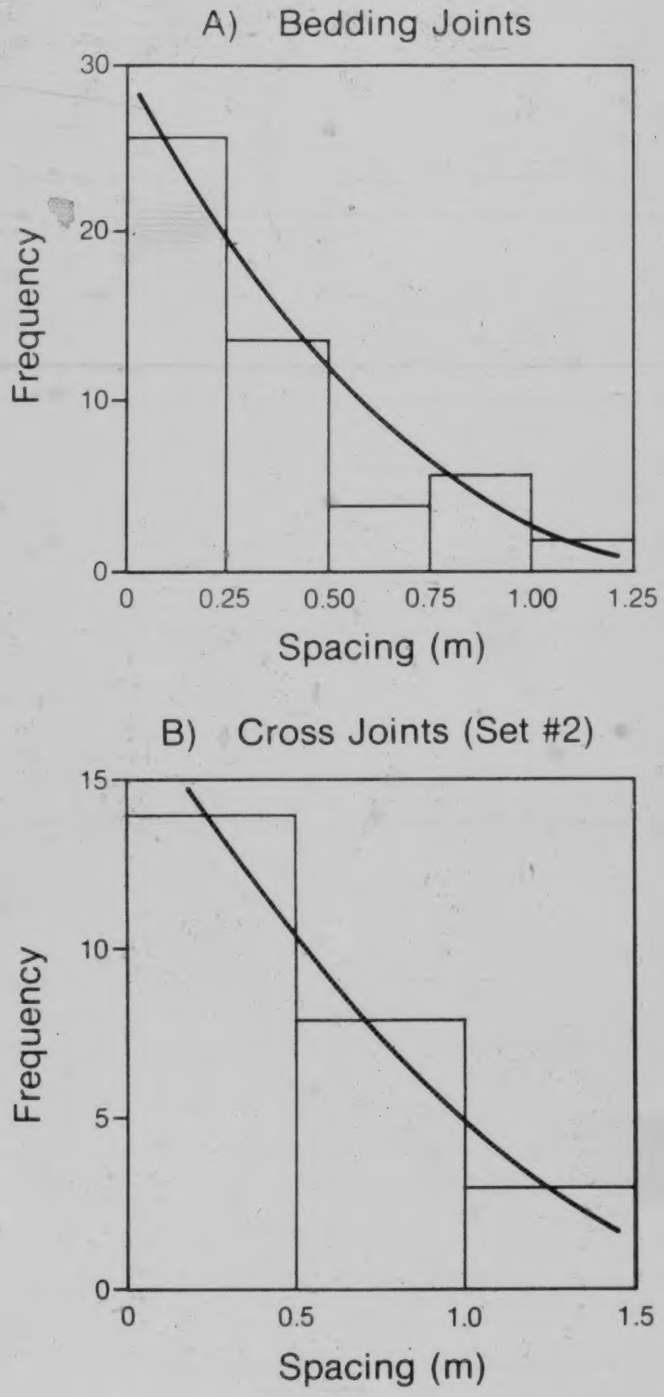

Figure G.3 51 Pit Discontinuity Spacing